EPA-IAG-79-D-X0513

NBS/EPA ENERGY ENVIRONMENT PROJECT

to the

Environmental Protection Agency

Office of Environmental Processes & Effects Research

Jan.-Dec. 1980

US Dept. of Commerce

National Bureau of Standards

Washington, DC 20234

TABLE OF CONTENTS

FOREWORD

The role of the National Bureau of Standards (NBS) in the Interagency Energy/Environment R&D program, coordinated by the Office of Research and Development, U. S. Environmental Protection Agency, is to provide those services necessary to assure data quality in measurements being made by a wide variety of Federal, state, local, and private industry participants in the entire program. The work at NBS is under the direction of the Office of Environmental Measurements and is conducted in the Center for Analytical Chemistry, the Center for Radiation Research, and Center for Chemical Physics. NBS activities are in the Characterization, Measurement, and Monitoring Program category and address data quality assurance needs in the areas of air and water measurement methods, standards, and instrumentation. NBS outputs in support of this program consist of the development and description of new or improved methods of measurement, studies of the feasibility of production of Standard Reference Materials for the calibration of both field and laboratory instruments, and the development of data on the physical and chemical properties of materials of environmental importance in energy production. This report is the last of a series of reports which had been issued every six months by NBS over the past five years (i.e. 1975-1980) as part of the Interagency Energy/Environmental program.

William H. Kirchhoff
Chief, Office of Environmental Measurements
National Bureau of Standards

INTRODUCTION AND SUMMARY

This report describes work performed by the National Bureau of Standards (NBS) during the period, January 1980 through December 1980, under the Interagency Agreement (EPA-79-D-X0513) between the U. S. Environmental Protection Agency and NBS. This Agreement authorizes NBS activities concerned with the development of measurement methods, techniques, Standard Reference Materials (SRM's), and instrumentation in support of other programs for evaluating environmental effects of increased energy use. The resultant measurement methods and SRM's are used to provide data quality assurance for measurements made in the laboratory and in field monitoring associated with energy production and use. The highlights for this reporting period in the eight sub-agreement areas are given below. Detailed project information is provided in the body of this report.

81 BCKa - ENERGY RELATED POLLUTANT MEASUREMENT AND INSTRUMENTATION DEVELOPMENT

Under the task, "Energy Related Water Pollutant Analysis Instrumentation", internal standard mixtures required for testing the Master Analytical Scheme (MAS) were prepared. Three different standard mixtures, "purgeable", "extractable", and "intractable" organic compounds, each at two concentration levels were prepared. Since time did not permit extensive stability testing, accelerated aging studies were performed on test mixtures similar to the internal standard mixtures to allow a preliminary assessment of stability. Although some decomposition was observed, the rates were such that properly stored mixtures (0-5 °C) were expected to be usable for the required several months of evaluation of the MAS. Approximately 600 individually sealed ampoules of the various internal standard mixtures were prepared, and the 400 required for initial tests of the MAS were delivered as requested. Ampoules from all six internal standard mixtures prepared have been stored at 0-5 °C here at NBS. Periodically, selected ampoules will be removed from storage and the concentrations of individual components checked by gas or liquid chromoatography to permit another evaluation/assessment of stability.

A patent application covering the NBS developed interface device for a conventional liquid chromatograph and a conventional mass spectrometer was approved. Several LC/MS experiments have been performed to evaluate and optimize this system for quantitative measurements.

Work related to liquid chromatography-electrochemical detection (LC-EC) focused on the development of new chromatographic separations and the optimization of the electrochemical detection response. A manuscript on NBS activities in LC-EC has been submitted to Analytical Chemistry. Work related to the inductively coupled plasma (ICP) technique focused on the characterization and correction for interferences which degrade the quality of analytical results.

In an effort to develop/improve methodologies for characterizing and quantitating chemical species in various energy related matrices, activities focused on the use of high performance liquid chromatography/ atomic absorption spectrometry, plasma emission spectrometry and ion exchange/atomic absorption spectrometry.

81 BCKb - ENERGY RELATED WATER POLLUTANT ANALYSIS INSTRUMENTATION

Work performed under the task, "Development of Measurement Methods for Non-Volatile Organic Pollutants in Water Due to Energy Technologies", focused on the development of a fluoroimmunochemical procedure for detection and quantitation of dinitrophenols in water. Specific immunoglobulins were prepared and used in quantitative competitive assay experiments to assess their effectiveness.

Additionally, installation of the Fourier transform infrared (FTIR) spectrometer was completed. Plans have been made to use the FTIR in four specific areas: high resolution/low pressure gas work, liquid samples, liquid chromatography and gas chromatography. Construction and testing of an interface for wall coated open tubular gas chromatographic columns (WCOT), which allow real-time FTIR analysis of compounds, and other gas chromatographic studies were conducted this reporting period.

Previous reports included progress of activities related to Coherent Anti-Stokes Raman Spectroscopy (CARS). An evaluation of CARS and its application to high performance liquid chromatography is summarized in Appendix 2.

81 BCLa - ENERGY RELATED POLLUTANTS AND EFFECTS MONITORING AND ASSOICATED METHODS AND TECHNIQUES DEVELOPMENT

Under the task, "Development of SRM's for Stationary Sources Associated with Energy Production", measurement of the concentration of nitrogen dioxide (NO_2) in gas mixtures on a relative basis has been completed. Work related to determining the final concentration value of the 250, 500, 1000 and 2500 ppm NO_2 mixtures and the length of the period of certification must continue before final issuance of the mixtures as SRM's. Two new SRMs consisting of 50 and 100 ppm nominal concentration of sulfur dioxide in nitrogen are nearing completion. Standard Reference Materials have been issued for 1500 and 3000 ppm NO in N_2. Two new SRM's (SRM 2657 and SRM 2658) consisting of two and ten mole percent O_2 in N_2 are now available (see certificate in Appendix).

Under "Development of SRM's for Monitoring Ambient Air Impacted by Emissions Resulting from Energy Production", work has been completed on the analysis of the air which will be used to prepare the CO_2 in Air SRM's. Fifty sample lots of approximately 320, 330, and 340 ppm CO_2 in air are being prepared. A third COGAS system has been constructed for the automation of permeation tube calibrations. A traceability procedure/protocol for gas standards has been developed which in essence transfers the responsibility for producing large numbers of accurate standards (Certified Reference Materials) to the specialty gas industry. A document has been prepared for publication under the Interagency Energy-Environment program, entitled "A Procedure for Establishing Traceability of Gas Mixtures to Certain National Bureau of Standards Standard Reference Materials".

The goal of work under task "Develop Methods for Dispersal of Particulates on Filter Media and Methods for Determining and Controlling the Composition and Morphology of such Dispersed Particulates", was to perform the research and development required to produce thin standard samples especially useful for calibration of x-ray fluorescence analysis of collected airborne particulate matter. Several candidate methods for preparing such samples have been investigated and the results are described in this report.

Under "Particulate Physical and Chemical Charaterization", results of studies to improve and verify the particle size and count measurements with particle Doppler Shift Spectrometry (PDSS) is described. Several publications detailing NBS work with PDSS are included in the appendix.

Final certification of SRM 2673, Sulfate and Nitrate on Filter media, and SRM 2674, Lead on Filter media, has been completed (see Certificates in Appendix).

81 BCLb - ENERGY RELATED AIR POLLUTANT ANALYSIS INSTRUMENTATION

Under the task, "Development of an Instrument to Measure Airborne Sulfate Particulate Matter", the development and characterization of the pulsed Electrostatic Precipitator-Flame Photometric Detector (PEP-FPD) system for the measurement of ambient level aerosol sulfur concentrations has been completed and a final report is in the review process. A summary of these characterization and optimization activities is described in this report.

81 BCLc - ENERGY RELATED POLLUTANTS AND EFFECTS MONITORING AND ASSOCIATED METHODS AND TECHNIQUES DEVELOPMENT

Work under the task, "Radiocarbon as an Environmental Trace", has continued with the objective of utilizing the natural $^{14}C/^{12}C$ ratios to distinguish

between biogenic and fossil pollutant sources. A rather detailed description of activities related to radiocarbon measurements (e.g. research advances, statistical evaluations of interlaboratory data, advances in small sample radiocarbon measurement techniques) is included in this report.

81 BCMa - ENERGY RELATED POLLUTANTS AND EFFECTS MONITORING AND ASSOCIATED METHODS AND TECHNIQUES DEVELOPMENT

Under the task, "Energy Related Water Pollutant Standard Reference Materials", certification and issuance of SRM 1644, (Polynculear Aromatic Hydrocarbons) was completed. This SRM includes three generator columns (anthrancene, benz(a)anthracene, and benzo(a)pyrene) which can be used to produce known concentrations of these PAH's in aqueous solutions. The first natural matrix SRM for trace level organic constituents (Organics in Shale Oil, SRM 1580) was also issued. SRM 1580, is intended primarily for evaluating the reliability of analytical methods used for the determination of trace level polynuclear aromatic hydrocarbons, phenols, and nitrogen heterocyclic compounds in shale oil, coal-derived liquids, or petroleum products. In addition, this SRM may be used as a surrogate standard for any complex environmental extract containing classes of compounds for which the SRM is certified.

A work plan was developed and approved to intitate evaluation/feasibility studies of drilling fluid reference standards. The objective of this activity is to prepare a drilling fluid mixture which could be useful in evaluative/assessment studies of chemical constituents on aquatic and terrestrial environment, as well as provide an important reference standard in a quality assurance protocol for measurements made on discharges from drilling and production operations.

Work continued on the development improvment, and application of laser Raman spectroscopy to the analysis of organic pollutants. An optical

mulitchannel analyzer and a commerical gas chromatograph were acquired. The sampling system has been refabricated to provide for higher sensitivity and sample through-put. A publication describing matrix isolation Raman spectroscopy is included in the Appendix.

81 BCMb - ENERGY RELATED POLLUTANTS AND EFFECTS MONITORING AND ASSOCIATED METHODS AND TECHNIQUES DEVELOPMENT

Activities under the task, "Develop Organic SRM's for the Calibration of Energy-Related Water Pollutant Measurement Methods", focused on the development of SRM's for organic pollutants associated with emerging energy technologies. Experience and knowledge gained from research studies conducted with the LC-MS technique (see BCKa) have been applied to direct quantitative analysis of individual organic compounds in complex mixtures.

Studies have continued for the development of a phenol in water SRM. A comparison of the stability of selected phenols in distilled water and in industrial wastewater using HPLC was performed and the results are included in this report.

81 BCN - ENERGY RELATED POLLUTANTS AND EFFECTS MONITORING AND ASSOCIATED METHODS AND TECHNIQUES DEVELOPMENT

Work performed under the task, "Radiological Pollutant Quality Assurance", resulted in the preparation and characterization of two hundred ampoules of thorium-232 solution for EPA/LV. Also, two concentration levels of a mixed radionuclide solution standard were prepared and issued to EPA/LV. Reports of calibration for these standard solutions are included in the body of this report.

81-BCK-a-ENERGY RELATED POLLUTANT MEASUREMENT AND INSTRUMENTATION AND DEVELOPMENT

1. Energy-Related Water Pollutant Analysis Instrumentation

1.a. Development of Marker Compounds

The internal standard mixtures required for testing the Master Analytical Scheme have been prepared and delivered.

A final list of 23 deuterium labeled compounds was agreed upon for use as internal standards in the trial implementation of the Master Analytical Scheme. The standards each consist of seven to eleven compounds in a solvent. Three different mixtures, "purgeable," "extractable," and "intractable" organic compounds, each at two concentration levels were prepared. The components and gravimetric concentrations are shown in Tables 1, 2, and 3.

Table 1

Internal Standards for "Purgeables"

	Set No. 1		Set No. 2	
	µg/ampoule[a]	µg/L in H_2O[b]	µg/ampoule[a]	µg/L in H_2O[b]
Bromoethane-d_5	0.15	0.2$_9$	1.47	2.9
Diethyl ether-d_{10}	1.36	2.7	13.5	27.0
Anisole-2,4,6-d_3	1.25	2.5	12.4	24.9
Chlorobenzene-d_5	0.17	0.3$_4$	1.69	3.4
n-Decane-d_{22}	1.40	2.8	13.9	27.8
Naphthalene-d_8	1.24	2.5	12.4	24.7

[a]Each ampoule also contains 1 µL of methanol.

[b]Concentration is µg/L if the contents of one ampoule are added to a 500 mL water sample.

Table 2

Internal Standards for "Extractables"

	µg/ampoule = µg/L in H_2O[a]	
	Set No. 1	Set No. 2
o-Xylene-d_{10}	11.3	551
Nitrobenzene-d_5	519	2463
Naphthalene-d_8	95.0	383
Anthracene-d_{10}	41.1	40.0
Di-n-octyl ether-d_{34}	590	2561
Acridine-d_9	98.2	499
Phenylethylamine-d_4	10.0	517
Hexamethylenetetramine-d_{12}	98.8	500
Phenol-d_6	460	2134
Benzoic Acid-d_5	11.4	499
Bisphenol A-d_{16}	499	2502

[a]When added to 1 L of water.

Table 3

Internal Standards for "Intractables"

	µg/ampoule = µg/L in H_2O[a]	
	Set No. 1	Set No. 2
n-Butylamine-d_9	570	2058
n-Butyric Acid-d_7	51	2342
2-Naphthalenesulfonic Acid-d_7	99	501
n-Dodecyl Phosphate-d_{25}	484	2047
Ethanol-d_5	120	512
Acetonitrile-d_3	544	2709
t-Butanol-d_9	112	519

[a]When added to 1 L of water.

Synthesis of Labeled Compounds

Two labeled compounds, 2-naphthalenesulfonic acid-d_7 and mono-n-dodecyl-phosphoric acid-d_{25}, were synthesized. The preparation of the 2-naphthalenesulfonic acid-d_7 was briefly described in the previous report. Mono-n-dodecylphosphoric acid was prepared from the commercially available n-dodecyl alcohol-d_{26} according to the scheme:

$$CD_3(CD_2)_{11}OD \xrightarrow[\text{pyridine}]{(C_6H_5O)_2POCl} CD_3(CD_2)_{11}O\overset{O}{\overset{\|}{P}}(OC_6H_5)_2$$

or

$$\xrightarrow[HOAc]{H_2/Pt} CD_3(CD_2)_{11}O\overset{O}{\overset{\|}{P}}(OH)_2$$

The purity of the material was 98 percent as established by gas chromatography of the trimethylsilyl derivative. The impurity was identified as phosphoric acid.

Chemical and Isotopic Purity of Marker Compounds

Each compound was checked for purity by gas chromatography (GC) or liquid chromatography (LC) for quantitative data and also by mass spectrometry. The results are summarized in Table 4.

Isotopic purities shown in Table 5 were calculated from an average of six scans of the molecular ion cluster of the underivatized compounds except for: (1) bisphenol-A-d_{14} which was measured from the molecular ion of the trimethylsilyl derivative; (2) n-butyric acid-d_7, ethanol-d_5, and phenol-d_5 which were measured on the molecular ions of the material formed by the simultaneous introduction of the corresponding fully deuterated compound and a large excess of water into the source of the mass spectrometer; (3) di-n-octyl ether which was measured at m/z 130 ($C_8D_{17}^+$); (4) t-butanol-d_9 which was measured at m/z 64 ($C_4D_8^{+\cdot}$) at a resolution of 5200. This resolution is sufficient to eliminate interference from oxygen containing fragments. The t-butanol-d_9 was formed from t-butanol-d_{10} by the simultaneous introduction of a large excess of water.

Table 4

Chemical Purity of Marker Compounds

Compound	Chemical Purity	
	Quantitative Method	% Impurities
Acetonitrile-d_3	GC	<1%
Acridine-d_9	GC	<1%
Anisole-2,4,6-d_3	GC	<1%
Anthracene-d_{10}	GC	<1%
Benzoic-d_5 acid	GC	<1%
Bisphenol-A-d_{14}	LC	ND
Bromoethane-d_5	GC	<0.1%
t-Butanol-d_9	GC	ND
n-Butylamine-d_9	GC	ND
n-Butyric-d_7 acid	GC	<1%
Chlorobenzene-d_5	GC	ND
n-Decane-d_{22}	GC	ND
Diethyl ether-d_{10}	GC	ND
Di-n-octyl ether-d_{34}	GC	ND
Mono-n-dodecylphosphate-d_{25}	GC[a]	<2%
Ethanol-d_5	GC	<1%
Hexamethylenetetramine-d_{12}	GC	ND
Naphthalene-d_8	GC	ND
2-Naphthalenesulfonic acid-d_7	LC	<1%
Nitrobenzene-d_5	GC	ND
2-Phenylethyl-1,1,2,2-d_4-amine	GC	ND
Phenol-d_5	GC	ND
o-Xylene-d_{10}	GC	ND

[a]As the trimethylsilyl derivative.

ND = non-detected

Table 5

Isotopic Purity of Marker Compounds

Compound	No. of Deuterium Atoms Present in Compound: As Supplied	No. of Deuterium Atoms Present in Compound: After Exchange[a]	Atom % Deuterium[b]	Mole % Completely Labeled[b]
Acetonitrile-d_3	3	3	99.3	98
Acridine-d_9	9	9	96.7	71
Anisole-2,4,6-d_3	3	3	96.1	88
Anthracene-d_{10}	10	10	99.4	94
Benzoic-d_5 acid	5	5	99.4	97
Bisphenol-A-d_{14}	16	14	98.6	81
Bromoethane-d_5	5	5	99.3	97
t-Butanol-d_9	10	9	99.5	94
n-Butylamine-d_9	9	9	99.3	94
n-Butyric-d_7 acid	7	7	99.3	95
Chlorobenzene-d_5	5	5	99.4	97
n-Decane-d_{22}	22	22	99.4	87
Diethyl ether-d_{10}	10	10	99.6	96
Di-n-octyl ether-d_{34}	34	34	99.7	94
Mono-n-dodecylphosphate-d_{25}	25	25	99.4	85
Ethanol-d_5	6	5	99.0	95
Hexamethylenetetramine-d_{12}	12	12	99.8	98
Naphthalene-d_8	8	8	98.6	89
2-Naphthalenesulfonic acid-d_7	7	7	98.6	87
Nitrobenzene-d_5	5	5	99.0	95
2-Phenylethyl-1,1,2,2-d_4-amine	4	4	99.2	97
Phenol-d_5	6	5	98.5	92
o-Xylene-d_{10}	10	10	99.4	94

[a]As used for spectra.

[b]For labeled positions after exchange.

Mass Spectra

Electron impact mass spectra at 70 eV were recorded for each marker compound in the labeled form expected to be recovered from aqueous solution with the exception of mono-n-dodecylphosphoric acid-d_{25} which did not give a mass spectrum representative of intact material. The mass spectrum of mono-n-dodecylphosphoric acid-d_{25} as the trimethylsilyl derivative was recorded. The complete mass spectra in both tabular and bar graph form are reported in NBS Interagency Report 80-2160, "The Mass Spectra and Isotopic Purity of Compounds Proposed for Use in the 'Master Analytical Scheme for the Analysis of Organic Compounds in Water,'" by E. White V, M. J. Welch, and H. S. Hertz.

Procedures for the Preparation of Internal Standard Solutions of Marker Compounds

"Purgeables". A small serum vial (approximately 1 cm diameter x 2 cm high)[1] was weighed to the nearest 0.01 mg on a semi-micro balance. Approximately 6 mg naphthalene was weighed into the vial. A circle of aluminum foil was put over the top followed by a liner of Teflon bonded to silicone rubber. An aluminum cap was crimped over these liners. The vial was weighed, 500 µL methanol was added through the septum with a syringe, and the vial reweighed. (A separate test of the weight loss of methanol was made under these weighing conditions and it was found to be 0.01 mg/min.) The remaining compounds were added by filling a syringe with the required volume, adding to the weighed vial through the septum, and reweighing the vial and its contents. Least volatile materials were added first. The order was decane, anisole, chlorobenzene, bromoethane, and diethyl ether. After all constituents were weighed in, the solution was mixed.

The dilute solution was prepared by a weighed dilution of the concentrated solution. A clean vial was capped as before, weighed, 450 µL of methanol was added through the septum by syringe, and vial and contents weighed. Then 50 µL of the concentrated solution was added, and vial and

---

[1]The small vials used for weighing were 1 mL Reaction Vessels, Cat. No. 3-3123, Supelco. Since the vials were too long to be used easily for filling 1-µL Microcaps, the vials were shortened from a length of about 3.2 cm to a length of 2 cm.

contents reweighed and then mixed. The remaining concentrated solution was put into a clean glass ampoule and sealed until needed, at which time it was transferred to a small serum vial.

To ampoule either solution, the vial was capped with aluminum foil only, 1-μL Microcaps were filled with the solution through a small hole in the cap, put into a melting point tube[2] already sealed on one end, and then the remaining end was sealed. Tweezers were used to handle the Microcaps.

In order to minimize concentration changes, the steps needed for ampouling were done as rapidly as possible. It took 35 minutes to aliquot and seal 100 samples.

The approximate amounts to be weighed for the preparation of the concentrated solution were as follows:

Naphthalene	6.25 mg
Decane	6.25 mg = 8.56 μL
Anisole	6.25 mg = 6.31 μL
Chlorobenzene	0.62_5 mg = 0.56 μL
Bromoethane	0.62_5 mg = 0.45 μL
Diethyl ether	6.25 mg = 8.83 μL

The concentration data for the two sets, prepared in April 1980, by the above procedures are shown in Table 1.

A total of 52 ampoules of Set No. 1 and 60 ampoules of Set No. 2 were delivered. Additional ampoules were held at NBS for stability studies.

"Extractable". Solutions for the preparation of the ampoules of internal standards for "extractable" samples were made by weight. For each set, solids were weighed and placed into an approximately 500 mL flask. Liquids were weighed by syringe, weighing the full and empty syringe. The required amount of methanol was added by pipet and the amount added checked by weight. After mixing the solution, 5 mL amounts were dispersed with a Micro-Medic automatic pipetter into 10 mL glass ampoules, which were then sealed.

[2]The melting point capillaries were cleaned before use. They were placed in a clean separatory funnel, HPLC grade methanol was added to cover the tubes, the tubes were filled by applying a vacuum, then inverted, refilled, and emptied. This process was repeated. The tubes were then dried in a vacuum oven at 7 Pa (0.05 mm Hg) and 140 °C, for 48 hours.

The concentration data for the two sets, prepared in May 1980, are shown in Table 2.

A total of 68 ampoules of Set No. 1 and 54 ampoules of Set No. 2 were delivered. Additional ampoules were held at NBS for stability studies.

"Intractables". Solutions for the preparation of the ampoules of internal standards for "intractable" samples were made by weight. For each set, n-butylamine-d_9 and dodecyl phosphate-d_{25} were weighed first and dissolved in distilled water before the addition of the other labeled materials. Liquids were weighed by syringe, weighing the full and empty syringe. The required amount of water was added by pipet, and the amount checked by weight. After mixing each solution, 7.5 ml (Set 1) or 10 mL (Set 2) amounts were dispensed with a Micro-Medic automatic pipetter into 10 mL glass ampoules, which were then sealed.

The concentration data for the two sets, prepared in June 1980, are shown in Table 3.

A total of 68 ampoules of Set No. 1 and 116 ampoules of Set No. 2 were delivered. Additional ampoules were held at NBS for stability studies.

Stability of Marker Compound Solutions

Accelerated Aging Studies. Although the time between the final decision on the constituents for the marker compound internal standard solutions and the required delivery did not permit extensive stability testing, it was recognized that some of the compounds, when stored in the mixtures, might react with other constituents or lose deuterium by exchange. As a consequence, several test mixtures similar to the "extractable" and "intractable" internal standards, but simplified and of undeuterated compounds in deuterated solvents, were prepared and subjected to conditions to accelerate aging. These solutions were examined by nuclear magnetic resonance spectroscopy. For the surrogate "extractable" standard decreases in the concentration of hexamethylenetetra-

mine and phenol were observed, but the rates were such that properly stored (0-5 °C) mixtures were expected to be usable for the several months required. A surrogate "intractable" standard containing acetonitrile, dodecylphosphoric acid, butyric acid, and a tertiary amine base showed no change.

Stability. Ampoules from all six internal standard mixtures prepared have been stored at 0-5 °C. Selected ampoules are periodically removed and the concentrations of individual components checked by gas or liquid chromatography. Initial results are encouraging, but the testing is not yet complete.

1.b. Liquid Chromatography - Mass Spectrometry

Coupling liquid chromatography (LC) and mass spectrometry (MS) has most widely been achieved by two methods. One operates by splitting off a small fraction of the LC stream and introducing it directly into the high vacuum of the MS. Another employs a moving belt onto which the stream is evaporated. The belt then moves into the high vacuum region where the solutes are desorbed.

The interface which we are developing is an attempt to combine advantages of both methods; the simplicity of direct liquid injection together with the solute preconcentration of the moving belt technique. Preconcentration of the LC stream is achieved by allowing it to flow down a heated wire where 90-95 percent of the solvent is evaporated. A portion of the residual liquid is admitted to the high vacuum through a probe which is, in essence, a miniature needle valve. Our early efforts were concentrated on development of the heated wire and its controls, and on the construction of a probe which would give a steady, uniform spray of liquid droplets into the ion source of the MS. A slightly unsteady or intermittent spray gives rise to very noisy signals from the MS.

A patent application covering the device has been approved and a paper describing it has been accepted for publication in ANALYTICAL CHEMISTRY. A preprint of the latter is appended.

Normal-Phase LC/MS Experiments:

Encouraged by the stability of the spray of hydrocarbon solvents from the LC/MS probe, we initiated experiments to make quantitative measurements. The determination of phenol and o-cresol in shale oil ordinarily requires several steps: extraction followed by GC or GC/MS quantitation. It was found to be possible to quantitate these materials directly by LC/MS, using either external standards or the method of standard addition, monitoring m/z = 94 (phenol) or m/z = 108 (cresols). One μL of undiluted shale oil was injected. Even with so volatile a compound as phenol, it was found that the concentrator device gave a six-fold concentration enhancement. Standard deviations of the determined values were about 10 percent, and the means were within about 10 percent of the certified concentrations of about 400 ppm. A UV trace and single ion record for the phenol determination are shown in Figure 1.

Reversed-Phase LC/MS Experiments:

Considerable difficulty was encountered in getting droplets to detach from the probe tip when solvents containing large concentrations of water were used.

In an attempt to get a more uniform spray of water-containing solvents, a new probe was constructed. This used a threaded cap to retain a replaceable seat against the end of the probe. The orifice was formed by allowing a tungsten wire to pierce the seat material. Seats tried were aluminum and gold foils, mylar, teflon, TFE-100X, Kapton, and poly(vinylidene fluoride). The latter seems to have the most satisfactory mechanical properties.

Owing to the high surface tension and high heat of vaporization of water, it does not explosively vaporize into the vacuum as do the hydrocarbon solvents. Also, our design does not permit application of increased pressure to the stream to impart sufficient momentum to detach droplets. Therefore, a concentric tube was added through which a nebulizing gas (e.g., argon or methane) could be passed. With this system, it was possible to get molecular

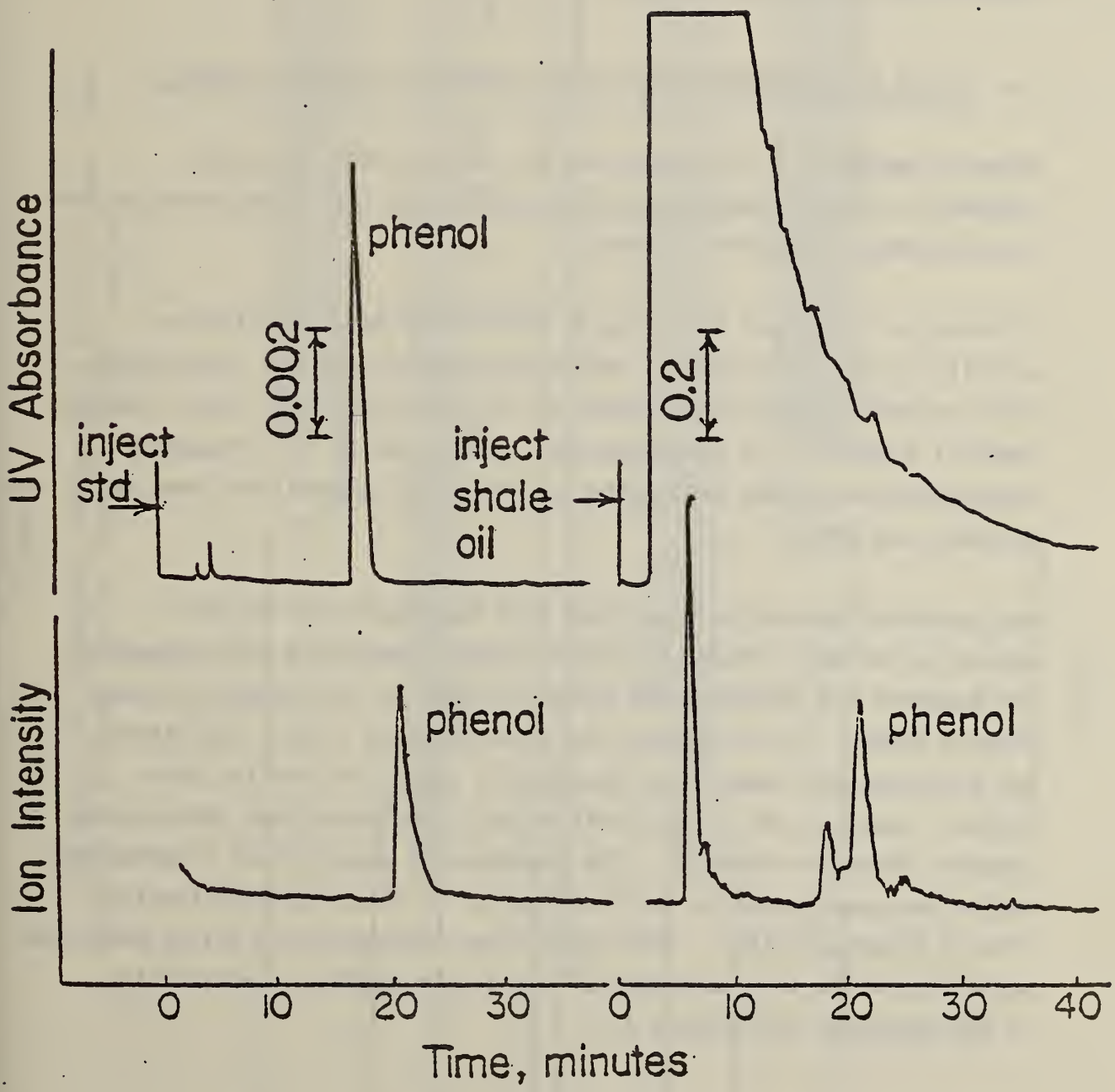

Figure 1 Chromatogram of shale oil obtained during phenol quantitation. Upper trace: ultraviolet detector recording at 254 nm. Lower trace: single ion record at m/z 94.

ions of the non-volatile compound adenosine. This apparatus is shown in Figure 2.

The results obtained from these experiments were encouraging, but not optimum for this system. A number of experiements with the LC/MS probe were planned for the near future; however, timely implementation of these plans may be hampered due to lack of funding.

1.c. Liquid Chromatography with Electrochemical Detection (LC-EC)

Research emphasis in this past year has been focused on the development of new chromatographic separations and the optimization of the electrochemical detector response.

Following a literature survey by A. Cohen (NBS/CAC), the electroactivity of over 30 currently used organic pesticides was investigated using current-sampled polarography to provide a basis for their electrochemical detection. A chromatographic separation of six frequently encountered pesticides (including parathion and guthion) has been developed (see Figure 3).

Many possible separation conditions have been evaluated for the separation of the cationic organotin species, employing such methods as ion exchange and reverse-phase chromatography in the presence of complexing agents. Little success has been obtained in this laboratory, but Brinckman and Jewett have developed a separation for the monocationic species, and this separation was used to evaluate the electrochemical detection approach. The amperometric detection of triphenyltin cation was complicated by the formation of an electrode deactivating film of hexaphenylditin. This problem was overcome using pulsed detection wave-forms which take advantage of the electrochemical reversibility of the reduction (see Figure 4).

Figure 2

New probe for concentric admission of atomizing gas. The diaphragms (shaded) are of poly(vinylidene fluoride).

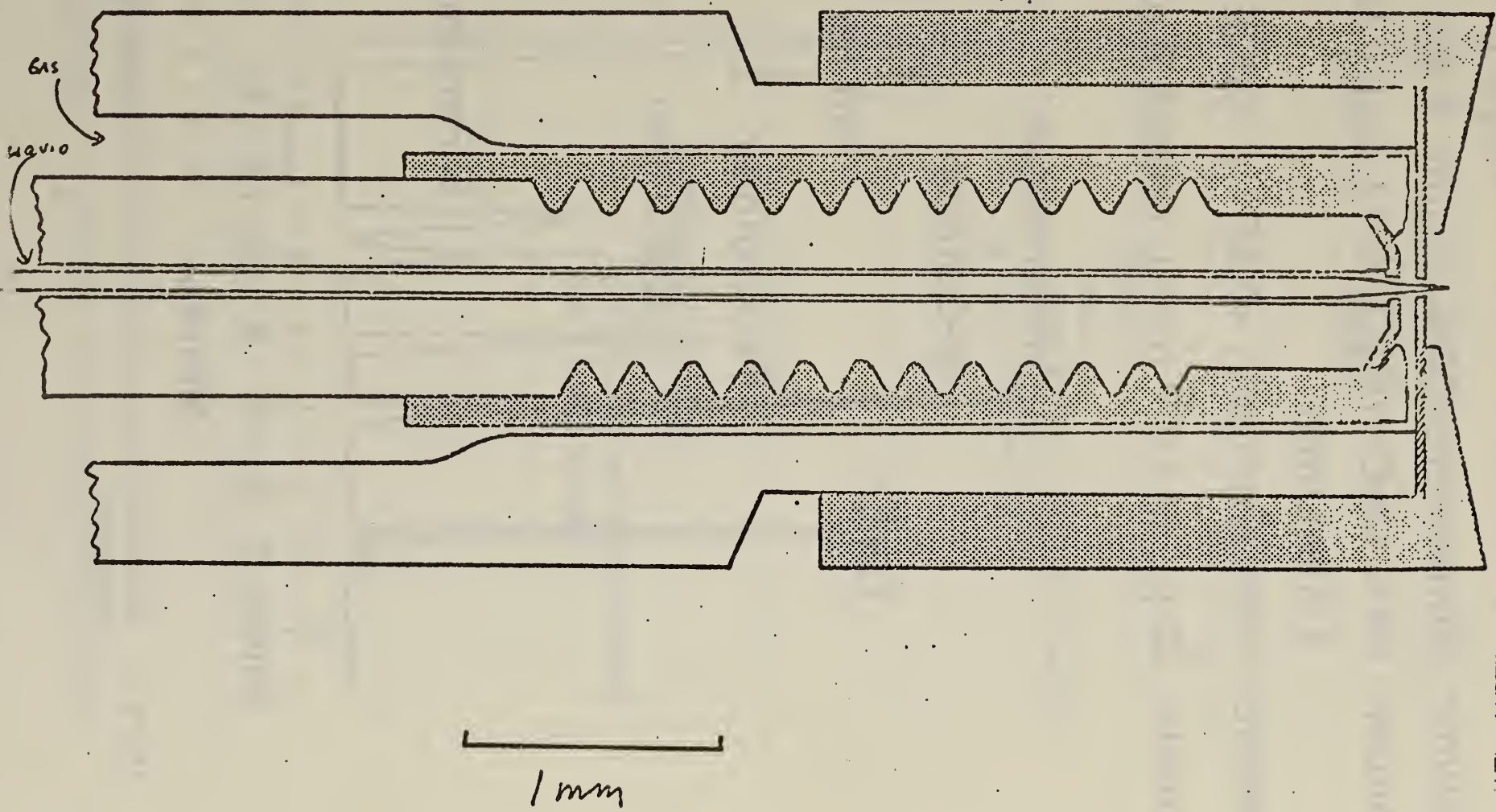

SEPARATION OF SOME INSECTICIDES

Column: Spherisorb ODS, 5 µm, 4.6 x 250 mm

Soluent: 60% MeOH/H_2O, 0.12 mol/L NH_4OAc

1.5 mL/min

Detector: Amperometry, -0.85 V, HMDE

Sample: 20 µL of 10^{-5} mol/L (about 3 ppm) of each

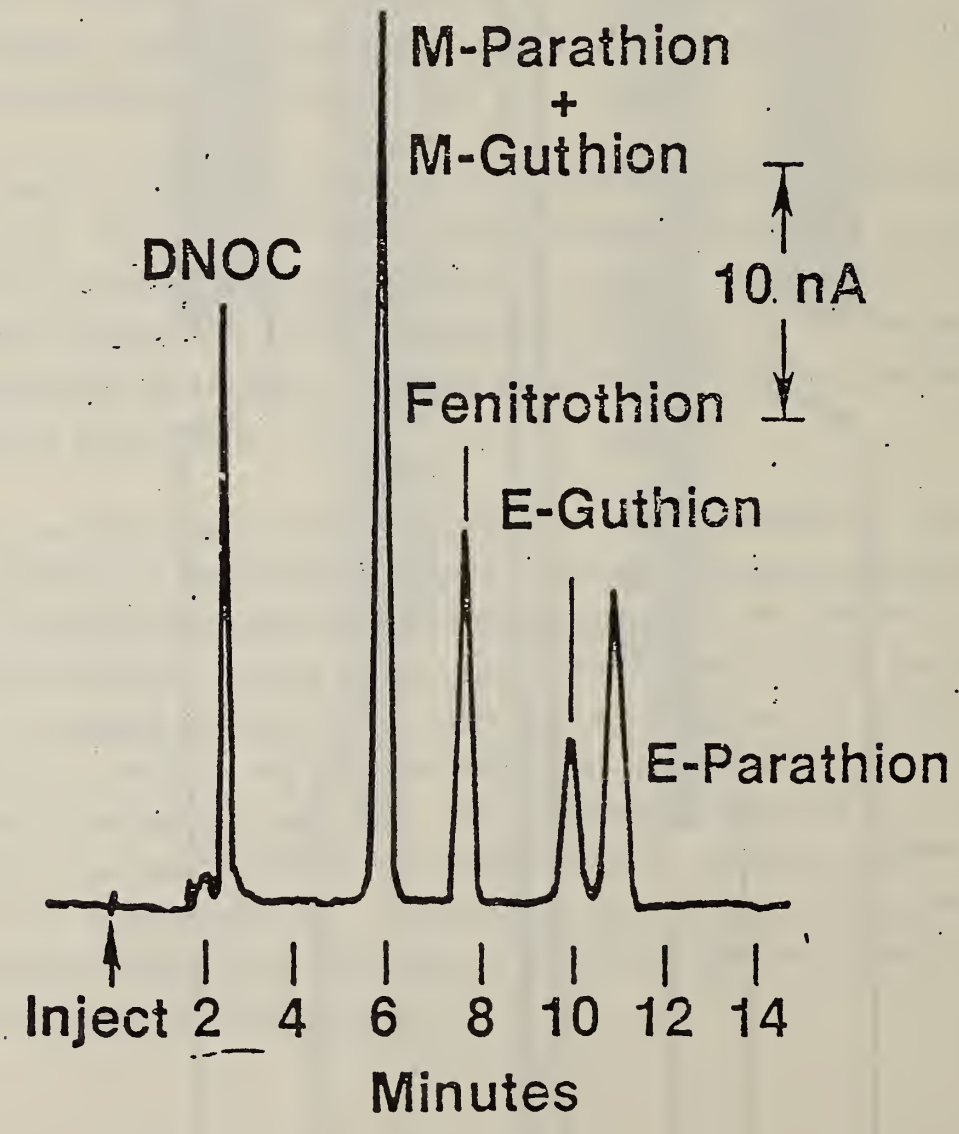

Figure 3. Reverse-phase insecticide separation employing amperometric detection.

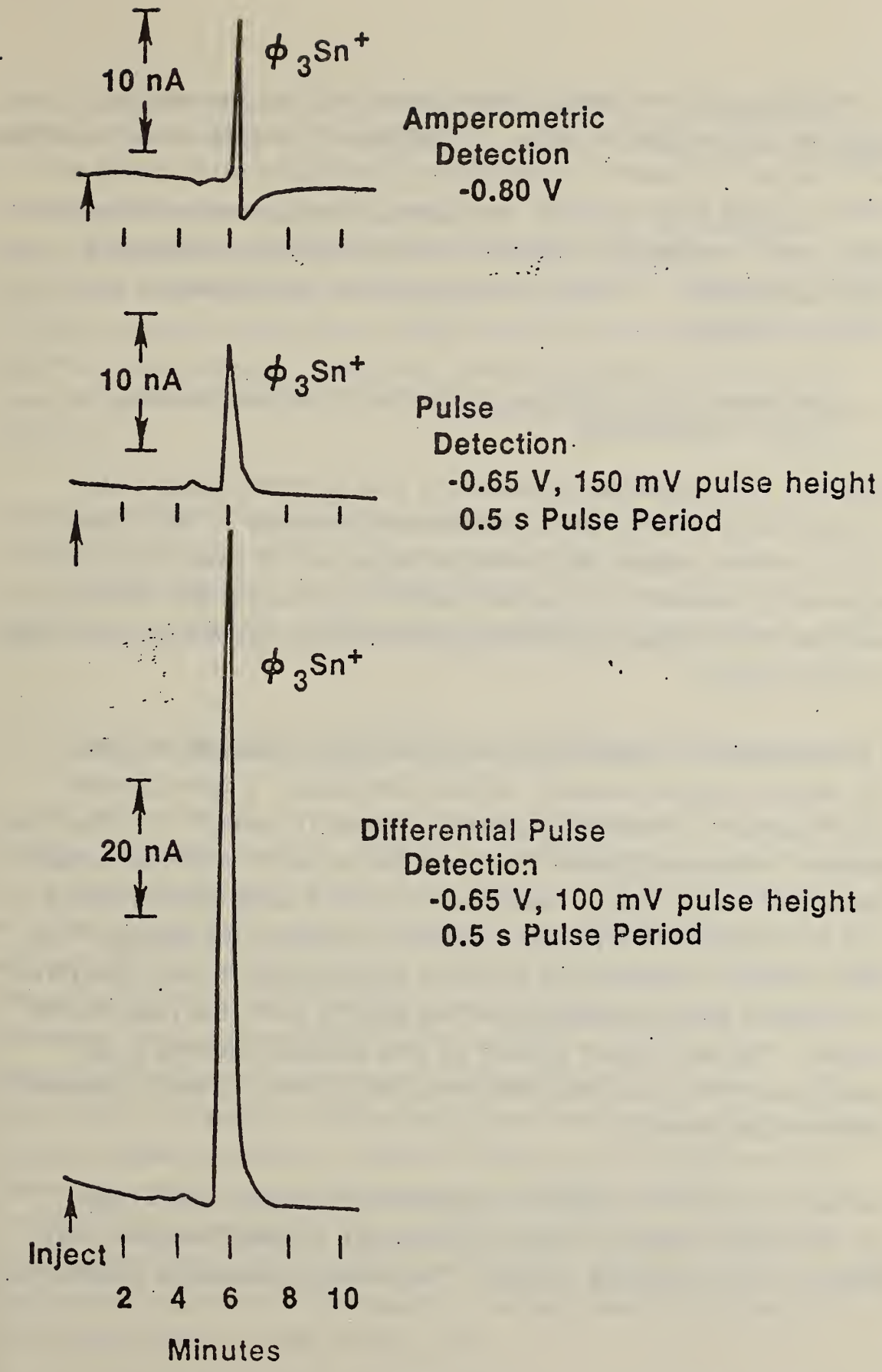

Figure 4 . Detection of triphenyltin cation using different detector waveforms.

A comparison has been made of several materials for the working electrode of the detector cell. A dropping and hanging mercury electrode cell, as well as several solid-electrode thin-layer cells (based on mercury-coated gold, platinum, and glassy carbon), were evaluated for their negative potential range and detection limits for reducible organic pesticides. A manuscript on LC-EC has been submitted to Analytical Chemistry.

Development of a High-Sensitivity Dual-Electrode Detector for Liquid Chromatography

Reductive electrochemical detection in liquid chromatography (LC) is potentially a very powerful measurement technique in the determination of trace organic pollutants by virtue of its sensitivity and selectivity. However, for the best sensitivity, oxygen exclusion is required. This makes the technique cumbersome to use and has restricted its application.

A new approach for reductive LC detection that eliminates the need for complete oxygen exclusion has been developed. A two-electrode, thin-layer cell is used in a manner conceptually similar to a ring-disc system. Two closely spaced electrodes are poised at different potentials. The first electrode encountered by the flowing electrolyte is held at a potential sufficiently negative to reduce the analyte. The second detector electrode is held at a potential sufficiently positive to reoxidize the generated species and also to avoid the reduction of oxygen. The low residual current at this potential assures a low background noise, upon which the analytical current is easily measured with high sensitivity.

The best analytical response is obtained for analytes that either are reversibly reduced or that have chemical followup reactions that generate easily oxidized products. The reductive/oxidative behavior of

three important industrial/environmental pollutants - nitrobenzene, dichlone, and tributyltin - have been studied by reverse pulse voltammetry.

The sensitivity and linearity of the dual electrode technique has been evaluated by comparison to direct reductive detection. Two chromatograms with equal concentrations are pictured in figure 5. The baseline noise of direct reductive detection without use of an inert atmosphere box is apparent (upper figure). The lower chromatogram shows the very low baseline noise of the dual electrode approach achieved with a minimum of difficulty.

Current experiments involve the evaluation of the technique's selectivity by application to the measurement of organic analytes in environmental samples. Also, investigation is in progress on the use of modulated waveforms and phase selective detection to improve selectivity.

1.d. Interferences in the Inductively Coupled Plasma (ICP) Technique

In the application of the ICP technique to high-accuracy analysis of Standard Reference Materials (SRM's), interferences have been found which can degrade the quality of analytical results. These interferences can be traced to spectral and matrix-related interactions which must be characterized and corrected for in order to minimize their effect. The problem of spectral interference in the ICP technique is well known. Procedures for background and spectral overlap corrections have been established and are presently being employed in this laboratory. The first step is to expose a photographic plate with spectra of the sample and pure-element standards. Spectral lines are then chosen from considerations of sensitivity and absence of spectral overlap. The exit-slit carriage is mounted on the microdensitometer with the reference photographic plate, and slits are positioned in alignment with the chosen lines on the plate. Final alignment is accomplished by adjustment of a refractor plate in front of each slit.

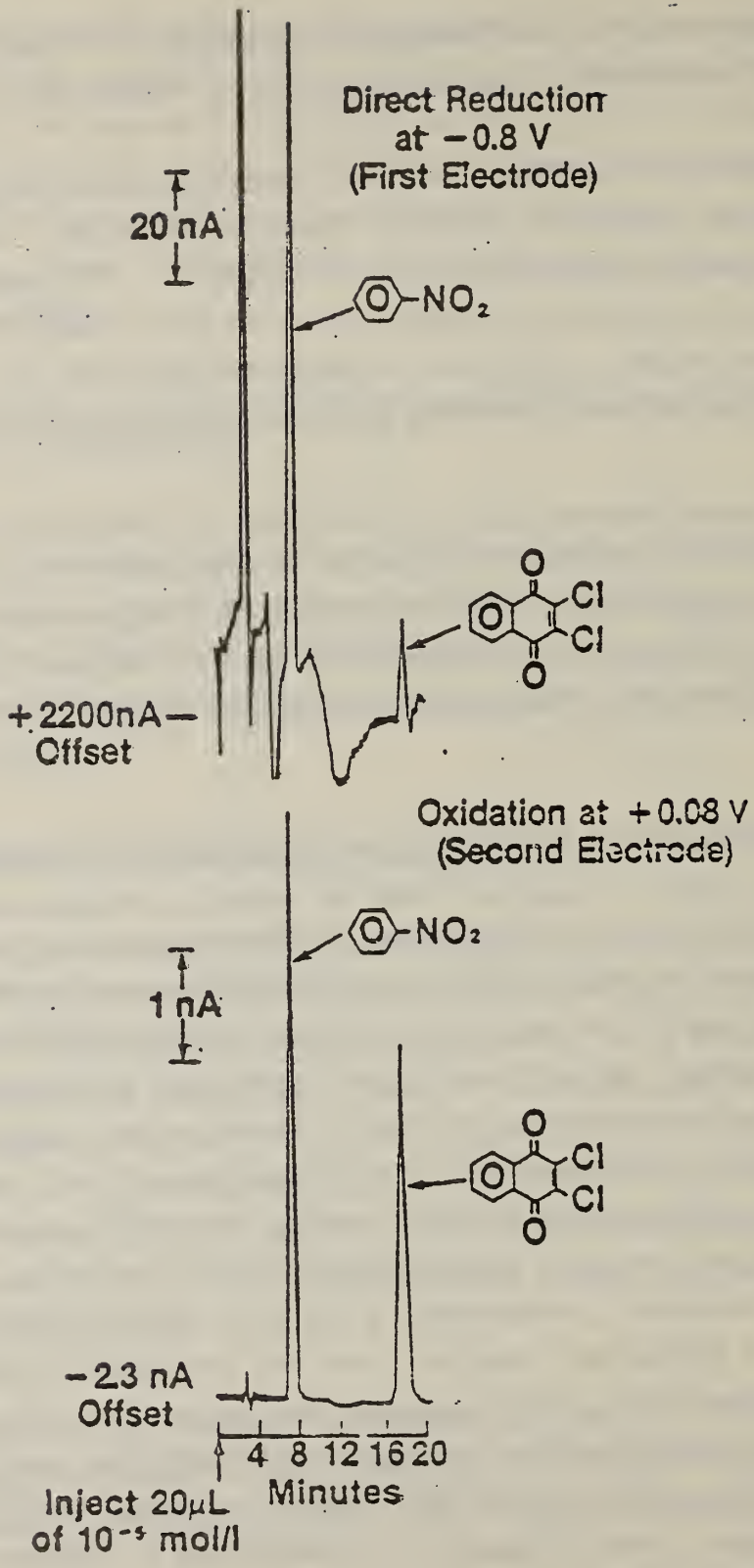

Figure 5. Different Reductive Detection Modes. Conditions: Analytes--1.0×10^{-5} mol/L of nitrobenzene and dichlone; Solvent--60 percent MeOH/H_2O, 0.1 mol/L NH_4OAc pH 5.2 at 1.0 mL/minute; Column--Whatman Partisil PXS 5 µm. Upper figure--direct reductive detection at -0.8 V without enclosure of the LC in an inert atmosphere box. Lower figure--dual electrode detection, -0.8 V on generator electrode, -0.08 V on detector electrode.

A wavelength scan of each element is stored in the computer for output on the terminal. From plots of intensity-versus-wavelength for each element, the spectral peak position is checked and background correction points on either side of the peak are chosen. Spectral scanning and background sampling are accomplished by computer-controlled rotation of a refractor plate positioned behind the spectrometer entrance slit. In this manner, true net intensities for the spectral lines are calculated and either stored in the computer for calibration or displayed on the terminal.

Evidence has been found indicating differences in analytical response between pure-element standards and samples of complex matrices which are not due to spectral interference. These effects become significant when applying the ICP technique to high-accuracy analysis of SRM's. Chemical matrix effects in the plasma itself can cause up to fifteen percent relative enhancement or depression of the analyte element intensity depending on the spectral line and plasma operating conditions. Complete definition of the problem has involved examination of compromise conditions for simultaneous multielement analysis both from the point of view of sensitivity as well as matrix effect suppression.

One way to estimate a suspected matrix effect is to record net intensities for various elements at constant concentrations, with and without an excess (3000 μg/mL) of potassium present. The ratio of intensity with potassium to intensity without potassium can be plotted with respect to an instrument variable such as power, or observation height. The objective is to find operating conditions which result in a ratio close to 1.00 without significantly affecting the signal-to-background ratio. At present, no serious degradation in signal-to-background ratio has been caused by tuning the ICP for minimum matrix effect. However, the data include only five elements thus far; therefore the results must be considered to be preliminary. These data, as well as extension to additional elements and matrices, will provide the information necessary to minimize analytical bias in simultaneous multi-element analysis using the ICP techniques.

1.e Metal Speciation Using High Performance Liquid Chromatography/Atomic Absorption Spectrometry

During recent years it has become increasingly apparent that total metal data alone may not provide complete and accurate descriptions of the complicated roles which many metals play in our ecosystem. It is generally believed that alkylated forms of certain metals (e.g., Hg, Pb, and Se) are much more toxic than the inorganic salts of the metals or even the metals themselves. Some microorganisms are capable of chemically and biochemically transforming certain toxic elements into more toxic organometallic compounds which may then be released into the environment. Additionally, chemical speciation of trace metals can be a real problem in defining nutrient composition of foods because the biological activity of a metal such as chromium or iron depends on the chemical species to which the metal is bound.

The rapidly increasing interest in metal speciation in diverse scientific disciplines has prompted the immediate need for development of analytical instrumentation which allows the determination of not only the total metal content but also the different chemical forms in which the metal may be distributed. Atomic spectrometric techniques (absorption, emission, and fluorescence) have long been regarded as being sensitive and metal-specific spectrochemical technqiues for total metal analyses are limited in their ability to differentiate between various chemical forms of the metal within the sample. Chromatographic techniques can be successfully employed to separate various chemical forms of the analyte, but poor detector specificity frequently limits their analytical utility when highly complex mixtures are encountered. However, interfacing chromatographic and atomic spectroscopic instrumentation into a single analytical hybrid system which has the combined advantages of both techniques presents a viable means of potentially solving analytical problems which otherwise would not be possible by either individual technique.

In an effort to gain more knowledge about the metal distribution in complex matrices, an investigation has been undertaken using the combined instrumentation of a flame atomic absorption spectrometer interfaced to sample the mobile phase exiting at the outlet of the analytical column of a high performance liquid chromatograph (HPLC). To demonstrate the analytical feasibility of HPLC/AAS for molecular characterization of metals in complex matrices, tetraalkyl lead (TAL) compounds were determined directly in gasoline. Baseline resolution of the TAL mixture consisting of tetramethyl lead (TML), trimethyl ethyl lead (TMEL), dimethyl diethyl lead (DMDEL), methyl triethyl lead (MTEL), and tetraethyl lead (TEL) was effected by reverse-phase HPLC using a 70 percent acetonitrile (CH_3CN)/30 percent H_2O mobile phase. The eluted tetraalkyl lead species were then sequentially atomized in an air/ acetylene flame. The lead absorbance for each TAL compound was measured by atomic absorption spectrometry using the 283.3. nm lead resonance line. Analyses were conducted free of spectral interferences. Detection limits for lead by this hybrid technique were about 10 ng for each TAL compound. Using our instrumental configuration and analytical conditions, the 5 tetraalkyl lead compounds were separated and detected in less than 10 minutes. A number of different commercial gasolines were analyzed for their tetraalkyl lead content. The TAL distribution was found to vary widely among manufacturers.

Atomic absorption spectrometry has been compared in terms of analytical performance to UV absorbance spectrophotometry as a detector for HPLC for the determination of tetraalkyl lead compounds in petroleum refinery products. Preliminary data indicate that for certain applications the metal-specific AA detector is more analytically useful as an HPLC detector than UV absorbance spectrophotometry for the study of different metal species in complex matrices. In some cases, the UV absorbance detector is severely plagued by spectral interference at 254 nm due to coeluting aliphatic, olefinic, and aromatic hydrocarbons of the gasoline matrix which absorb at this wavelength. As shown in figure 6, a clean chromatograph of tetraalkyl lead compounds in gasoline is obtained with

Direct Determination of Tetraalkyl Lead Compounds in Gasoline by Reverse-Phase HPLC

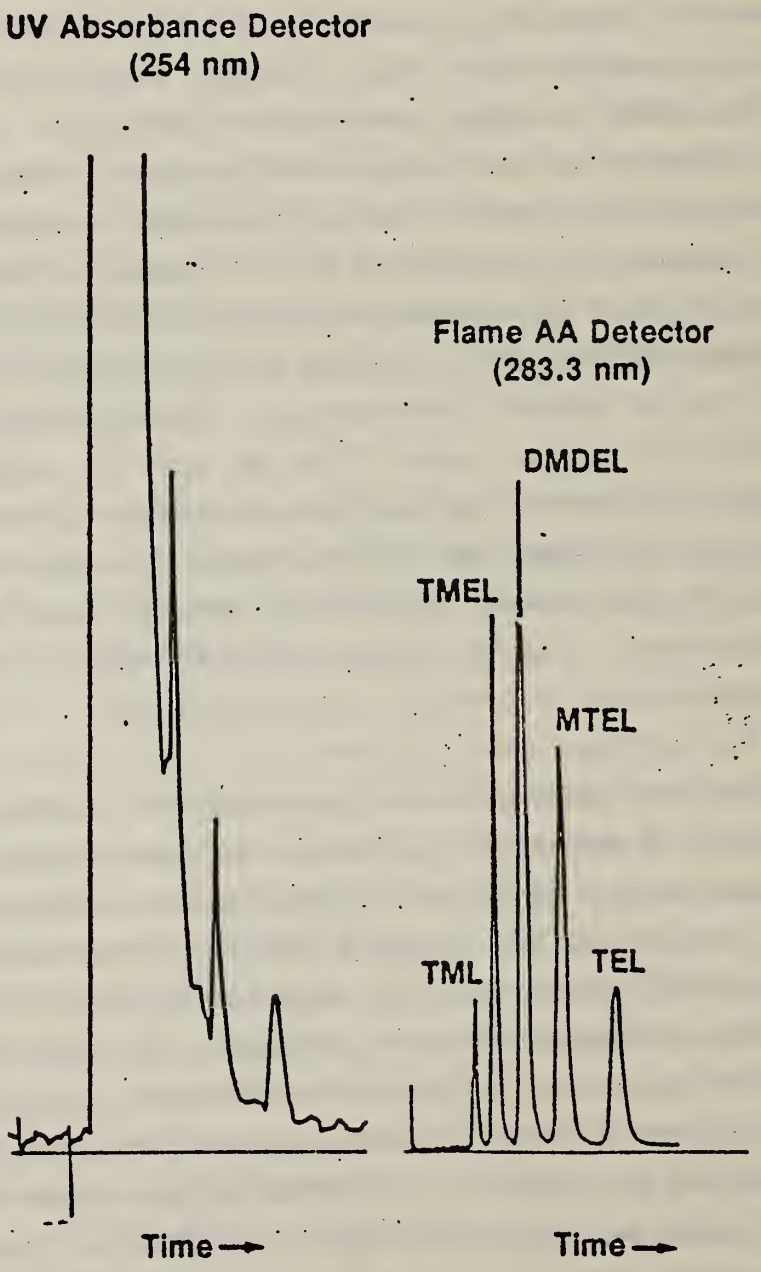

Figure 6

the AA detector because it responds to only lead-containing compounds at the 283.3 nm line.

In order to improve the analytical performance of the HPLC/AAS system described in this preliminary report, it is necessary to optimize the chromatographic conditions and to decrease the dead volume present between the column and the detection system. In addition, the detection limits can be significantly lowered by using a flameless atomic reservoir.

The HPLC/AAS technique can be easily extended to the determination of different organometallic compounds in diverse matrices by simply tuning the monochromator to the analytical line of the metal of interest. This inherent specificity of AAS cannot be realized by existing commercial HPLC spectroscopic detectors. Moreover, the specificity of AAS considerably relaxes the constraints of the analytical conditions required for the separation. With AAS, only the compounds containing the metal of interest need to be separated from one another; the metal-containing compounds need not necessarily be separated from the sample matrix.

1.f. Sulfur Speciation in Coal

This methodology is based on the measurement of the characteristic vaporization temperatures at atmospheric pressure of the various forms of sulfur, using plasma emission spectrometry to monitor each vaporized sulfur species. The resulting spectrometric thermogram consists of a series of relatively broad peaks, each peak being a different sulfur species.

For this experiment, the 190.027 nm sulfur atomic emission line was used with a HTV R-919 photomultiplier tube and a one-meter monochromator with air purging. This system, using the 190.027 nm line can detect 100 μg of sulfur. If air is purged and the 182.625 nm line is used, the detection limit can be lowered to 5 μg. Previously, three sulfur species in coal

have been reported in the literature, pyritic sulfur (FeS_2), sulfate sulfur ($FeSO_4$), and an "organic" sulfur. In the present experiments, sulfur and iron emission intensities were monitored as a function of temperature.

From these experiments, four sulfur species have been found, FeS_2, $FeSO_4$, organic sulfur, and a low evaporation temperature sulfur. This low evaporation temperature sulfur starts to evaporate at 28 °C. SRM 1635 Western Coal has been found to contain about 18 times more of this species than SRM 1632a Penn Coal. Also, organic sulfur has been found to be linked with iron. In a previously described analytical technique, organic sulfur was calculated by substracting pyritic and sulfate sulfur from the total. Therefore, the value obtained from the "organic" sulfur species included the low evaporation temperature sulfur. In the future, an attempt will be made to identify the chemical forms of these species using thermal separation and a cold trap collection technique. Also, an investigation will be undertaken in which two monochromators are used simultaneously to detect both sulfur and iron or any other elements which may be bound with sulfur.

Sulfur species analysis still needs work on the development of a standardization procedure, but it is a simple technique and has potential for the direct determination of each species present.

1.g. Ionic Chromium Speciation Measurements

An anion-exchange method has been developed for the separation of trivalent and hexavalent forms of chromium in synthetic aqueous solutions. The aqueous sample is made 1N in HCl and is then introduced onto the anion-exchange column. In a 1N HCl medium, Cr (III) elutes from the column while Cr (VI) is adsorbed by the active sites of the anion-

exchange resin. After Cr (III) has eluted from the column, a solution of 1N ascorbic acid in 1N HCl is added to the column which then reduces the Cr (VI) species to Cr (III) species directly on the column. The newly-formed Cr (III) species are then eluted from the column as in the first part of the procedure. Atomic absorption spectrometry is used for on-line detection of the chromium species as they elute from the column. The aspiration uptake capillary of the AAS nebulizer is replaced by a Teflon microsampling cup. The anion-exchange column is positioned so that the eluent drops directly into the microsampling cup for continuous nebulization and atomization of the sample. A chromatogram which illustrates the direct speciation of trivalent and hexavalent chromium by ion exchange-atomic absorption spectrometry (IE-AAS) is shown in Figure 7.

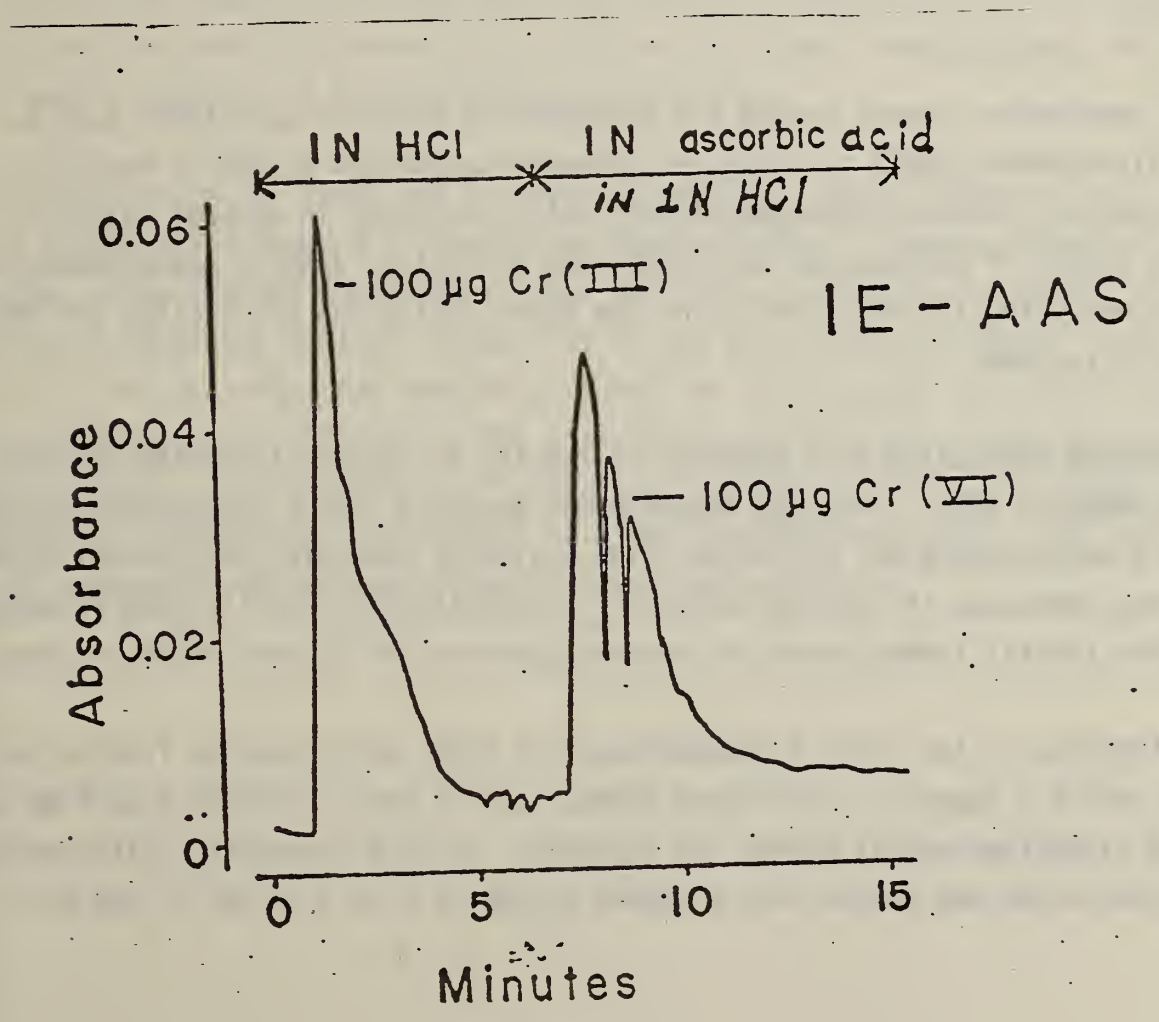

Figure 7

2. Development of Measurement Methods for Non-Volatile Organic Pollutants in Water Due to Energy Technologies

2.a. Fluoroimmunoassay Procedure Developed for Dinitrophenols in Water

Detection of trace amounts of the toxic pollutant 2,4-dinitrophenol in water is an analytical problem that presents many challenges to the analytical chemist. Laboratory investigations have shown that gas chromatography and high-performance liquid chromatography, while suited for analytical determinations of most of the toxic pollutants, are not as efficient in the separation and identification of the nitrophenols. The development of an immunochemical procedure for detection and quantitation of dinitrophenols in water has been the focus of efforts during 1980.

In developing a model system for detection of priority pollutants such as dinitrophenols (DNP) in water, we prepared conjugates of DNP by reacting proteins, 2,4-dinitrobenzenesulfonic acid, and K_2CO_3 in aqueous solution. The extent of conjugation was calculated by optical density measurements at 360 nm, using 17,350 at pH 7.4 as the molar extinction coefficient for DNP-lysyl residues.

Selected conjugates were injected in rabbits at monthly intervals beginning in February 1980. Antibody response was measured versus homologous conjugates in a micro-double-gel diffusion slide system by observing the precipitation lines developed in the agar matrix. The rabbits were finally bled 25 weeks after initial immunization via cardiac puncture for optimal yield of serum.

Antibodies in the form of immunoglobulin G (IgG) were obtained from serum by use of a beaded, cross-linked agarose gel to which Cibicron Blue F3GA dye and diethylaminoethyl groups are attached. In this procedure, buffer-equilibrated serum was passed over a packed column (2.0 cm x 18 cm) of the gel.

Protease-free IgG was obtained as the first peak eluted with a wash of the starting buffer. To obtain a specific solid-phase binding reagent for assay purposes, the purified IgG was covalently bound to hydrophilic polyacrylamide beads, 5-10 μm in diameter.

For assay purposes, we have focused our research efforts on fluorimmunoassay rather than radioimmunoassay. The use of a fluorescently-labeled ligand in a fluoroimmunoassay has the advantage of longer shelf life, less expensive instrumentation, ease of counting, and less stringent disposal procedures. In fact, the use of fluorescence labels in immunoassays has the potential to replace many existing radioimmunoassay procedures. The fluorescent ligand we first used in the assay system was a complex of 2,4-dinitrobenzenesulfonic acid and 5-[(4,6-dichlorotriazin-2-yl)-amino]fluorescein hydrochloride. While having adequate fluorescent activity, specific binding was low. More recently, labeled ligands have been developed by (a) reacting 2,4-dinitrobenzenesulfonyl chloride with fluorescein isothiocyanate (FITC) in anhydrous pyridine and isolating the reaction product by exclusion gel column chromatography, or (b) double labeling of RSA with DNP and with FITC.

Characterization of ligand (a) is still in progress, while ligand (b) has been successfully used in a competitive binding assay. Current detection limits are at the 100 microgram/L level for DNP in water. To be useful in pollution analysis, sensitivity must be in the submicrogram/L level. Sensitivity of this order has been established for immunoassays in clinical use. By combining the specificity of the assay with capabilities of concentrating dinitrophenols with an affinity "accumulator" column, detection of ultra-trace amounts of dinitrophenol pollutants in water should be achieved. This will be of importance in the monitoring of industrial effluents.

2.b. Development of a Fourier Transform Infrared Spectrometer-Gas Chromatograph Interface and Its Application to Pollutant Identification

Installation of a Nicolet 7000 Fourier transform infrared (FTIR) spectrometer was begun in September 1979, and essentailly completed by January 1980. The instrument was found to meet all design specifications and even exceed some, such as resolution and signal-to-noise ratio. The instrument is being used for four distinct research and/or service functions: high-resolution low-pressure gas work, liquid samples, liquid chromatography, and gas chromatography.

The studies of gas chromatographic applications have progressed through the utilization of packed column chromatography to the construction and testing of an interface for wall coated open tubular gas chromatographic columns (WCOT), which will allow real-time FTIR analysis of compounds eluting from the WCOT. The use of packed columns was not pursued because they were not found to have the resolving power required for the separation of the complex samples we wished to analyze. The WCOT columns used in this project were chosen to maximize sample capacity of the column, since the FTIR instrument requires ∿100 ng of component for the collection of a reasonably identifiable spectrum. Also, an on-column injector was fabricated to facilitate injection of a maximum amount of sample onto the column without undue loss of efficiency. The first interface design consisted of a Pt/Ir tube which connected the output of the thermal conductivity detector (TCD) to the FTIR light pipe. This interface was found to be unsuitable because too much dead volume (located mostly in the TCD and connecting fitting) caused unacceptable peak broadening. In addition, the Pt/Ir tube thermally trapped out and/or reacted with all solutes boiling above 300°C.

The present interface consists of a 50 cm length of deactivated, methyl silicone-coated quartz capillary of 0.15 mm internal diameter. The TCD has been bypassed and no other gas chromatographic detectors are

used. This interface is connected to a glass WCOT by use of AgCl cement; if a quartz WCOT were used, then the last 50 cm of the capillary itself could act as the interface. The quartz interface does not appear to react with or retard eluting compounds and spectra have been obtained for compounds such as methyl dibenzanthracene (b.p. <500 °C). Reconstructed gas chromatograms (from IR data) still show large losses in efficiency over those obtained from normal gas chromatographic detectors. This loss is most likely due to the large volume of the FTIR light pipe, and a new low volume light pipe is being procured. Even though the FTIR data does not fully reflect the high-efficiency separations obtained on the WCOT columns, very recognizable and identifiable spectra are being obtained from environmental samples being analyzed (e.g., phenols in shale oil, PCB's, etc.). This is, to a large extent, being made possible by some newly developed manipulative computer software which numerically regains some of this lost column efficiency.

81-BCL-a-ENERGY RELATED POLLUTANTS AND EFFECTS MONITOIRNG AND ASSOCIATED METHODS AND TECHNIQUES DEVELOPMENT

1. Development of SRM's for Stationary Sources Associated with Energy Production

1.a. NO_2 in Air Gas Blend SRM's

The analytical work necessary to establish the feasibility of nitrogen dioxide in air mixtures as Standard Reference Materials has not been completed. The areas in which work must continue are related to the assignment of accurate values to the concentration and to the length of the period of certification. Measurement of the concentration of all samples on a relative basis has been completed but the final absolute value has not been assigned pending further work. It appears that most samples are stable and if further analyses confirm the overall stability a certification period of one year will be assigned to these gas mixture SRM's.

There are virtually no accurate methods of analysis for NO_2 which result in concentration measurements uncertain to less than ±1% relative. Consequently, a considerable effort was expended to relate the concentration of NO_2 in these samples to the concentration of well characterized standards containing similar concentrations of NO. A double catalytic converter was assembled which appeared to give stable consistent ratios of conversion of NO_2 to NO. If it could be assumed that conversion in the second converter in series was 100% efficient then a direct comparison could be made between NO standards and the samples containing NO_2. However, this assumption cannot be made without confirmatory evidence. We have established that if the conversion in the second converter is less than 100% it isles by a constant percentage of the NO_2 entering the system. This was confirmed by comparing the concentration of NO_2 measured by a UV photometric method with that measured by conversion to NO and analysis by chemiluminescence. In the case of both instruments the relationship between samples was identical within the combined

uncertainties of the two methods. The table below relates the observed concentration of each sample to sample 1 for each method of analysis and is expressed as the ratio of the signal measured for each sample divided by the measured signal for sample 1.

Sample	Ratio of Sample Signal to Sample 1	
	Chemiluminescence	UV
1	1.000	1.000
2	.425	.425
3	.217	.217
4	.109	.108

All of the 250 ppm and the 1000 ppm samples were reanalyzed approximately one year after the first analysis. The data for the 250 ppm samples indicates that only one sample out of 50 has changed by more than 1% relative. This one sample appears to have decreased about 2% relative. However, the results for the 1000 ppm lot show a number of samples to have either increased or decreased in concentration but in no case by more than 1% relative. It should be noted that while more variability was observed with the 1000 ppm samples it does not necessarily follow that these samples are less stable. The precision with which a sample can be analyzed is roughly ±2 ppm. Thus at the 1000 ppm level a relative change of 0.2% could be recognized but at 250 ppm a relative change of this size would not be apparent.

At this time it appears that it will be possible to assign an accurate final concentration to each sample but the uncertainty will be somewhat greater than with the less reactive gaseous SRMs. We estimate that the final total uncertainty with which the 250 ppm samples will be certified will be ±3% relative (7.5 ppm) and that at 1000 ppm it will be ±1% (10 ppm).

The analysis of NO_2 by chemiluminescence requires a very long equilibration time if the sample lines are exposed to atmospheric moisture such

as occurs when samples are changed. For this reason and because of the reactivity of NO_2 toward other parts of the COGAS system it was decided that attempts to automate the analysis would be fruitless. Consequently, a special sample manifold was constructed to facilitate the manual analysis. The system consists of a "spider" to which 5 or 6 samples can be attached. The spider and associated tubing which connects the spider to the instrument are flushed with gas containing a concentration of NO_2 similar to that of the samples to be analyzed. It is then sealed and not exposed to the atmosphere until analysis of the 5 or 6 samples has been completed. This procedure has reduced the equilibration time considerably and has reduced the amount of sample needed for analysis.

The remainder of the samples, 500 and 2500 ppm will be analyzed by January 31, 1981. Following this step, the data for all samples will be examined and the final decision necessary for issuance on SRMs will be made.

1.b. SO_2 in N_2 SRM's

Two new SRMs consisting of 50 and 100 ppm nominal concentration of sulfur dioxide in nitrogen are nearing completion. Each SRM will consist of 50 samples each. The analysis of the 50 ppm samples has been completed and the analysis of the 100 ppm samples will be completed by the end of 1980.

The use of an automated analytical system (COGAS) for the analysis of these samples was not attempted. Preliminary results using an instrumental method (NDIR) suggested strongly that problems due to adsorption of SO_2 on the stainless steel parts of COGAS could lead to erroneous results. Considerable investigation of the problem was anticipated and it was decided to analyze each sample manually in which case the problems of adsorption could be minimized. However, when these SRMs are completed the use of COGAS will be investigated using a small number of the analyzed SRMs.

The final concentration of the samples in the 50 ppm lot cover a range of about 1 ppm (2% relative) and at this time there is no evidence of instability of any samples in the lot. The range of concentration in the 100 ppm lot is about the same on an absolute basis (1 ppm) but smaller on a relative basis (1%).

The final uncertainty to be assigned to each sample in the 50 ppm lot will probably be about 2% relative. This value is based on the uncertainty of the chemical method used to analyze the reference sample and on the imprecision with which this reference sample is compared to each sample in the lot. The uncertainty of the 100 ppm lot is expected to be smaller than that of the 50 ppm lot. It is not likely that the uncertainty of the 50 ppm level can be reduced significantly. Several techniques were investigated including gas chromatography, precise dilution and measurement with a flame photometric detector and non-dispersive infrared measurement (NDIR). Measurements by NDIR was found to be the most precise but because of the relative insensitivity of the technique to SO_2 the results at 50 ppm probably represent a practical lower limit for analysis of SRMs.

The material for a new SRM (SO_2 in N_2, 3500 ppm) has been ordered and is in preparation. Analysis of a reference sample to be used by the commercial supplier has been completed and delivery of the lot of 50 samples should occur before the end of 1980. Previous analytical experience with concentration of SO_2 of 2500 ppm suggests the absence of any significant analytical problems at the 3500 ppm level and further suggest that a certification to ±1% relative will be feasible.

It is planned to issue these as SRMs by June 30, 1981.

1.c. <u>NO in N_2 SRM's</u>

SRM's have been issued for 1500 and 3000 ppm NO in N_2.

1.d. O_2 in N_2 SRMs

All work is complete

Two SRMs consisting of 2 and 10% oxygen (SRM 2657 and SRM 2658) in nitrogen are now available.

2. Development of SRMs for Monitoring Ambient Air Impacted by Emission Resulting from Energy Production

2.a. CO_2 in Air SRMs

Specifications were developed and a commercial supplier is currently preparing three lots of 50 samples each at approximately 320, 330, and 340 ppm carbon dioxide in air. Work has been completed on the analysis of the air with which the samples will be prepared, to assure that the composition in terms of both the major and trace constituents is identical to "normal" air.

2.b. Automation of Gas Analysis

A third system (COGAS-III) has been constructed for the automation of permeation tube calibrations. Preliminary results indicate that the system will operate as intended.

Under a separate program with the Motor Vehicle Manufacturers Association, ten new carbon monoxide in nitrogen mixtures were developed involving measurements which demonstrated the usefulness of high-pressure injection from large sample loops into a gas chromatograph to increase detector response for carbon monoxide mixtures at concentrations of less than 100 ppm. The technique allowed the intercomparison of samples with standards with a precision of ± 0.2 percent. Certification of these SRM's involved the first test of the software used to control the combined gas chromatography NBS-developed computer operated-gas analysis system (COGAS). COGAS had previously been used only with continuous flow gas analyzers.

2.c. Development of a Traceability Procedure for Gas Standards

The demand for gas standards is increasing at an accelerated rate. Improvement in instrumentation during the last two decades and mandated requirements for accuracy in gas measurements related to environmental concern have both contributed to the demand. Limitations imposed on the gaseous SRM program resulted in severe shortages of standards which on occasion has caused concern among regulatory agencies, users and producers. Since it is not realistic, either philosophically or physically, to consider expanding the gaseous SRM program beyond its present bounds, it has become essential to establish some alternative supply of accurate standards. As a result of this need a protocol has been developed which in essence transfers the responsibility for producing large numbers of accurate standards (Certified Reference Materials) to the specialty gas industry. The protocol makes provision for monitoring by the regulatory agencies and at the same time NBS retains the responsibility for assuring traceability of the Certified Reference Materials (CRM's) to NBS gaseous SRM's.

According to the protocol, the specialty gas producer will prepare CRM's at concentrations equal to or very close to the concentration of existing SRM's. These will be prepared in large homogeneous batches. The producer will analyze each CRM from the batch by comparison to an SRM. The regulatory agency will select samples from each batch for analysis. The analysis by the regulatory agency will be performed using SRM's as calibrants. Both the producer and the regulatory agency will furnish NBS with complete information concerning the production and analysis of the CRM's including the data for both calibration of the instruments used and the analysis of the CRM's. NBS will then statistically compare the results reported by the producer with those found by analysis by the regulatory agency. In addition, NBS will examine all the results reported by the producer to ascertain the homogeneity of the batch. From these data it will be possible to verify the total uncertainty of the concentration claimed by the producer. At this point the concerned

parties will be notified that the particular batch of CRM's has been prepared in accordance with the protocol and that the stated concentration is correct within the defined limits of uncertainty.

The protocol in its present form has been extensively modified in response to comments from the gas industry, users of SRM's and the principal regulatory agency, the Environmental Protection Agency. It is not a "cook book" by which CRM's can be prepared. Rather, it recognizes the experience and expertise of the specialty gas industry while at the same time it recognizes the reservations which the user may have regarding the industry and which the industry may have regarding the regulatory agency. It is expected that the role of NBS as an independent overseer will inspire confidence not only in the quality of the CRM's but in the integrity of the entire procedure.

The availability of CRM's should moderate the demand for the corresponding SRM's, so that the latter would be used largely as primary standards, which was the purpose for which they were originally produced. A document has been prepared for publication under the Interagency Energy-Environment Program, entitled "A Procedure for Establishing Traceability of Gas Mixtures to Certain National Bureau of Standards Standard Reference Materials".

3. Develop Methods for Dispersal of Particulates on Filter Media and Methods for Determining and Controlling the Composition and Morphology of Such Dispersed Particulates

3.a. Thin Glass Films Produced by Focused-Ion Beam Sputtering

X-ray fluorescence spectrometry has proven to be a versatile and rapid method for multielement analysis in many analytical applications. Of particular interest are substances which can be analyzed in the form of a deposit on a filter, mesh or membrane, or as a thin pressed pellet. Collected airborne particulate matter, particulates in waste water and

geochemical samples are just a few examples of this type. In some respects such "thin samples" are ideal for x-ray fluorescence analysis because the detection limits are suitably low and interelement effects such as x-ray absorption and/or enhancement are negligible. The absence of any sizable interelement effects makes possible a linear instrument response to element mass per unit area. Spectrometer calibration for analysis of such samples is usually performed with thin samples containing known concentrations of the analyte(s) of interest. Some problems associated with the "thin specimen model" are x-ray self-absorption in particles (notably for the light elements such as Al, Si, P, and S) commonly referred to as particle-size effects, and self-absorption in the substrate. Both of these effects require the application of correction factors. Therefore, the basic premise is that accurate multielement analysis of thin samples can be performed based on the thin specimen model, together with empirical or theoretical correction factors.

There are several important criteria which need to be met if thin samples are to be acceptable for calibration purposes. First, the uniformity of the sample as well as its homogeneity must be within an acceptable well-defined tolerance limit. If the sample contains particulate matter, both the size and distribution should be characterized. Secondly, the mass loading of the sample must be known to an acceptable degree of accuracy. And finally, the sample should possess sufficient durability and integrity.

The goal of a joint program between NBS and the U.S. Environmental Protection Agency (EPA) was to perform the research and development required to produce thin standard samples especially useful for calibration of x-ray fluorescence analysis of collected airborne particulate matter. For this purpose we have investigated several candidate methods for preparing such samples.

One method which shows great promise is the deposition of thin films of glass containing known concentrations of several elements of interest on polycarbonate substrates by a technique known as focused

ion-beam sputtering. Ion-sputtering essentially involves the transfer of atoms and/or molecules from a target to a substrate by the action of an ion beam (usually argon) incident upon the target. The ion beam is accelerated at high potential (700-1100 volts) with a flux of about 0.5 mA/cm^2 toward the target at a 45° angle. Since the substrate is not in the plasma environment, substrate damage does not occur. This is a distinct advantage of this particular sputtering technique. Other advantages to be gained are: (1) production of thin films from synthetic materials such as glasses of known elemental composition which can be varied as desired; (2) high adherence of the glass to the substrate which obviates the need for overcoating to maintain sample integrity; and (3) easy control of the glass mass loading on the substrate by variation of the sputtering time.

Several studies were performed with glass targets fabricated at NBS which allowed up to eight 47 mm substrates to be coated at one time. Instrumental parameters such as ion acceleration voltage and ion current were systematically varied to determine their effect on film composition. It was found that rather severe changes in these parameters often do not affect the film composition by more than ± 15 percent. Glass films sputtered from targets containing phosphorous and sulfur were also prepared to demonstrate the feasibility of preparing films containing elements of low atomic number.

In Table 6 are summarized the elemental compositions of three sets of films at mass loadings ranging from 167 to 185 $\mu g/cm^2$ which were prepared at various times. These data demonstrate that the compositional reproducibility of thin films from set to set is satisfactory for the purposes of preparing standard films.

Multi-element thin standards suitable for calibration purposes can be fabricated by the focused ion-beam sputtering technique. In order to include all the elements of interest in any particular film, several glass targets would need to be fabricated. It is believed that these films would be useful to monitoring agencies such as EPA for assessing environmental impact of airborne particulate matter. Work is now in progress to prepare several sets of films which will be certified by the Office of Standard Reference Materials as NBS Standard Reference Materials.

Table 6 Composition of Glass Films at Higher Mass Loadings[a]

Set No.	Film No.	Mass Loading Glass Film $\mu g/cm^2$	Percent SiO_2	Percent CaO	Percent ZnO	Percent PbO
1	1	180.4	43.1	23.3	12.8	16.6
	2	184.0	42.1	22.7	12.3	16.1
	3	184.2	41.5	22.5	12.4	16.0
	4	181.0	43.6	23.5	12.5	16.7
	5	179.6	43.4	23.3	12.8	16.7
	AV.		42.7 ± 0.4[b]	23.1 ± 0.2[b]	12.6 ± 0.1[b]	16.4 ± 0.2[b]
2	1	179.4	45.4	24.5	12.6	15.7
	2	178.0	45.0	24.4	12.6	15.7
	3	185.4	44.9	23.7	11.9	15.0
	4	178.8	44.7	24.0	12.5	15.5
	AV.		45.0 ± 0.2[b]	24.2 ± 0.2[b]	12.4 ± 0.2[b]	15.5 ± 0.2[b]
3	1	167.1	47.0	24.9	12.4	15.4
	2	170.0	47.4	24.8	11.5	15.2
	3	182.6	46.2	24.0	11.2	15.2
	4	173.2	47.2	24.4	11.5	15.1
	AV.		47.0 ± 0.3[b]	24.5 ± 0.2[b]	11.7 ± 0.3[b]	15.2 ± 0.1[b]

[a] Ion-acceleration voltage = 1000V; Ion-current = 90 mA; Time = 5 1/2 hours.

[b] Standard deviation of the mean value i.e., $(S/\sqrt{n})$ where S is the standard deviation of a single measurement.

4. Particulate Physical and Chemical Characterization

4.a. Particle Doppler Shift Spectrometer (PDSS)

Two major areas of study to improve and verify the particle size and count measurements with the Particle Doppler Shift Spectrometer (PDSS) have been the extension of the measurement range to submicron particles and the development of a "diagnostic" parameter measure to detect and quantitate particle velocity components arising from sources other than gravitational settling, such as thermal-induced or particle-induced flows in the measurement cell.

Low Pressure PDSS Measurements: Submicron particle and slip effect studies

We attempted to extend the measurement range of the PDSS to submicron diameters by evacuating the measurement cell in order to enhance the sedimentation velocity of smaller particles by the slip effect, a pressure-dependent phenomena. We were able to extend the range from 5 μm diameter down to about 2 μm, but were unable to get any lower due to experimental difficulties. The limiting problem is the difficulty of generating aerosols in an evacuated system at 10-15 torr or less. A spray nozzle system was used to generate particles at low pressure. The nozzle does not develop a spray below about 10 torr. We also attempted to introduce aerosols generated at high pressures (760 torr) by control-leaking them into the evacuated measurement cell. Dilution of the sample particle concentration is so severe however, that the counting statistics become unacceptable.

These experimental difficulties will require a large effort to overcome. In order to make the slip effect study feasible it would be necessary, in addition to solving the sample generation-introduction problem, to a) incorporate a method of rapid, four-place, accurate pressure measurement in the torr pressure range and to b) build either a thermally insulated or thermally controlled measurement cell. Accurate, precise pressure

measurement is necessary because pressure and settling velocity are the only independent parameters measureable in the PDSS experiments. Thermal control of the cell is required because even in the 10-20 torr pressure region, thermal convections can become the major particle velocity driving force, destroying spectrum resolution.

Detection and quantitiation of non-gravitational settling particle velocity components

The accurate particle diameter measurement by the PDSS is described in the paper "Particle Doppler Shift Spectrometry. Accurate determinations of 5-15 μm aerosol." by Fletcher, Bright and Chabay in J. Phys. Chem., 84: 1607 (1980). The ability to detect and quantitate spurious velocity components has been described in "Low Reynolds number fluid flow induced by settling aerosol and detected by Particle Doppler shift spectrometry" by Fletcher, Bright and Chabay, J. Phys. Chem., 84: 1611 (1980). A complete study was made on the settling droplet induced flow effect and is described in the paper "Droplet Induced Flow Effect" by Bright, Fletcher and Baum which has been submitted for publication in the J. of Fluid Mech. These papers are included as the report of these studies.

4.b. Particulates on Glass Fiber Filters: Certification of SRM's for Pb, Sulfate, and Nitrate on Filter Media

Final certification of SRM 2673, Sulfate and Nitrate on Filter Media, and SRM 2674, Lead on Filter Media, has been completed. These materials are intended for use in the evaluation of apparatus and methods used in the determination of lead, sulfate, or nitrate in atmospheric particulates collected on filters.

Certification measurements for the anions were accomplished by ion chromatography. Lead for SRM 2674 was determined by both voltammetry and atomic absorption spectrometry (AAS). Statistical analysis of the data indicated no significant effects of biases in the AAS due to undissolved solids from the glass filter matrix.

81-BCL-b-ENERGY RELATED AIR POLLUTANT ANALYSIS INSTRUMENTATION

1. Development of an Instrument to Measure Airborne Sulfate Particulate Matter

Work continued on the characterization and optimization of the pulsed precipitator/flame photometric detector (FPD) aerosol sulfate measurement technique. As indicated in the preceding report, we made an evaluation of the feasibility of doping the hydrogen gas with SO_2 or ethyl mercaptan in order to increase the total FPD response into a range where the instrument is more stable, and to increase the sensitivity of the response. The sensitivity of the system is a function of the total signal, because the FPD response (R) is nonlinear with sulfur concentration(s); (i.e., $R \propto [S]^n$, where n = 1.8, therefore Sens. = $\frac{dR}{d[S]} \propto n[S]$). We have experimentally verified this prediction; viz., an increase in total sulfur concentration of a factor of 2.6 is predicted to give an increase in sensitivity of 4.7, in good agreement with an observed increase of 5.1.

An important limitation in the application of the FPD for airborne sulfate particulate measurement is the slow response time of the burner to changes in sulfur concentration. The rise time for 90 percent of full equilibrium response is about 15 seconds, and the fall time is 2.8 seconds. For a precipitator operating frequency of 0.2 Hz we can obtain only 60 percent of the potentially available response. This is equivalent to a loss in sensitivity of almost 50 percent. We therefore have looked for better burner designs. We recently evaluated a burner and detector system built by Dr. Don Stedman at the University of Michigan and found that it was much faster (rise time = 1 sec; fall time = 0.2 seconds). We will obtain this instrument through a collaborative study arrangement, evaluate the burner for sensitivity, and optimize it for application with the pulsed precipitator technique. Table 7 shows a comparison of the percent of full response vs. precipitator frequency for the instrument we have been using, and for the University of Michigan burner/detector.

Table 7

Recovery of Potentially Available Response vs. Precipitation Frequency

	Percent of Full Response	
Frequency (hertz)	Meloy[a] FPD	U. of Mich. FPD
.2	60	100
.5	17	85
1.0	5	65
2.0	2	30
4.0	--	10

The development and characterization of the Pulsed Electrostatic Precipitator-Flame Photometric Detector (PEP-FPD) system for the measurement of ambient level aerosol sulfur concentrations has been completed this year and a final report to EPA is in the review process. The basis of the technique is the use of the PEP to selectively modulate the aerosol component of the sample while leaving the gas phase component unaffected, resulting in a signal from the detector (FPD) which has two separable components corresponding to the particle and gas phase sulfur concentrations. Because the FPD response to sulfur concentration is non-linear (Response $\sim[S]^n$ where n = 1.5 to 2 depending on various flame and flow parameters) the sensitivity of the FPD is a function of the total sulfur concentration in the sample. The following data shows the sensitivity (dI/dS) and sensitivity relative to sensitivity at 1 ppb for our FPD:

[S] (ppb)	dI/dS (amp/ppb)	dI/dS relative to 1 ppb
1	1.42×10^{-10}	(1)
5	4.81×10^{-10}	3.4
10	8.13×10^{-10}	5.7
50	2.75×10^{-9}	19.4
100	4.65×10^{-9}	32.7
200	7.86×10^{-9}	55.4
500	1.57×10^{-8}	110.8
1000	2.66×10^{-8}	187.3

[a] In order to adequately describe materials and experimental procedures, it is occasionally necessary to identify commercial products by manufacturer's name or label. In no instance does such identification imply endorsement by the National Bureau of Standards nor does it imply that the particular products or equipment is necessarily the best available for that purpose.

One consequence of this operational characteristic is that it is possible to increase the sensitivity of the PEP-FPD system by increasing the total sulfur concentration in the flame. We have verified this by adding a constant concentration of CH_3CH_2SH to the hydrogen. A second consequence, however is a complication of data reduction when one is attempting to measure more than one sample component because the sensitivities are related to total sulfur concentration, not to sample component concentrations. We have solved this problem by developing a data acquisition/reduction procedure that enables us to achieve simultaneous measurement of aerosol and gas phase sulfur concentrations with sensitivities of 0.2 $\mu gm\ S/m^3$ and 1 ppb respectively. Initial data comparison from an intercomparison study shows a very high correlation coefficient with data obtained by a dichotomous sampler-x-ray-fluorescence system.

We have shown the major limitation in response time of the technique is in the FPD. (The commercially available FPDs have > 60 sec rise times and $\sim$ 1.5 sec fall times.) We have completed characterization of a new FPD design which has symmetric rise and fall times of less than one second. This faster response time means the PEP-FPD system will be capable of real-time measurements of ambient SO_2/SO_4 concentrations under conditions where the concentrations are dynamic, such as in plume traverses. Additional research will be needed to improve the sensitivity and flow stability of the fast-flame FPD to its full potential, though it now is comparable to commercially available FPDs in those respects.

81-BCL-c-ENERGY RELATED POLLUTANTS AND EFFECTS MONITORING AND ASSOCIATED METHODS AND TECHNIQUES DEVELOPMENT

1. Radiocarbon as an Environmental Trace

1.a. Applications

The use of miniradiocarbon measurements with 5-10 mg (carbon) environmental samples (gases, atmospheric particles, sediment) has continued with the objective of utilizing the natural $^{14}C/^{12}C$ ratios to distinguish between biogenic and fossil pollutant sources. Important progress has been made in our understanding of the source of carbonaceous particles, especially of those collected in urban areas, through several cooperative studies with industry* and universities**. A critical element in these investigations has been the utilization of sample selectivity (chemical and physical) in combination with the radiocarbon measurements. That is, because small samples can be used, we have been able to increase the "information content" of our measurements by examining samples that have been preselected according to geographical region, known activities, chemical nature, and stable isotopic composition. A summary of our recent radiocarbon results, together with an indication of these critical supporting data, is given in Table 8. The general conclusions to be drawn from these studies are (i) urban particles tend to show predominately fossil carbon (though with a non-negligible biospheric contribution); and (ii) particles from remote locations contain less organic carbon, which is primarily biogenic. An extremely important exception occurred in the Portland Study***, where the combustion of biospheric material (field, slash, and residential wood burning) led to the first observations of urban carbonaceous particles containing up to 100 percent biogenic carbon. These results have caused us to focus on the air pollution potential of residential wood combustion - a problem which will be a subject of our continuing studies (see Table 9).

---

* General Motors, Global Geochemistry Corporation.

** Oregon Graduate Center, Colorado School of Mines, University of Washington.

*** The Portland Aerosol Characterization Study measurements were carried out in cooperation with the Oregon Graduate Center and the Oregon Department of Environmental Quality.

1.b. Research Advances

Research activities have been directed toward the analysis of atmospheric gases, high accuracy natural radiocarbon measurements, chemical-mathematical investigations of the Radiocarbon Dating Calibration Curve, and extension of the state of the environmental radiocarbon art to microgram samples using Accelerator Mass Spectrometry. Work with the atmospheric gases is still in the initial stages; thus far milligram quantities of atmospheric methane**** have been extracted for radiocarbon measurement. High accuracy radiocarbon measurements are underway in connection with calibration of the new NBS International Radiocarbon Dating Standard, and concomitant chemical-statisitical investigations have been performed in cooperation with the Australian National University on an International Laboratory Intercalibration exercise involving some 20 laboratories and three calibration materials (Oxalic Acid, 1850 Tree Rings, Sucrose). Evaluation of the fluctuations of the Radiocarbon Dating Calibration Curve is underway in cooperation with the Statitistical Engineering Division of NBS under the auspices of an international committee formed for this purpose. Information to be derived includes the assessment of accuracy, development of an accepted calibration curve for accurate dating, and geophysical model information for the assessment of past climatic variations. Studies initiated in 1979 show outstanding promise for the analysis of extremely "old" and extremely small samples. Our exploratory work, which utilized the NBS variable geometry isotope separator and the University of Rochester Tandem Van de Graaff Accelerator, demonstrated the feasibility of measuring natural radiocarbon in the 10 μg range. All of the above activities are intended to increase our ability to extract reliable information on anthropogenic and natural contributions to both environmental pollutants and chemically-induced climatic perturbations, now and in the past.

**** The methane study, of interest for climatic reasons and to learn about man's perturbation of the carbon cycle, is being carried in cooperation with NOAA (Air Reserves Laboratory).

RADIOCARBON IN AEROSOLS AND SEDIMENT

	Mass-Carbon (mg)	% Contemporary [$^{14}C/^{12}C$] (± one standard deviation)	Supporting Data
Ambient Particles			
Los Angeles	7.8	23 ± 16	Organic (insoluble)
Salt Lake City	5.3	28 ± 13	Composition
Utah Desert	10.2	88 ± 16	
Impact Particles (<3 µm)			
Portland, OR.	5.1-10.7	62. – 107.	Inorganic Composition
Sediment			
Puget Sound, WA. FA	60.	86 ± 21	Isotopic ($^{13}C/^{12}C$)
Puget Sound, WA. PAH	14.	19 ± 21	Composition

(FA = Fatty acid fraction, PAH = Polycyclic Aromatic Hydrocarbon fraction).

Table 8. Percent of contemporary (biogenic) carbon deduced from radiocarbon measurements on small (∿ 10 mg) environmental samples. Supporting inorganic, organic, and isotopic (^{13}C) data aided in source resolution/confirmation. References: Ambient Particles (Currie et al., 1978), Impact Particles (Cooper, Currie, and Klouda, 1979b), Sediment (Swanson, Fairhall, and Currie, 1979).

WOOD BURNING

Utilization

- **Scandinavia:** Finland projects 30% (by end of 1980's); Sweden, 58% (by 2015)
- **U.S.:** A major fuel, ranks with hydroelectric and nuclear (wood stove sales: 10^6/yr.)

Environmental Significance

- Particle emissions: 20–50 times oil, gas/Btu, primarily fines (respirable)
- Incomplete combustion→soot, PAH, HCHO, phenols, . . .

Observed Impacts

- Bangor, ME: 8 $\mu g/m^3$ (inventory)
- Portland, OR: 24 $\mu g/m^3$ (radiocarbon)

Table 9. Wood as a fuel: Utilization and particulate pollution. Information on wood utilization may be found in Brooke (1979) and Trefil (1978); on environmental significance and impacts, in Cooper, Currie, and Klouda (1979a) and Butcher (1978).

1.c. Statistical Evaluations of the International Radiocarbon Cross Calibration Exercise, and of the Natural Radiocarbon Fluctuations

High accuracy natural radiocarbon measurements are of critical importance in a number of fields, ranging from archeology to climatology to environmental science. In addition to our current activities related to the calibration of the new International Standard for Radiocarbon Dating (replacement for SRM 4990B), we have contributed to the numerical evaluation of interlaboratory data representing a) high precision measurements of homogeneous primary and secondary natural radiocarbon standards, and b) the "calibration" relationship between radiocarbon concentrations and calendar age as deduced from dendrochronology (tree ring measurements). The first activity is important for assessing the relative activity of the three "standards" and for identifying error sources and limits (random and systematic) among the best laboratories internationally. Deliberations on the second topic culminated in the organization of the International Committee for the Calibration of the Radiocarbon Time Scale, to which NBS scientist, Lloyd A. Currie, is an advisor. The fine structure of the radiocarbon dating calibration curve -- i.e., long-term trends and short-term fluctuations about the simple exponential decay model -- is important for two major reasons: a) fine structure must be adequately evaluated/fitted to achieve accurate dating, b) modeling of the fine structure provides a means for us to learn more about the history of the earth (climate, environmental changes, ocean circulation, solar activity, etc.).

i. Exploratory Analysis of the International Radiocarbon Cross-Calibration Data: Consensus Values and Interlaboratory Error

Data from the international cross-calibration exercise have provided an important opportunity to assess the state-of-the-art of high-precision natural radiocarbon measurement and to derive consensus values for two relatively pure and homogeneous materials relative to the international radiocarbon dating standard (NBS Oxalic Acid, SRM-4990B). Performance was good: some fifteen laboratories returned results for the two indepen-

dent ratios -- Australian National University Sucrose/Modern Standard (S/M) and 1850 Wood/Modern Standard (W/M) -- with a typical imprecision (standard deviation) of about five percent per mil; and the distribution of results was relatively narrow. The primary limitations encountered were incomplete laboratory data and variable reporting practices.

Analysis of the data led to the following observations:

- Imprecisions (standard deviations) reported varied from about two percent per mil to eight percent per mil, with one laboratory reporting 28 percent per mil. Most, but not all, imprecisions represented counting statistics only.
- Apparent blunders (large deviations from consensus values) occurred in a few cases, especially for estimates of the ratio S/M.
- "Laboratory error," σ_x -- i.e., a non-Poisson error component -- was estimated from the data distributions for both sample ratios. Results were similar: for S/M, σ_x = 3.5 percent per mil; for W/M, σ_x = 1.8 percent per mil. These error estimates, though rather uncertain because of the limited number of degrees of freedom, are consistent with earlier estimates, and the may reflect the accuracy limit for current counting techniques.
- Consensus ratios, following the use of exploratory techniques to identify blunders, and taking into account "laboratory error" and varying Poisson imprecision, were $\Delta^{14}C$ = 508.1 ± 2.0 percent per mil (1850 Wood, age-corrected for decay to 1950). (Uncertainties represent one standard error, and both S and W are normalized to $\delta^{13}C$ = -25 percent per mil).

Further results of the evaluation include $\delta^{13}C$ distributions and the search for measurement method-, sample nature-, and isotope fractionation-related effects. (See Figure 8 for histograms of the intercomparison results).

ii. Calibration of the Radiocarbon Time Scale

Evaluation of the structure of the radiocarbon calibration curve is critically important both for accurate dating (as shown in Figure 9)

CROSS-CALIBRATION HISTOGRAMS

(corrected ^{14}C deviations, in ‰)

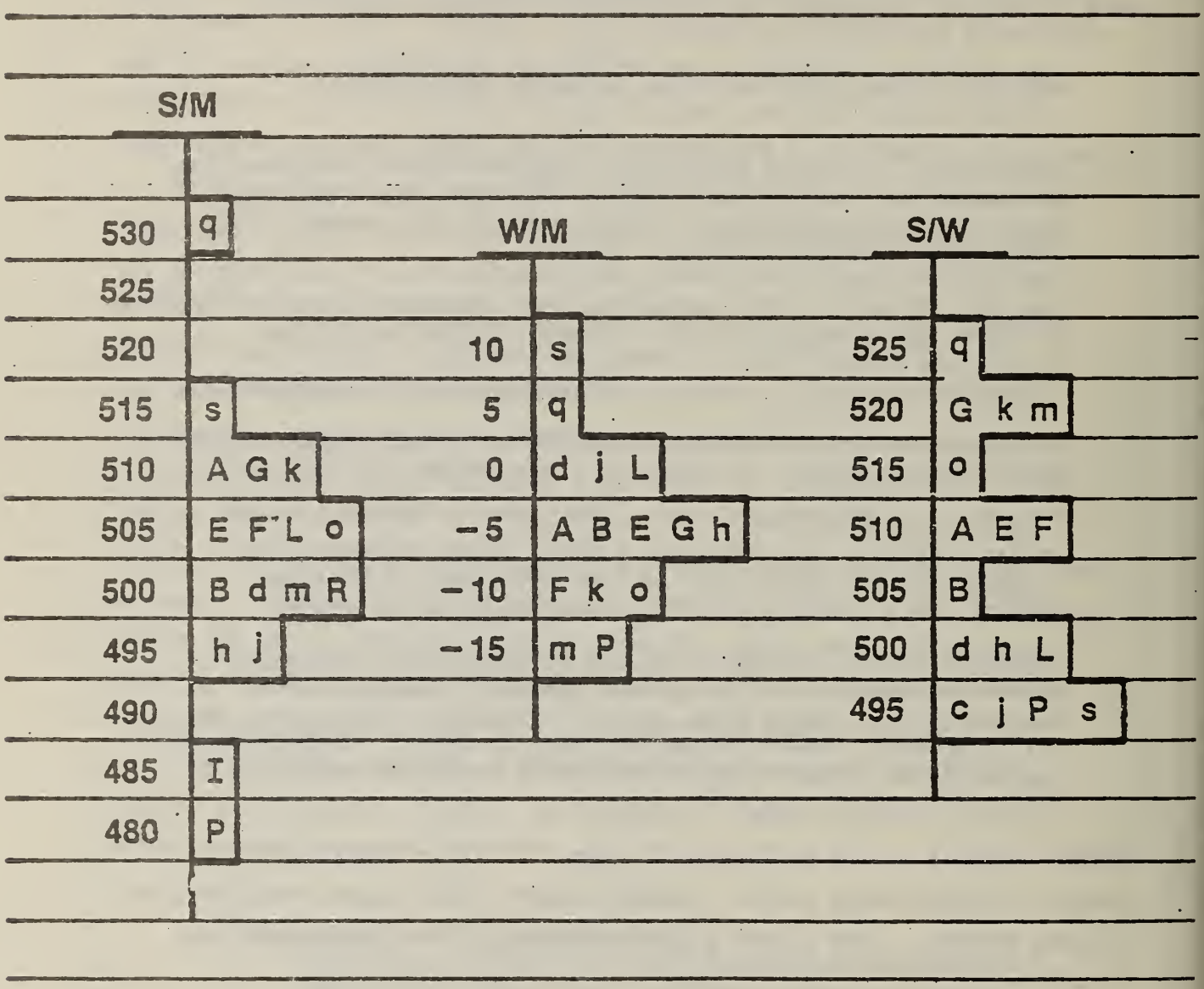

- S, M, W = Sucrose, Modern Standard, Wood
- σ_i = 2‰ – 4‰ (Cap.); 5‰ – 8‰ (Lower Case)

Figure 8 Histogram of the radiocarbon ratios for ANU sucrose (S), 1850 wood (W) and the modern standard (M; 0.95 x NBS oxalic acid). Numerical scales are expressed as deviations (in parts-per-thousand) from unity from each of the three ratios; and laboratories are coded alphabetically.

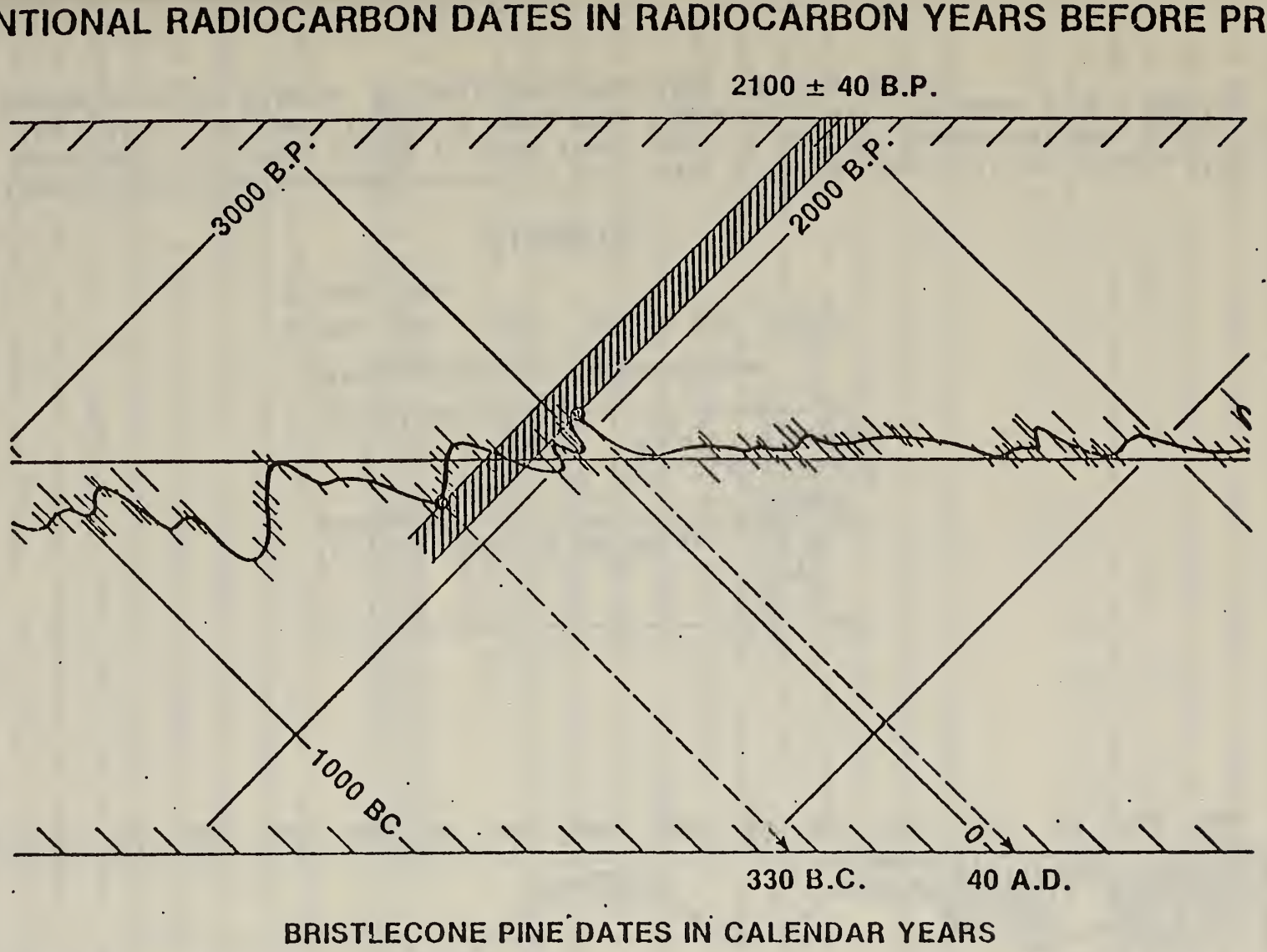

Figure 9 Magnification, due to fluctuations of the radiocarbon calibration curve, of the age uncertainty interval for an archaeological wood sample prepared at NBS. The underlying radiocarbon calibration curve was adapted from: Suess, H. E., Radiocarbon Variations and Absolute Chronology, I. U. Olsson, ed., Wiley-Interscience, New York, 595 (1970).

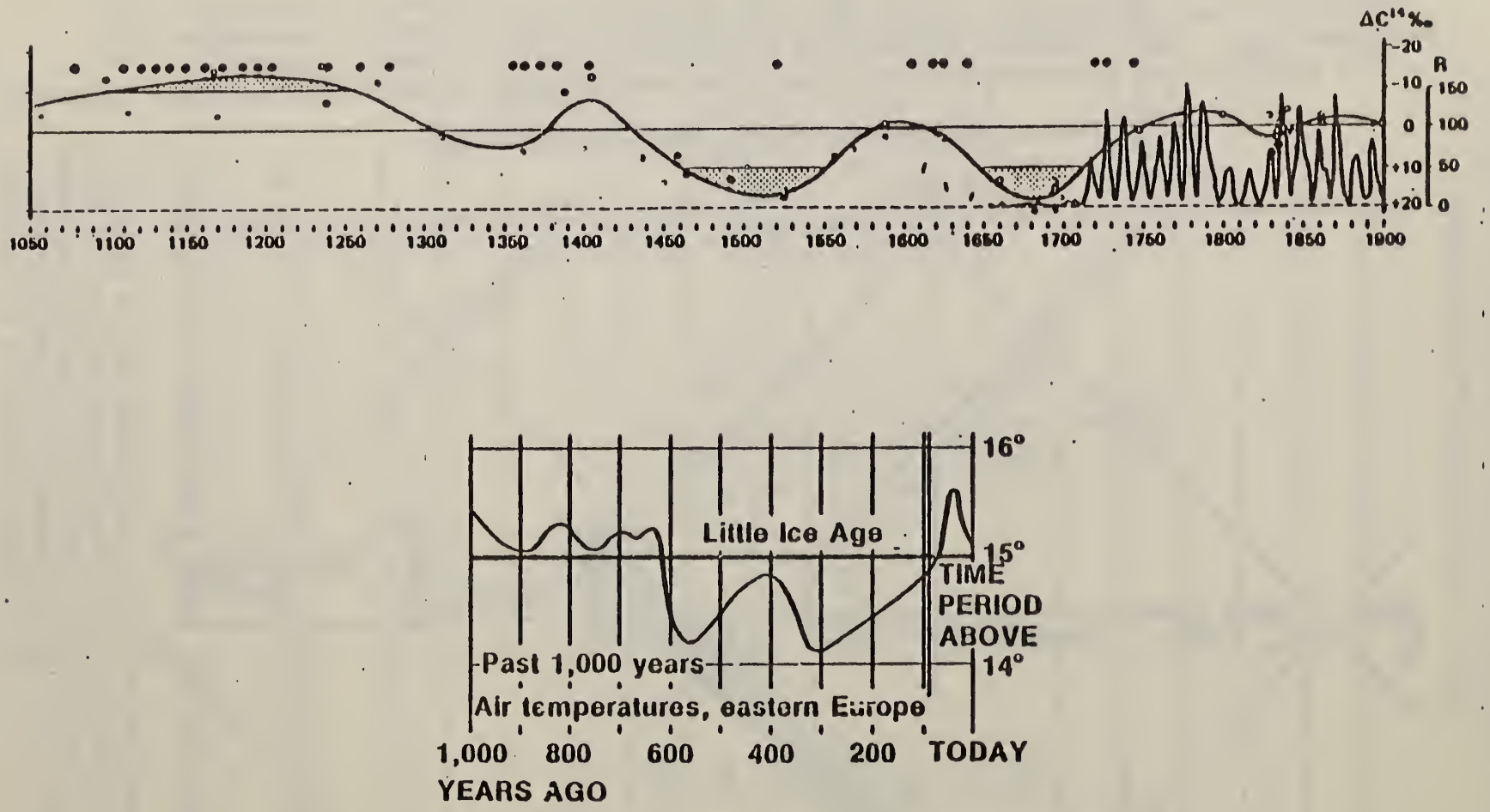

Figure 10 Correlation of radiocarbon fluctuations with solar activity (sunspots) and climate (^{18}O in ice cores). The upper figure is taken from: Eddy, J. A., The Maunder Minimum, Science 192, 1189 (1976). The lower figure is taken from figure on p. 615: Mathews, S. W., What's Happening to Our Climate, National Geographic 150, 576 (Nov. 1976).

and for geophysics and climatology (Figure 10). At the present time, because of the remarkable precision of natural radiocarbon measurements and the unique time (8000 year) record provided by dendrochronology, radiocarbon is the only radionuclide capable of giving us direct information on past fluctuations in solar activity. When combined with geophysical modeling and ice core measurements of the ancient atmosphere (CO_2), the ^{14}C variations will yield further insight into the history of the carbon cycle and prognosis for "the CO_2 problem."

Objectives of the International Committee are to assemble high quality data and to utilize geophysical and statistical-mathematical approaches to "fitting" the data. More specifically, the Committee seeks to identify means for combining all (reliable) ^{14}C measurements of tree-ring dated wood specimens into a single radiocarbon scale calibration scheme, preserving as much of the high frequency components as seem warranted by the data. During the past year cooperative efforts by L. A. Currie (Center for Analytical Chemistry), C. Spiegelman (Center for Applied Mathematics), and J. C. Lerman (Univ. of Arizona) have produced important insights into measurement and interlaboratory errors (see also part 1, above), assumed functional models, and best estimates for the calibration curve and its uncertainty band.

1.d. Advances in Small Sample Radiocarbon Measurement Techniques: Application to the Assay of Individual Atmospheric Chemical Species

During the past year the NBS program to utilize natural radiocarbon as a tracer for sources of carbonaceous pollutants has been directed toward a) fundamental advances in measurement and data evaluation techniques and b) critical studies of urban air pollution episodes (such as the Denver "brown cloud") and basic investigations of sources of atmospheric gases and particles. The importance of these investigations rests upon the impact of both natural and man-made carbonaceous contaminants on health, stratospheric ozone, and climate. The success of this program, the only such program extant, is due to the ability of NBS to perform

reliable radiocarbon measurements on ambient samples containing microgram to milligram quantities of carbon.

Measurement advances are continuing through the development of miniature gas proportional counter and nuclear accelerator ("atom-counting") techniques which provide sensitivity gains of 10^2 to 10^5 compared to conventional radiocarbon dating techniques. Important meetings treating these topics (among others), organized by individuals in the group, included an ACS Symposium ("Nuclear and Chemical Dating Techniques", March 1980) and a meeting at NBS (August 1980) on sample preparation for accelerator measurements. Our work with the accelerator, which last year demonstrated the capability of precise measurement using less than 40 μg (carbon) of the new international radiocarbon dating standard, is continuing with studies in alternative source preparation methods, isotopic enrichment, and baseline tests with the first "dedicated" tandem accelerator constructed exclusively for atom-counting measurements. This particular machine is considered a National Science Foundation Regional Facility, and it will be located at the University of Arizona. The accelerator approach will make possible the radiocarbon assay of μg quantities of individual hydrocarbons and halocarbons, and individual chemical and size fractions of non-urban atmospheric particulates.

Applications to urban pollution and source studies of carbonaceous particles have centered on vegetative burning in the Portland, Oregon region, vegetative vs. oil shale aerosol contributions in a remote Utah location, urban pollution in Los Angeles and Denver, and an international effort (joint US - USSR AFAEX-79 project) to investigate "processes and mechanisms of formation and transformation of natural aerosol" in a remote forested region in the Soviet Union. In all of these studies, which were broadly interdisciplinary in nature, our group provided the only isotopic data; and the natural radiocarbon results yielded the only unique measure of the biogenic (non-fossil) contribution. This was especially important in the Denver and Portland studies where as a

result of our measurements it was concluded that residential wood burning constituted one of most significant sources of inhalable (< 2.5 μm) and visibility-reducing particles. In Denver for example, it was concluded that 18 percent of the visibility reduction of the winter time atmosphere arose from wood burning. Furthermore, 39 percent of the most effective visibity-reducing species -- elemental ("graphitic") carbon -- has been ascribed to wood burning.

It should be noted that the foregoing regional studies have included considerable data on chemical and physical characteristics of the ambient particles, together with supporting emission inventory and meteorological data. Although radiocarbon techniques provided the only direct measure of contemporary carbon, the other (indirect) indicators supported the conclusions from radiocarbon measurements in every case. A major challenge exists in selecting and evaluating the entire multidimensional data patterns from such experiments; this need formed the basis for the first Receptor Modeling Workshop (March 1980 in Durham) and the resulting committee on chemical mass balance and multivariate analysis methods of source reconciliation. Our program at NBS has been expanded to include such modeling efforts, in cooperation with NBS Center for Applied Mathematics. The combined use of isotopic data (^{13}C and ^{14}C) with particle size and chemical data (pyrolysis mass spectrometry, inorganic composition and elemental vs. organic carbon) has, in fact, been an intrinsic part of the above urban and remote particulate studies.

A summary of our recent radiocarbon measurements, which now include atmospheric gases as well as particles, is given in Table 10. Future work will be directed toward further sampling of selected gases (hydrocarbons, carbon monoxide), sources of urban run-off and sediment studies, high-altitude sampling, investigations of arctic haze and climatological consequences, and paleoatmospheric (isotopic) composition via ice core samples.

Table 10

Recent Radiocarbon Results

Sample		Objective	Result - Contemporary Carbon Fraction	Supporting Data
^{14}C Standard[a]	Direct	Minimum size	0.95 ± 0.03	^{13}C
	Implant	Enrichment	(^{14}C-pulse)	
Atmospheric CH_4		CH_4 budget	0.98 ± 0.22	—
Sediment	Fatty Acids	Source of PAH	0.86 ± 0.21	^{13}C
	PAH		0.19 ± 0.21	

[a]Accelerator $m_c \leq 40$ μg; all others, proportional counter, $m_c \approx 5$-10 mg

Atmospheric Particles

Sample		Objective	Result - Contemporary Carbon Fraction	Supporting Data
Urban	Volatile	Natural Component	0.69 ± 0.17	Inorganic
	Non-volatile	(chem.)	0.06 ± 0.08	Composition
Regional	Urban	Natural Component	0.23 ± 0.15	Organic
	Rural	(locale)	0.88 ± 0.16	Composition
Vegetative Burning	Slash		0.94 ± 0.21	Particle Size
	Field	Urban Impact	1.07 ± 0.15	and
	RWC[b]		0.67 ± 0.14	Inorganic Composition

[b]Residential wood combustion

81-BCM-a-ENERGY RELATED POLLUTANTS AND EFFECTS MONITORING AND ASSOCIATED METHODS AND TECHNIQUES DEVELOPMENT

1. Energy Related Water Pollutant Standard Reference Materials

1.a. Aqueous Polynuclear Aromatic Hydrocarbons in Water (SRM 1644)

Generator columns for the production of saturated aqueous solutions of anthracene, benz(a)anthracene, and benzo(a)pyrene constitute SRM 1644. The columns were prepared commercially and have been certified by two independent analytical techniques.

The first technique involves quantitative extraction of the PAH from the aqueous stream by an "extractor column" packed with C_{18} bonded phase, use of an acetonitrile-water eluent to transfer components from the extractor column to an analytical C_{18} column for separation of the analyte from non-analyte components, and detection of the analyte by absorbance at 254 nm.

The second technique uses a "standard addition" technique for "on stream" analysis. The effluent from the generator column is mixed with PAH standards dissolved in acetonitrile, and the resultant PAH in the mixed solvent determined by fluorescence.

Preliminary data from the certification are given in Table 11. The final certified values will result from a compilation of the data obtained from both methods. Such a compilation has been completed for benzo(a)pyrene, where:

$$\ln (\text{conc.}) = 20.35 - 5924 \left(\frac{1}{K}\right)$$

where conc. is in units of µg/kg.

or

$$\ln (\text{conc.}) = 1.00 - 5924 \left(\frac{1}{K}\right)$$

where conc. is in moles/liter.

Table 11

Preliminary Results of Analysis Using Two Techniques for Generator Column Aqueous Effluents

Anthracene

Temperature (°C)	Concentration (µg/kg)	
	Technique 1	Technique 2
30	58.8	59.6
25	42.8	42.9
20	31.1	30.9
15	22.6	22.2

Benz(a)anthracene

Temperature (°C)	Concentration (µg/kg)	
	Technique 1	Technique 2
30	12.3	13.0
25	8.86	9.32
20	6.37	6.67
15	4.58	4.78

Benzo(a)pyrene

Temperature (°C)	Concentration (µg/kg)	
	Technique 1	Technique 2
30	2.28	2.26
25	1.62	1.60
20	1.14	1.14
15	0.80	0.81
10	0.57	0.58

Table 12a

Fitted Concentrations Utilizing the Equation for Benzo(a)pyrene Data (in µg/kg)

Temp., C	Concentration	Lower Limit	Upper Limit
10.0	.5616	.5382	.5859
11.0	.6045	.5811	.6288
12.0	.6503	.6270	.6745
13.0	.6993	.6761	.7233
14.0	.7516	.7287	.7753
15.0	.8074	.7848	.8307
16.0	.8669	.8447	.8897
17.0	.9303	.9085	.9527
18.0	.9979	.9764	1.0199
19.0	1.0699	1.0486	1.0916
20.0	1.1465	1.1252	1.1683
21.0	1.2281	1.2062	1.2503
22.0	1.3148	1.2918	1.3382
23.0	1.4070	1.3821	1.4323
24.0	1.5050	1.4774	1.5331
25.0	1.6091	1.5777	1.6410
26.0	1.7196	1.6836	1.7563
27.0	1.8369	1.7952	1.8795
28.0	1.9613	1.9130	2.0108
29.0	2.0932	2.0373	2.1507
30.0	2.2331	2.1685	2.2996

Table 12b

Fitted Concentrations Utilizing the Equation for Benzo(a)pyrene Data in S.I. Units (mol/L)

Temp., C	Concentration	Lower Limit	Upper Limit
10.0	2.2261	2.1336	2.3226
11.0	2.3962	2.3035	2.4926
12.0	2.5780	2.4854	2.6739
13.0	2.7721	2.6802	2.8672
14.0	2.9794	2.8884	3.0732
15.0	3.2005	3.1109	3.2927
16.0	3.4364	3.3482	3.5268
17.0	3.6878	3.6013	3.7764
18.0	3.9557	3.8706	4.0427
19.0	4.2411	4.1568	4.3271
20.0	4.5448	4.4602	4.6310
21.0	4.8680	4.7815	4.9562
22.0	5.2118	5.1208	5.3045
23.0	5.5773	5.4788	5.6776
24.0	5.9657	5.8563	6.0773
25.0	6.3783	6.2541	6.5050
26.0	6.8164	6.6737	6.9621
27.0	7.2813	7.1162	7.4502
28.0	7.7745	7.5832	7.9708
29.0	8.2976	8.0759	8.5253
30.0	8.8520	8.5960	9.1156

*NOTE: Concentrations are reported in units of 10^{-9}.

K is degrees Kelvin in both equations.

The maximum uncertainty for either of the equations between 10 °C and 30 °C (273.15 and 303.15 K) is ± 0.042. Tables 12a andl 2b express the concentrations at one degree intervals between 10 °C and 30 °C.

1.b. First Natural Matrix Trace Organic SRM Issued for Shale Oil

The Center for Analytical Chemistry has in the past conducted several collaborative studies aimed at assessing the accuracy of data obtained from trace organic analytical methodologies. The results of a recent study involving the determination of specified phenols, polynuclear aromatic hydrocarbons, and N-heterocyclics in a shale oil sample by several laboratories revealed large systematic biases among laboratories. One method for enhancing the accuracy of analytical measurements is the use of suitable quality assurance standards or Standard Reference Materials (SRM's). However, until now, SRM's for environmental trace organic analyses were nonexistent due to the lack of analytical methodologies necessary for certification.

Over the past few years, analytical methodologies have been developed and used to certify the first natural matrix SRM for trace-level organic constituents, Organics in Shale Oil, SRM 1580. The quantitation of individual compounds in the complex shale oil matrix necessitated the use of multi-dimensional chromatographic procedures, i.e., gas or liquid chromatography on two columns of different selectivity and/or extremely selective detection methods.

Three different methods of sample preparation were used prior to analysis: simple dilution of the shale oil with methylene chloride (or other suitable solvent); acid/base extraction to isolate acidic, basic, and neutral components; and a high-performance liquid chromatographic

fractionation. Two of the following techniques were employed to determine the certified values for the organic compounds in shale oil: capillary gas chromatography (GC), gas chromatography/mass spectrometry (GC/MS) with single ion (monitoring) for selective detection, and high - performance liquid chromatography (HPLC) with selective fluorescence detection. All GC/MS analyses used the standard addition method for quantitation. The GC and HPLC analyses employed either internal standard, external standard, or standard addition methods. The excellent comparability of the values determined by these different analytical methods is illustrated in Table 13. Table 14 lists values for other compounds determined by only one technique. These values will appear on the SRM certificate for information only. The methods developed for the certification of this SRM are applicable to the determination of similar compounds in other complex natural matrices. Standard Reference Material 1580, Organics in Shale Oil, is intended primarily for evaulating the reliability of analytical methods used for the determination of trace level polynuclear aromatic hydrocarbons, phenols, and nitrogen heterocyclic compounds in shale oil, coal-derived liquids, or petroleum products. In addition, this SRM may be used as a surrogate standard for any complex environmental extract containing classes of compounds for which the SRM is certified.

Table 13. Summary of Results for Organic Compounds in Shale Oil Determined by Two Independent Techniques.

Compound	Sample Preparation Technique	Analytical Technique	Concentration (µg/g)
benzo(a)pyrene	Direct Injection	GC/MS	20 ± 1 (6)[a]
	HPLC	HPLC	23 ± 1 (8)
benzo(e)pyrene	Direct Injection	GC/MS	17 ± 1 (6)
	HPLC	HPLC	20 ± 3 (8)
fluoranthene	Direct Injection	GC/MS	55 ± 5 (6)
	HPLC	HPLC	53 ± 2 (9)
perylene	Direct Injection	GC/MS	2.8 ± 0.5 (5)
	HPLC	HPLC	4.0 ± 1 (11)
pyrene	Direct Injection	GC/MS	101 ± 6 (6)
	HPLC	HPLC	106 ± 10 (9)
phenol	HPLC	GC/MS	412 ± 35 (8)
	Acid/Base Extraction	GC	402 ± 4 (8)
o-cresol	HPLC	GC/MS	386 ± 42 (8)
	Acid/Base Extraction	GC	384 ± 9 (8)
2,6-dimethylphenol	HPLC	GC/MS	183 ± 23 (10)
	Acid/Base Extraction	GC	168 ± 12 (8)
5,6-benzoquinoline	Acid/Base Extraction	Multi-dimensional GC	15.1 ± 1.2 (8)
	HPLC	HPLC	16.3 ± 1.5 (7)

[a] = number of ampoules analyzed.

Table 14. Summary of Results for Organic Compounds in Shale Oil Determined by One Technique.

Compound	Sample Preparation Technique	Analytical Technique	Concentration (µg/g)
benzo(k)fluoranthene	HPLC	HPLC	13
phenanthridine	HPLC	HPLC	45
m-cresol	Acid/Base Extraction	GC	330
p-cresol	Acid/Base Extraction	GC	270
2,4-dimethylphenol	Acid/Base Extraction	GC	380
2,5-dimethylphenol	Acid/Base Extraction	GC	320
2,5,6-trimethylphenol	HPLC	GC/MS	360
2,4,6-trimethylphenol	HPLC	GC/MS	120

a. Shale Oil Round Robin:

Many laboratories are currently involved in the quantitative analysis of individual toxic organic compounds in alternate fuels and energy effluents. For many of these environmental analyses there is little knowledge of the comparability of data from different laboratories, and in most cases probably little knowledge of intralaboratory precision. To gain insight on this matter aliquots of the shale oil sample were sent to six laboratories currently involved in characterizing alternate fuels. The labs were requested to determine the concentrations of selected compounds in the shale oil. The results of this limited interlaboratory exercise are presented in Table 15. The scatter of the results indicates the variability of state-of-the-art quantitative analyses for individual compounds in a complex matrix. It also stresses the need for an SRM such as the shale oil which laboratories can use to guage the accuracy of their analytical methods.

Table 15. Interlaboratory comparison of results of shale oil analyses (ppm).

Compound	NBS[a]	2	3	4	5	6	7
pyrene	107	155	360	150	168	212	141
fluoranthene	61	102	220	80	108	104	112
phenol	395	392	180	-	-	-	399
o-cresol	338	350	150	-	-	-	381
2,4,6-trimethylpyridine	1060	468	460	-	950	-	1092

[a]Results reported by NBS represent the mean of values obtained by GC, GC/MS, and HPLC.

1.c. Work Plan and Evaluation/Feasibility Study of Drilling Fluid Reference Standards for Chemical Analysis

Background

Man's activities in off-shore drilling (as well as on-shore drilling) must proceed in order to locate new sources of oil and gas to satisfy the increasing demands for energy resources. If we are to preserve our renewable resources as we extract oil and gas from the continental shelf, research, development, and monitoring are needed to provide a better foundation for rational decisions on minimizing risks and protecting other resources.

Drilling fluids are now recognized as one of the major factors involved in the success or failure of drilling operations. The composition of a drilling fluid depends upon the formation to be drilled. Drilling fluids normally consist of colloidal suspensions of clay and minerals in water with chemical additives, and are used in production operations to support the borehole, to remove cuttings, and to cool the drill bits. In order to control the physical and chemical properties of drilling fluids, several types of inorganic and organic chemicals are used in conjunction with the clays, minerals, thinning and dispersing agents, etc. Since disposal of the drilling fluids is into water or onto adjacent land, it is essential to characterize these fluids for their chemical constituents in order to evaluate and assess the fate of the chemical constituents (many of them toxic) on the aquatic and terrestrial environment.

Scope

NBS will develop and provide EPA/Gulf Breeze with drilling fluid reference standards for use in characterization efforts and in a quality assurance program to improve and maintain reliability of measurements made on discharges from drilling and production operations.

Milestones:

(1) Obtain candidate reference material(s) from EPA/Gulf Breeze and assess the feasibility for preparing a dry mixture of four major drilling fluid components

(2) If milestone (1) proves feasible, prepare a batch (i.e., grind, blend, sieve) of material and establish homogeneity

(3) Characterize the drilling fluid mixture for several trace elements to be determined by NBS and EPA/Gulf Breeze

(4) Package, label, and provide EPA/Gulf Breeze with drilling fluid reference standard for specified trace elements

(5) Initiate studies on a drilling fluid material chosen in concert with EPA/Gulf Breeze for future (FY81) issuance as a more complex or more characterized standard

Progress

EPA/Gulf Breeze provided NBS with three test "fluids" for feasibility and assessment studies. As a result of these studies, EPA/Gulf Breeze and NBS have agreed that the reference drilling fluid sample should consist of a dry mix of the components found in drilling mud. NBS has ordered and received the five major components of drilling mud - barite, bentonite, chrome lignosulfonate, lignin, and caustic soda. The first three components have been blended in a dual V blender. Samples of this blend will be analyzed to confirm or deny the apparent homogeneity of the sample. Conceivably, some re-segregation of the sample may occur on storage due to the large difference in component densities. Therefore, some effort will be made to determine the degree to which this may happen. Packaging in small units and requiring use of the entire sample in an experiment would be another way around this problem.

If lignin is added in the solid state with caustic soda, two problems arise. First, the oil companies believe that the total mixture of dry components will not mix with water to yield the normal mud. Secondly, caustic soda is hygroscopic and in a flake form (all other components are powders, 200-400 mesh). It would have to be ground (difficult to do) in order to blend well with the other components. At this point, it would be appropriate to solicit reaction to a three component dry mix because of the problems associated with a 5 component mix.

1.d. Laser Analysis of Pollutants in Cryogenic Matrices

Scientists in the NBS Center for Thermodynamics and Molecular Science (CTMS) have designed and completed the first stage of testing of a molecule specific measurement technique for the analysis of complex environmental samples for evaluation or compliance with EPA standards. In the past several years it have been recognized that realistic legislation impacting environmental quality must be targeted at a small number of potentially harmful chemicals, rather than gross regulation of, for instance, total organic carbon. Of the existing techniques, the computer controlled gas chromatograph-mass spectrometer system is the most powerful in terms of sensitivity and specificity. A high degree of sensitivity is required since many of these regulated chemicals have toxic or carcinogenic effects at levels in the ppt level; specificity is required since in many cases the toxicity of a given chemical species may vary as much as several orders of magnitude between isomers. This is particularly true for the dioxins.

The laser technique offers a quantiative sensitivity comparable to that obtained by state-of-the-art GC-MS systems, a much higher degree of selectivity, and should, when fully implemented, be suitable for certification of environmental SRM's and performance of referee-type measurements. This technique involves laser Raman scattering from molecules isolated in a cryogenic matrix. Raman spectroscopy provides a valuable fingerprint of the vibrational modes of the molecules present allowing for identification based on comparison to a library file of known spectra. Since the molecules are physically trapped in an inert matrix, there is no interference in the Raman spectrum of the first species due to the presence of a second or other species, the signals from a complex mixture such as expected from real environmental samples is simply the sum of the individual components.

To date, NBS scientists have successfully demonstrated the potential sensitivity and selectivity of this sytem in the analysis of lab-

oratory samples of complex mixtures of volatile organic species at the sub nanogram level (corresponding to recapture of environmental samples at the ppt level). In these studies isomeric species were readily resolved with a 0.3 cm^{-1} resolution (isomeric peaks often show Raman shifts of 10 -50 cm^{-1}). The group recently acquired an LSI-11 controlled optical multichannel analyzer (OMA) and commercial gas chromatograph and have refabricated the sampling system to provide for higher sensitivity and sample through-put and to allow analysis of real world samples.

The status of this work is now at the point that within 6 months our operative system should be ready for the acquisition, separation and analysis of environmental samples. Considerable help was received from colleagues at Argonne National Laboratory. The initial tests of this system will include analysis of laboratory and real world samples of the tetrachlorodibenzo-dioxin isomers which cannot currently be distinguished by any existing technique at any concentration.

81-BCM-b-ENERGY RELATED POLLUTANTS AND EFFECTS MONITORING AND ASSOCIATED METHODS AND TECHNIQUES DEVELOPMENT

1. Development of Organic SRM's for the Calibration of Energy-Related Water Pollutant Measurement Methods

1.a. Analysis of Phenolic and Polynuclear Aromatic Hydrocarbon Species in Alternate Fuels and Effluents

Several coal gasification, oil shale refinery, and oil refinery aqueous effluents have been analyzed for selected phenolic and polynuclear aromatic hydrocarbon (PAH) species. A simple one-step organic extraction has been developed to isolate the phenolic and PAH compounds prior to quantitative analysis by selected ion monitoring (SIM) GC/MS. Individual compound concentrations were determined by an internal standard method (where suitable internal standards were available) or by comparison with a series of external standards.

Samples

The aqueous effluents were obtained from the Gulf South Research Institute, New Orleans, Louisiana. They were stored in amber glass bottles at 4 °C until analyzed. Prior to analysis, each sample was equilibrated at room temperature, homogenized by mixing vigorously for 1 minute, and filtered through Whatman #41 paper to remove any suspended particulate matter and/or insoluble oil. One hundred (100) mL of each sample was analyzed as described below:

Polynuclear Aromatic Hydrocarbons: The effluent (100 mL) was spiked with an appropriate amount of pyrene-d_{10} internal standard (IS). The sample was filtered and extracted with 100 mL CH_2Cl_2. The organic extract was dried by filtering through a cone of anhydrous Na_2SO_4. The sample volume was reduced to ~100 µL under a stream of dry N_2 for GC/MS analysis. All samples were analyzed in duplicate, and a sample blank consisting of 100 mL deionized H_2O was also analyzed. 1 to 2 µL of the concentrated extract was chromatographed on a 30 m SE-30 fused silica wall-coated open tubular (WCOT) column, which was

interfaced directly to the ion source of a quadrupole mass spectrometer. The mass spectrometer was operated in the selected ion monitoring mode. The molecular ions for the analytes (fluoranthene m/z 202, pyrene m/z 202, benzo(a)-pyrene [B(a)P] m/z 252, benzo(e)pyrene [B(e)P] m/z 252, perylene m/z 252) and the pyrene-d_{10} internal standard (m/z 212) were monitored with a mass spectrometer dwell time of 100 ms (see Figure 11).

Relative response factors for the analytes relative to the pyrene-d_{10} internal standard were determined from a gravimetrically prepared solution of the pure compounds. Individual compound concentrations were determined from the analyte and internal standard peak areas and the experimentally determined relative response factors. The results of these determinations are shown in Table 16. PAH concentrations were also determined in a separate series of experiments using an external standard method. No precision data is reported for these values as only one determination of each compound was made. In most cases, however, the agreement between the internal standard and the external standard determinations is very good.

Phenols: The following phenols were determined in the aqueous effluents: phenol, o-cresol, m-cresol, p-cresol, 2,4- + 2,5-dimethylphenol, and 2,6-dimethylphenol. One hundred (100) mL of the effluent was spiked with an appropriate amount of 2-chlorophenol as an internal standard. The pH of the sample was adjusted to ~1 with H_2SO_4 and the sample extracted with 50 mL CH_2Cl_2. The sample volume was reduced to 100-200 µL under a stream of dry N_2, and 1-2 µL aliquots analyzed by GC/MS. Chromatographic separations were carried out on a 20 m Pluronics PL-64 WCOT column which gives excellent resolution of all the phenols except the 2,4- and 2,5-dimethylphenols which are unresolved (the values determined represent a sum of the concentrations of the two isomers). The molecular ions for the analytes and the internal standard were monitored in real time with a 100 ms dwell time in order to insure at least 20 data points across the chromatographic peak (see Figure 12).

Relative response factors for the analytes relative to the 2-chlorophenol internal standard were determined from a gravimetrically prepared solution of

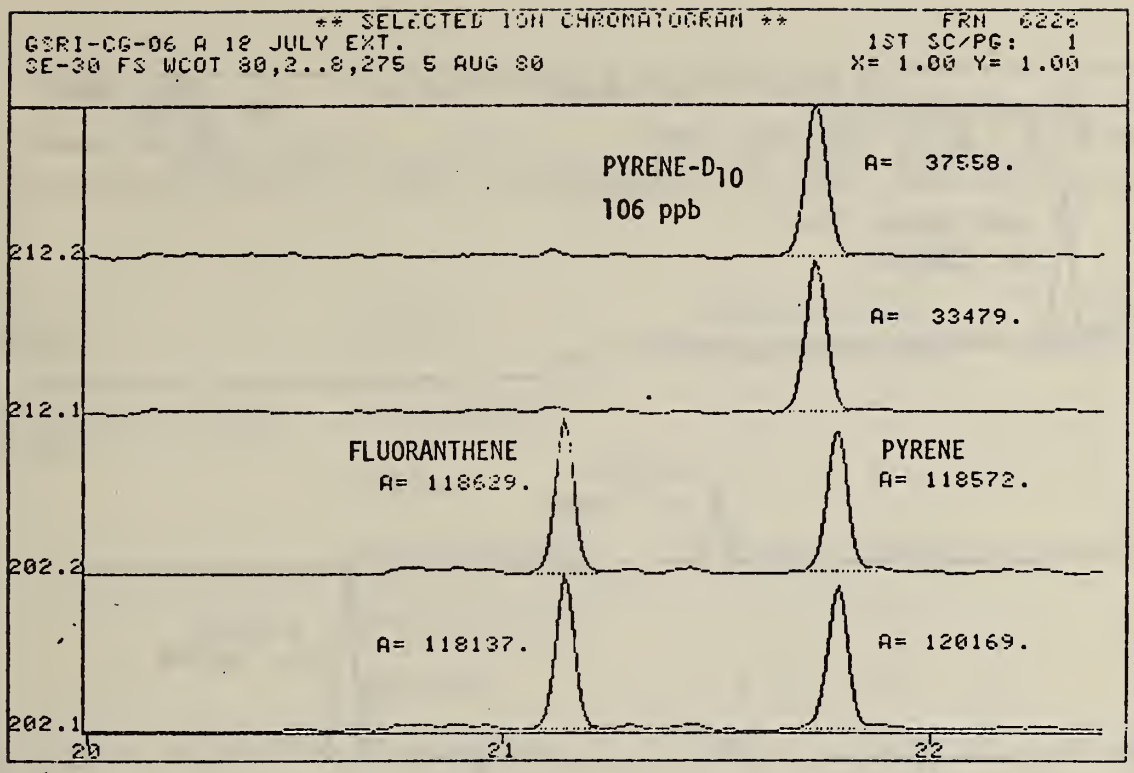

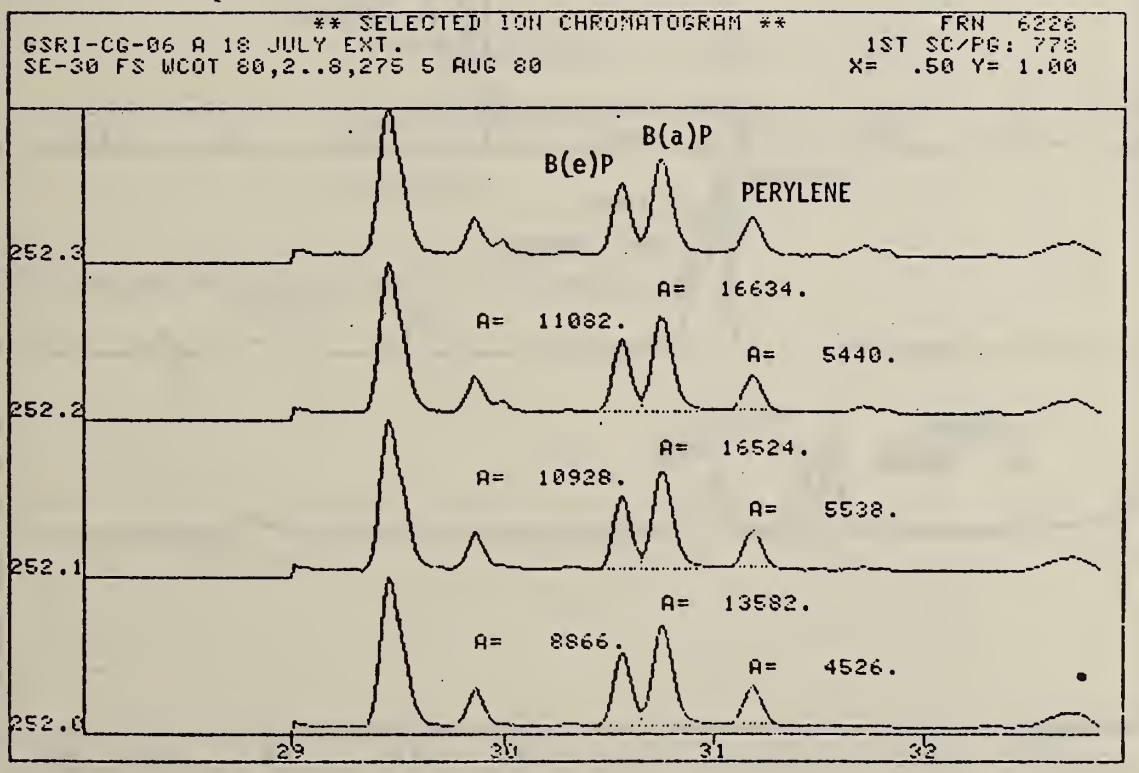

Figure 11

GC/MS SIM Analysis of PAH in Coal Gasification Effluent

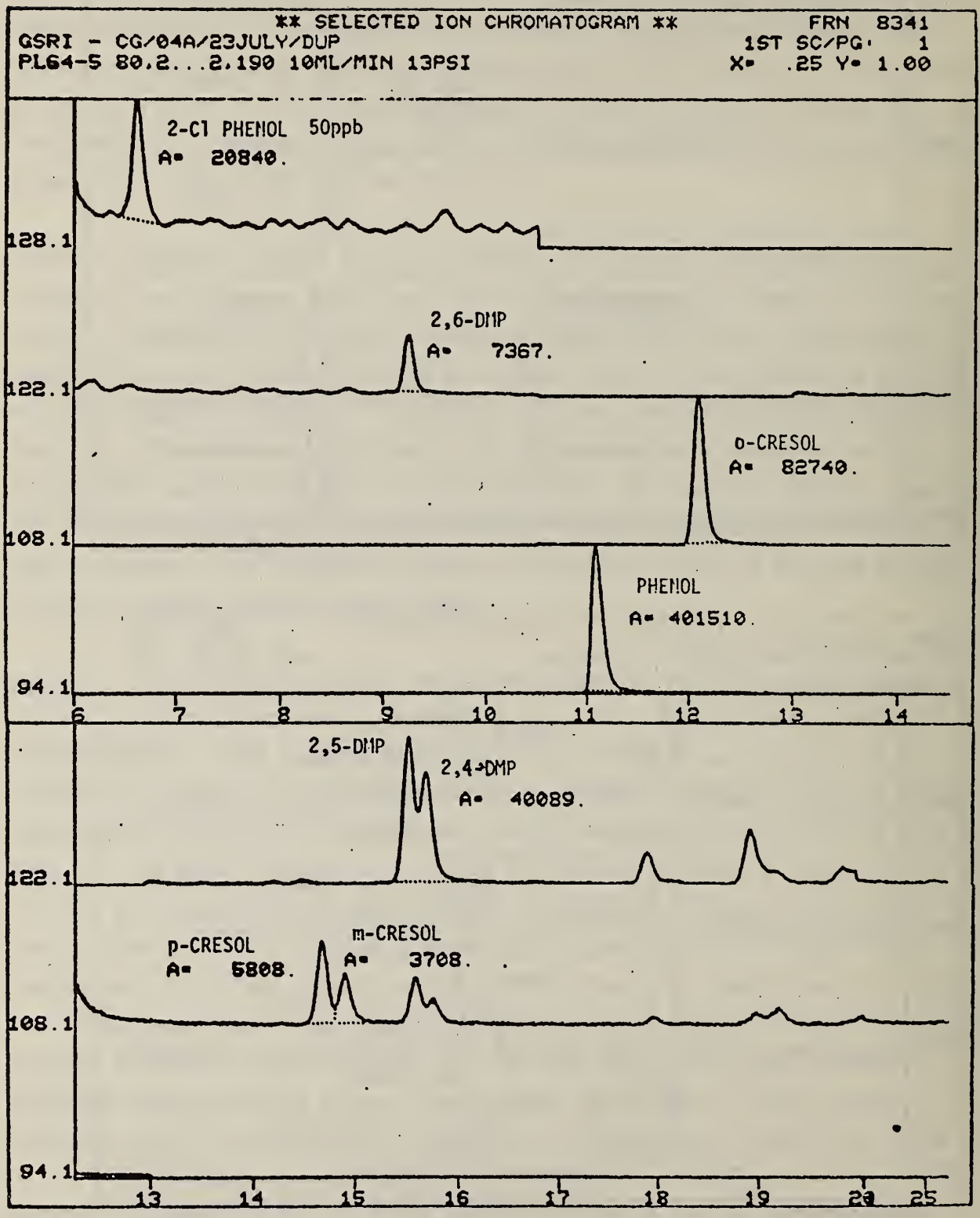

Figure 12

GC/MS SIM Analysis of Phenols in Coal Gasification Effluent

Table 16

Polynuclear Aromatic Hydrocarbons in Energy Effluents
(ppb)

Sample	Analyte	Concentration Internal Standard	External Standard
Coal gasification effluent CG-04	fluoranthene	11.6 ± 0.2	7.5
	pyrene	11.0 ± 0.1	7.6
	benzo(e)pyrene	0.92 ± 0.02	0.7
	benzo(a)pyrene	1.6 ± 0.3	1.5
	perylene	0.5 ± 0.1	0.5
Coal gasification effluent CG-06	fluoranthene	303 ± 2.8	296
	pyrene	281 ± 12	244
	benzo(e)pyrene	30 ± 0.7	37
	benzo(a)pyrene	58 ± 1.4	57
	perylene	18 ± 0	86*

*non-analyte interference co-eluting with perylene.

Table 17

Phenols in Energy Effluents
(ppb)

	Analyte					
Sample	Phenol	2,6-DMP	2,4- and 2,5-DMP	o-Cresol	m-Cresol	p-Cresol
CG-04 (IS)*	1038	27	191	311	16	27
CG-04 (ES)**	730	27	157	249	7	16
CG-06 (ES)	732	289	887	492	329	250
OS-42 (ES)	< 10	< 10	< 10	< 10	< 10	< 10
OS-42 (IS)	< 10	< 10	ND***	< 10	ND	ND
OR-21 (IS)	< 10	< 10	< 10	< 10	< 10	< 10
OR-23 (IS)	< 10	< 10	ND	< 10	ND	ND
OR-25 (IS)	< 10	< 10	< 10	< 10	ND	ND

Values represent an average of 2 determinations.

Notes: DMP ≡ dimethylphenol
CG ≡ coal gasification effluent
OS ≡ oil shale effluent
OR ≡ oil refinery effluent

*IS = internal standard
**ES = external standard
***ND = not detected

the pure compounds. Individual analyte concentrations were determined from the analyte and internal standard peak areas and the experimentally determined relative response factors. The results of these determinations are shown in Table 17. Concentrations in the coal gasification effluent CG-06 and the oil shale effluent OS-42 could not be determined by the internal standard method because of a co-eluting interference at the retention time of the 2-chlorophenol internal standard (the co-eluting compound(s) produced a significant ion current at m/z 128, the Cl-35 molecular ion of the internal standard). Determinations for these samples were based on a series of external standards.

1.b. Combined LC/MS Technique for Direct Quantitative Analysis of Individual Organic Compounds in Complex Mixtures

An interface for a conventional liquid chromatograph and a conventional mass spectrometer has been constructed which operates on the principle of pre-concentrating a liquid stream and then admitting part of it to the ionization region of the mass spectrometer. The selectivity of the mass spectrometer and the reproducible behavior of the entire system allow the direct quantitation of substances in complex mixtures.

The pre-concentration is accomplished by allowing the effluent from the liquid chromatograph to flow down a heater wire. The evaporation of solvent has yielded up to a 20-fold enrichment of analyte, and it is believed that 100-fold enrichment is feasible.

The flow into the mass spectrometer is controlled by a small needle valve built into the tip of the inlet tube. The valve is formed by a 0.05 mm teflon film at the tip of the tube pierced by a pointed 0.1 mm wire which passes throught the bore of the tube. Flow rate into the mass spectrometer can be controlled in the range of 0-20 μL/minute. Since all of the pressure drop occurs at the high vacuum end of the tube, boiling within the tube with consequent unstable flow is avoided.

The stability of the system is such that quantitation can be done with external as well as internal standards. Figure 1 (pg. 11) shows typical chromatograms from the determination of phenol in a shale oil matrix using external standards. The level found was 400 ± 40 ppm, a value in good agreement with, and with precision comparable to, two other methods requiring lengthy sample pretreatment. The direct shale oil determination by LC/MS required about 15 minutes per run.

1.c. Development of Phenol in Water SRM

To date, a comparison of the stability of some selected phenols in distilled water and in industrial wastewater using high-performance liquid chromatography (HPLC) has been made. A standard solution of some of the phenols on the Priority Pollutant List were used to spike both the distilled water (Table 18) and industrial wastewater (Table 19). Since a detectable amount of phenol was initially found in the industrial wastewater, no additional phenol was added. The spiked solutions were stored in both amber and clear ampoules. This was done to observe any possible degradation of the sample due to light. Also, to observe the correlation between the loss of phenolic compounds and microbiological activity which possibly effects chemical stability in wastewater, a preservative technique used by Carter et al.[1] (pH 3.7 data), was employed for one set of the wastewater samples.

There is no clear explanation for the behavior of the phenolic compounds in the preserved industrial wastewater. Our results indicate that the solutions have been stable at neutral pH (see Table 19).

To determine the stability of some phenols in water during a more long-term study, a four-year-old phenol in distilled water solution was analyzed. The results are shown in Table 20.

---

[1]From the draft of "Preservation of Phenolic Compounds in Wastewater" by Mark Carter and Madeline Huston, Central Regional Laboratory, Environmental Protection Agency.

In the future, a similar study using two less concentrated (<10 ppm) solutions of some phenols in distilled water and in industrial wastewater without sample preservation will be carried out.

Table 18

Phenols in Distilled Water Stability Study

	Concentration (ppm)									
	Concentration Added	Day 2[a]	Day 6[b]	Day 56[b]	Day 58[a]	Day 58[b]	Day 84[a]	Day 185[a]	Day 202[a]	Day 20
Phenol	24.05	24.06±2.0	23.57±0.7	23.42±1.1	22.24±1.1	23.33±1.1	23.93±1.4	24.29±0.4	24.39±1.3	23.56±1.
2-Chlorophenol	35.92	37.16±1.8	35.46±1.9	34.78±1.4	33.09±1.4	35.12±1.4	35.90±1.9	36.27±0.6	35.12±0.6	32.85±0.
2-Nitrophenol	23.09	21.77±1.4	21.88±0.3	20.77±0.4	20.58±0.3	18.74±0.5	23.05±1.1	22.84±0.2	22.58±0.2	21.41±0.
2,4-Dimethylphenol	14.58	13.90±0.9	13.21	14.62±1.2	13.50±0.6	14.52±0.6	13.59±0.8	14.62±0.5	14.34±0.7	13.85±0.
4,6-Dinitro-o-cresol	35.26	30.85±1.9	32.57±0.5	36.64±2.5	36.53±2.5	31.60±2.2	36.31±0.7	31.37±0.2	34.98±1.4	34.33±1.
Pentachlorophenol	14.00	13.32±1.1	14.61±1.5	13.13±1.7		14.08±1.8		14.06±0.4	14.09±0.5	14.56±0.

[a]Solution stored in amber ampoules

[b]Solution stored in clear ampoules

Table 19

Phenols in Industrial Wastewater Stability Study

	Concentration (ppm)										
	Concentration Added	Day 2 pH Neutral	Day 2 pH 3.7	Day 47 pH 3.7	Day 61 pH Neutral	Day 61 pH 3.7	Day 96 pH Neutral	Day 96 pH 3.7	Day 139 pH Neutral	Day 141 pH Neutral	Day 175 pH Neutral
Phenol		55.76±1.2	56.38±3.6	18.24±0.5	56.10±0.6	15.55±0.5	54.48±2.6	16.10±1.9	54.0 ±2.5	53.68±1.8	54.29±2.3
2-Chlorophenol	18.55	17.99±0.4	22.04±0.3	13.19±0.3	17.88±0.4	20.04±0.3	17.92±0.9	11.55±0.6	18.26±0.5	20.29±1.4	18.89±1.0
2-Nitrophenol	10.80	10.69±0.2	10.66±0.3	10.46±0.3	10.81±0.2	10.25±0.2	11.04±0.5	11.29±0.5	11.97±0.2	11.37±0.5	10.70±0.2
2,4-Dimethylphenol	19.65	19.48±0.9	16.31±0.4	16.37	19.22±0.9	11.42±0.9	19.05±1.2	16.20±1.3	18.80±0.9	17.89±0.9	19.61±0.5
4,6-Dinitro-o-cresol	17.20	17.71±1.0	17.70±0.9	17.39±3.6		25.94±0.3	18.55±0.8	21.25±1.0	19.02±1.0	17.03±0.2	18.50±0.2

[c]Ampuules were stored at 16 °C.

Table 20

Stability of Selected Phenols in Distilled Water

Compound	Gravimetric Concentration Added (mL/L)	Day 1[b]	Day 92[c]	Day 175[c]	Day 491[c]	Day 608[c]	Day 804[c]	Day 1525[d]
Phenol	21.0	19.9 ± 0.4	22.2 ± 1.1	21.7 ± 0.5	21.0 ± 0.4	20.5 ± 0.3	20.8 ± 0.6	21.0 ± 0.1
p-Cresol	54.3	53.9 ± 0.2	57.2 ± 1.2	55.0 ± 0.8	54.6 ± 1.3	52.8 ± 0.7	54.0 ± 1.6	53.0 ± 1.0
o-Cresol	34.3	35.3 ± 0.4	37.6 ± 1.1	34.5 ± 0.9	33.5 ± 0.9	32.5 ± 0.5	33.1 ± 0.7	32.6 ± 0.5
2-Naphthol	71.4	71.4 ± 0.4	70.6 ± 0.9	69.5 ± 0.7	67.1 ± 0.7	67.6 ± 0.9	68.8 ± 3.4	62.9 ± 0.4
2,4,6-Trimethylphenol	38.3	38.8 ± 0.7	39.3 ± 3.3	35.4 ± 3.6	34.3 ± 0.3	33.8 ± 1.3	33.1 ± 3.9	28.1 ± 0.5

[a]Concentrations measured by high performance liquid chromatography

[b]Results represent the combined average obtained from triplicate analysis of five ampoules.

[c]Results represent the combined average obtained from triplicate analysis of two ampoules.

[d]Results represent the combined average obtained from triplicate analysis of one ampoule.

81-BCN-ENERGY RELATED POLLUTANTS AND EFFECTS MONITORING AND ASSOCIATED METHODS AND TECHNIQUES

1. Radiological Pollutant Quality Assurance

1.a. ^{232}Th Solution

Thorium-232 is a radionuclide whose presence is of concern when in effluent and run-off waters from some types of mines, ore mills, and tailing piles, and in certain drinking water supplies. This calibrated solution of ^{232}Th is for laboratories that assay these waters. The starting material was all thorium nitrate, chosen so that the ^{232}Th progeny would be in radioactive equilibrium. The ^{232}Th content was assayed by isotope-dilution mass spectrometry and confirmed by γ-ray counting. Two impurities were observed and measured: ^{230}Th by means of α-particle spectrometry with a silicon surface-barrier detector, and ^{226}Ra by means of Ge(Li) detector spectrometry. The α-particle spectrum is shown in Figure 13, and the Report of Calibration is given at the end of this section. Two hundred ampoules of this solution were provided to EPA-LV.

1.b. Mixed Radionuclide Solutions

Two mixed radionuclide solutions were needed by EPA to distribute to laboratories that assay for radionuclides in drinking water. One solution mixture is a ten-fold dilution of the other. Each mixture contains ^{3}H, ^{90}Sr-^{90}Y, ^{134}Cs, ^{226}Ra and its progeny, and natural uranium and its progeny. The ^{228}Ra and natural uranium components were developed earlier in this multi-year program; the ^{134}Cs solution was calibrated specifically for these mixtures. A Report of Calibration for one of the mixtures is given at the end of this section.

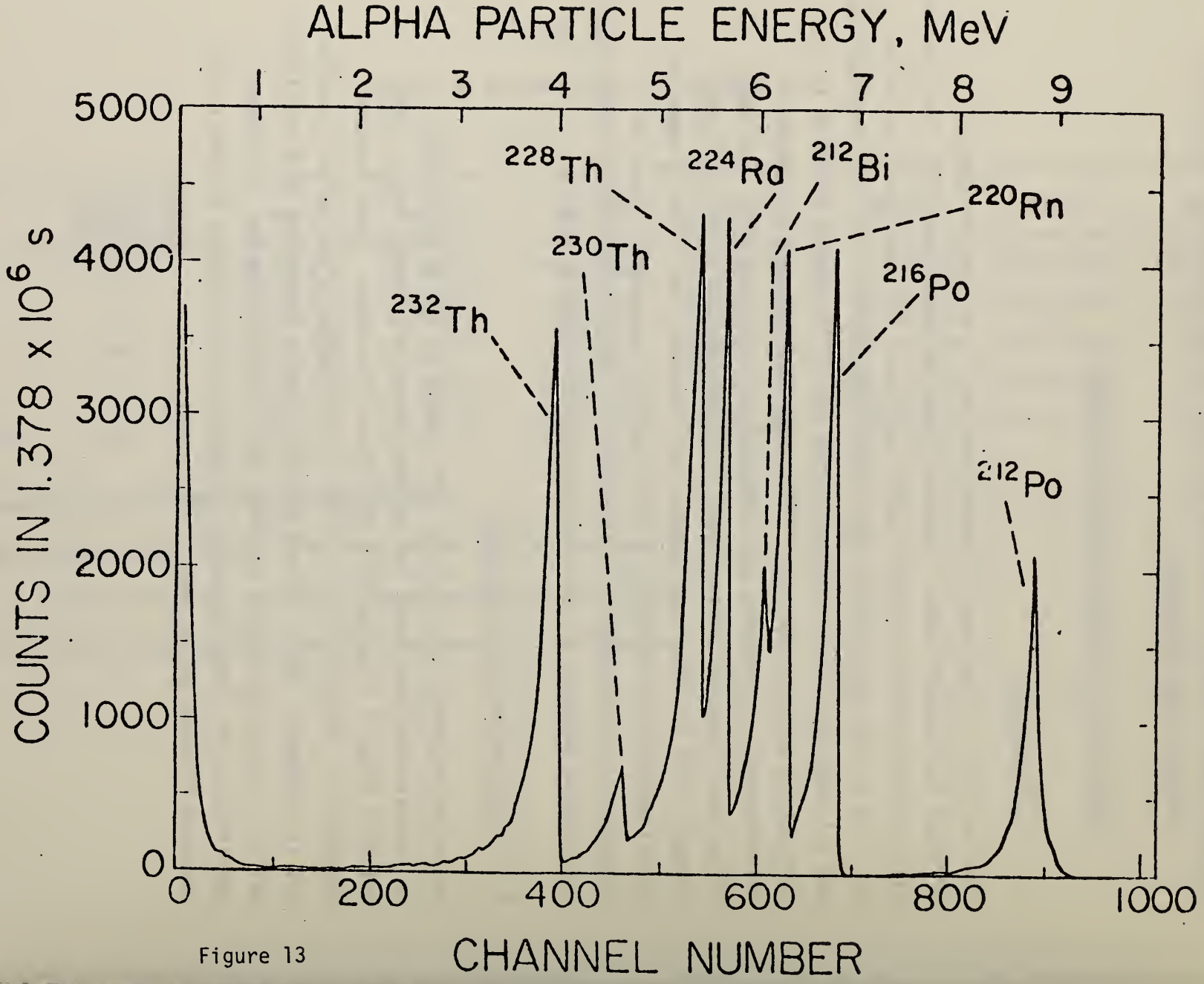
ALPHA PARTICLE ENERGY, MeV
1
2
3
4
5
6
7
8
9
5000
4000
3000
2000
1000
0
COUNTS IN 1.378 x 10^6 s
228Th
224Ra
212Bi
220Rn
230Th
216Po
232Th
212Po
0
200
400
600
800
1000
CHANNEL NUMBER

Figure 13

U.S. DEPARTMENT OF COMMERCE
NATIONAL BUREAU OF STANDARDS
WASHINGTON, D.C. 20234

REPORT OF CALIBRATION

THORIUM-232 SOLUTION

prepared for the

Quality Assurance Division

Environmental Monitoring and Support Laboratory
U.S. Environmental Protection Agency
Las Vegas, Nevada

This solution consists of thorium-232 and progeny in equilibrium in approximately 4.0 grams of one-molar nitric acid in a flame-sealed borosilicate-glass ampoule. The solution was prepared by dissolving old thorium nitrate in dilute nitric acid and filtering the solution through a membrane-type filter having 0.3-micrometer openings. Information from the supplier about the thorium nitrate is given in the appendix to this Report.

Two hundred and twenty ampoules containing approximately equal portions of this solution were prepared. Six of these ampoules were assayed for thorium concentration by isotope-dilution mass spectrometry in May 1979. These assays by the Inorganic Analytical Research Division, National Bureau of Standards, are described in the attached memorandum. The mean value from the assays is 0.04738 gram of total thorium per gram of solution. The total uncertainty in this value is 0.5 percent.

The radioactivity concentration of thorium-232 in the solution, which was calculated from the mass-spectrometric value and the conversion factors and constants in Table 1, is

$$*1.92 \times 10^{2}\ s^{-1}g^{-1} \pm 1.8\%*.$$

In making this conversion, all of the thorium was assumed to be thorium-232, on a mass basis.

The uncertainty in the radioactivity concentration, 1.9 percent, is the linear sum of the total uncertainty in the mass-spectrometric value and three times the uncertainty in the thorium-232 half life.

The thorium nitrate from which this solution was prepared contains radium-226 and thorium-230 impurities. An ampoule of the solution was assayed for thorium-232 and radium-226 by measuring the emission rates of gamma rays from the decay of their respective progeny with a Ge(Li)-detector spectrometer. The radioactivity concentra- of thorium-232 obtained from this assay agreed, to within four percent, with the value derived from the mass-spectrometric assays. The ratio of the radioactivity concentration of radium-226 to that of thorium-232 was 0.010 ± 0.003 in July 1979.

The thorium-230 to thorium-232 activity ratio of a dried deposit of this solution was calculated from the results of silicon surface-barrier-spectrometer measurements to be 0.15 ± 0.01. The radioactivity concentration of uranium-238 was estimated from the alpha-particle spectra to be less than 0.5 percent of that of thorium-232, and likewise for uranium-234.

TABLE 1. RELEVANT CONVERSION FACTORS AND CONSTANTS

Half life of ^{232}Th	= (1.405 ± 0.006) x 10^{10} y (1)
Atomic mass of ^{232}Th	= (232.038053805 ± 0.000002515) amu (2)
Avogadro constant	= (6.0220978 ± 0.0000010) x 10^{23} (3)
Length of tropical year	= 3.155693 x 10^{7} s (a)

(a) Based on the ephemeris second.

REFERENCES

1) M. R. Schmorak, "Nuclear Data Sheets for A=232, 236, 240", Nucl. Data Sheets, 20, 165 (1977).

2) A. H. Wapstra and K. Bos, "The 1977 Atomic Mass Evaluation, Part I. Atomic Mass Table", Atomic and Nucl. Data Tables, 19, 177 (1977).

3) Recent, unpublished value, National Bureau of Standards.

For the Director,

W. B. Mann

W. B. Mann, Principal Scientist
Radioactivity Group
Center for Radiation Research

March 12, 1980

APPENDIX TO REPORT OF CALIBRATION

THORIUM-232 SOLUTION

The following set of data about the tnorium nitrate used for this solution was provided by the supplier, and is given here for information only.

The thorium in the compound, $Th(NO_3)_4 \cdot 6H_2O$, was purified in 1906. Spectrophotometric assays of the compound in 1954 gave these results for some impurity metals.

Element	*Content, ppm*
Li	< 5
Na	< 25
K	< 5
Ca	3
Rb	< 5
Sr	< 3
Cs	< 25
Ba	3

FORM NBS-443
(REV. 12-43)

U.S. DEPARTMENT OF COMMERCE
NATIONAL BUREAU OF STANDARDS
WASHINGTON, D.C. 20234

REPORT OF CALIBRATION

MIXED RADIONUCLIDE CALIBRATED SOLUTION M1

prepared for the

QUALITY ASSURANCE DIVISION
U.S. ENVIRONMENTAL PROTECTION AGENCY
LAS VEGAS, NEVADA

This calibrated solution consists of hydrogen-3, strontium-90-yttrium-90, cesium-134, radium-226 and its progeny, radium-228 and its progeny, and uranium of natural isotopic composition and its progenies in approximately 4.2 g of carrier solution in a flame-sealed, borosilicate-glass ampoule. The carrier solution is 1 M HNO_3 containing approximately 10 μg each of stable strontium, yttrium, cesium, and barium per gram of solution, and is approximately 0.1 M in HCl. The ampoule contains part of a master solution which was prepared by gravimetric additions of calibrated solutions of the radionuclides to a known mass of the carrier solution.

The radioactivity concentrations on January 1, 1980, the total uranium concentration by mass, their uncertainties, and the half lives used in the decay calculations are given in the attached table.

The hydrogen-3 used in the preparation of this mixture was Standard Reference Material (SRM) 4927-B. The strontium-90-yttrium-90 was a portion of the solution from which SRM 4919-D was quantitatively prepared. The activity of the cesium-134 solution was measured using the National Bureau of Standards (NBS) pressurized "4π"γ ionization chamber that had previously been calibrated with a cesium-134 standard in terms of a radium-226 reference source. The radium-226 used in the preparation of this mixture was a portion of the solution from which SRM 4953-B was quantitatively prepared. The radium-228 was the NBS calibrated solution of July 1977. The uranium in the mixture came from the NBS calibrated solution of natural uranium of November 1978, plus part of the more concentrated solution from which the 1978 uranium solution was quantitatively prepared.

The total uncertainty in the radioactivity concentration of each radionuclide and in the total uranium concentration by mass is the linear sum of the 99-percent confidence limits for the mean and the estimated upper limits of conceivable systematic errors in the calibration, the decay calculation (where applicable), and the preparation of this solution.

Each radioactive component of the mixture was examined for gamma-ray-emitting impurities using germanium-spectrometer systems that covered the energy region from 90 to 1900 keV. Radium-226 and its progeny were observed in the radium-228 and uranium solutions. Radium-228 and its progeny were observed in the uranium solution. The radium-226 and radium-228 impurities are included in the total radioactivity concentrations reported for these nuclides. No other gamma-ray-emitting impurities were identified.

For the Director,

W. B. Mann

Attachment
March 1980

W.B. Mann, Principal Scientist
Radioactivity Group
Center for Radiation Research

MIXED RADIONUCLIDE CALIBRATED SOLUTION M1

PARENT RADIO-NUCLIDE	$s^{-1}g^{-1}$ ON JAN. 1, 1980	UNCERTAINTY, %			HALF LIFE, YEARS
		RANDOM (99% C.L.)	SYSTEM-ATIC	TOTAL	
^{3}H	2353	0.2	0.5	0.7	12.35 ± 0.01[b]
^{90}Sr	14.5	1.3	0.8	2.1	29.12 ± 0.24[b]
^{134}Cs	104.3	0.4	1.2	1.6	2.062 ± 0.005[b]
^{226}Ra	8.88	0.1	1.6	1.7	1600 ± 7[b]
^{228}Ra	7.28	1.4	1.9	3.3	5.75 ± 0.03[c]
^{234}U	12.2	3.9	1.3	5.2	(2.445 ± 0.010) x 10^{5}[c]
^{235}U	0.5851	0.1	0.3	0.4	(7.038 ± 0.005) x 10^{8}[d]
^{238}U	12.68	0.1	0.3	0.4	(4.468 ± 0.003) x 10^{9}[c]
TOTAL U	1.028[a]	0.1	0.1	0.2	----------

[a] Milligrams of U per gram of solution, by isotope-dilution mass spectrometry. The radioactivity concentrations of the uranium isotopes were determined from this concentration, the isotopic abundances measured by mass spectrometry, and the respective uranium half lives.

[b] NCRP Report No. 58, App. A, National Council on Radiation Protection and Measurements, Washington (1978).

[c] D.C. Kocher, ORNL/NUREG/TM-102, Oak Ridge National Laboratory, Oak Ridge, TN (1977).

[d] M.R. Schmorak, Nucl. Data Sheets, 21, 91 (1977).

APPENDIX 1

CONTEMPORARY PARTICULATE CARBON*

Lloyd A. Currie
Center for Analytical Chemistry
National Bureau of Standards
Washington, D.C. 20234

To be published in the Proc. of the International Symposium on Particulate Carbon: Atmospheric Life Cycle, sponsored by GM Research Labs., October, 1980.

---

*Contribution of the NBS, not subject to copyright.

ABSTRACT

Advances in natural radiocarbon measurement techniques have made it feasible, for the first time, to assess the contribution of biogenic (contemporary) carbonaceous sources to individual chemical fractions in milligram quantities of atmospheric particles. Isotopic measurements for source reconciliation are doubly important when dealing with pure species, such as methane, carbon monoxide or elemental carbon, because they represent the only compositional information obtainable. Elemental carbon is of special interest in this regard because of changing energy patterns associated with both contemporary (wood-burning) and fossil (diesel fuel and unleaded gasoline) carbon. Following a review of the assumptions underlying the use of radiocarbon as a biogenic tracer and the status of minicounter and accelerator techniques for the assay of milligram and microgram samples, a survey is presented of recent observations on urban and rural carbonaceous particles. Results for these particles, which have been fractionated according to size or volatility, have exhibited the full range from fossil to biogenic source dominance.

Keywords: Accelerator mass spectrometry; air pollution sources; atmospheric particulate matter; biogenic carbon; carbonaceous particles; carbon-13; contemporary carbon; elementary carbon; fossil fuel; natural tracer; radiocarbon; urban and rural carbonaceous aerosols.

INTRODUCTION

One of the foremost questions involved in our understanding of the atmospheric cycle of particulate carbon is the quantitative assessment of perturbations introduced through human activities. Although natural emissions of carbonaceous gases and particles clearly predominate on a global scale [1-3], man's use of coal, petroleum, natural gas and wood as fuel is known to have very severe consequences for particulate pollution ranging from local (especially urban) episodes to long-range effects [3-6]. A major objective of our research program is therefore the deconvolution of sources of atmospheric carbon through the analysis of ambient samples, with special emphasis on fine particle ($\lesssim$2 μm) elemental carbon, because of important effects on health, climate and visibility [7-9].

Naturally-occurring isotopes of carbon -- ^{12}C, ^{13}C, ^{14}C (radiocarbon) -- provide important tools for the deconvolution process, for their isotopic concentrations ($^{13}C/^{12}C$, $^{14}C/^{12}C$) differ significantly among different classes of potential source material. As indicated in Table 1, for example, measurement of $\delta^{13}C$ -- the deviation of the $^{13}C/^{12}C$ ratio from that of the PDB standard [10] -- allows one to distinguish between carbon originating from species such as carbonate minerals, marine plants, petroleum and natural gas, or carbon from C_3 and C_4 terrestrial vegetation [11,12]. Of greater importance, radiocarbon serves as a unique discriminator between contemporary biogenic (e.g., vegetation) and fossil organic matter [13]. The measurement of radiocarbon

thus serves as a very important complement to indirect methods (chemical element balance, factor analysis, dispersion modeling) for inferring sources of ambient carbonaceous particles. Its special characteristics are that it is a direct and unique indicator of biogenic carbon, and that, along with $\delta^{13}C$ it is robust with respect to changes during transport. Also, for single chemical substances such as elemental carbon, isotopic measurements provide the only compositional information attainable.

Since the preceding conference on atmospheric particulate carbon, at which we reported the first radiocarbon results for milligram quantities of carbonaceous particles [14], there have been some important societal and technical developments. In the first category, the need for a reliable, direct tracer for carbonaceous emissions has been magnified because of increases in wood-burning and in the use of diesel fuel and unleaded gasoline. (The relative decrease in the mix of pre-1975 automobiles is, in effect, causing the "loss of a tracer," i.e., lead upon which the chemical element balance method heavily depended.) Technical progress includes improved control and demonstrated reliability of our mini-gas proportional radiocarbon counting system, and most importantly, the introduction of the accelerator method of atom counting [15,16], which is likely to extend the range of sample sizes downward by another three orders of magnitude, to about 10 μg of carbon [17].

This development is of special consequence for elemental carbon, because this chemical form appears to be optimal for placement in the tandem accelerator sputter ion source [18], and the (sampling) blank for elemental carbon appears to be far lower than that for organic carbon [19].

Following a brief review of recent developments in small sample radiocarbon measurement and critical assumptions involved in interpreting the resulting data, we shall present a summary of several recent applications to urban and rural ambient aerosols which have helped to establish the validity of the method and which have provided a direct measure of the importance of biogenic sources on individual chemical and physical (size) fractions of carbonaceous particulate matter.

BIOGENIC CARBON TRACING -- METHODS AND CAUTIONS

The phenonemon which makes possible the use of radiocarbon as a direct tracer for sources of biogenic carbon is the same as that upon which radiocarbon dating is based [20]. That is, all living matter is in (approximate) isotopic equilibrium with atmospheric CO_2 which continually acquires radiocarbon following cosmic ray neutron capture on ^{14}N in the atmosphere. Unlike radiocarbon dating, in which ^{14}C concentrations are related to age, biogenic carbon tracing is based on isotope dilution -- the ^{14}C concentration in an ambient sample reflecting directly the mixing ratio of contemporary ("living") carbonaceous material and fossil material. Carbonaceous

substances of intermediate age -- e.g., 500 to 20,000 years -- are largely absent from atmospheric particulate matter.

Progress in the measurement of natural radiocarbon is indicated in Table 2. Following its discovery by W. F. Libby in the late forties, radiocarbon dating was recognized with a Nobel prize in 1960, and its use has continued to increase since that time. The method, as generally practiced, is characterized by excellent precision, but required sample sizes are extremely large (by air pollution standards) and chemical or physical separations are rare (with the exception of simple "pretreatment", and the extraction of cellulose for tree ring dating). Rapid progress in measurement techniques for small atmospheric samples was marked by (a) the introduction of mini-counter liquid scintillation and gas proportional counting in 1976 [21] for 100 mg and 10 mg size samples, respectively, and (b) the development in 1977 of direct ^{14}C atom (rather than β-decay) counting by means of high energy nuclear accelerators [15,16]. Although the first dedicated radiocarbon accelerator has not yet been installed, it has been demonstrated that natural radiocarbon may be measured in samples containing only 10-20 μg of carbon [17].

During the past three years, the mini-gas proportional counting method has been applied to a number of interesting problems, ranging from gas and particulate matter in the atmosphere to organic species in sediment [22], and it may be

considered validated and almost routine in operation. Atom counting (with accelerators) is still very much in an exploratory stage, but its enormous sensitivity (with consequent sample size reduction) will lead to very broad applications. As shown at the bottom of Table 2, based on current measurement parameters, decay counting of 10 mg of contemporary carbon yields a Poisson imprecision of about 6 percent (415 sample counts, S/B~2), whereas atom counting of 10 μg yields a value of 3 to 4 percent (786 counts, S/B>>1). The latter method requires an overall measurement time of hours rather than days. Many other factors which affect the time, cost and reliability of the alternative methods are beyond the scope of this paper. What the two methods share, however, is the exciting opportunity of determining the isotopic composition of individual chemical species and size fractions in atmospheric samples selected according to time and location.

A number of assumptions and cautions involved in the measurement and interpretation of radiocarbon data are highlighted in Table 3. With respect to the (two-source, isotope dilution) model the only currently significant assumption-limitation is connected with the ^{14}C variations in the biosphere. The three principal causes of these variations are (a) solar modulation of the cosmic rays, (b) dilution of atmospheric radiocarbon with fossil fuel generated CO_2 (Suess effect) and (c) artificial radiocarbon production (primarily associated with

atmospheric nuclear tests) [23]. As shown in Figure 1, the perturbation due to nuclear testing predominates, causing about a 30 percent radiocarbon excess in currently-living matter. Because of this, radiocarbon concentrations, relative to the "modern standard" (0.95 x NBS Oxalic Acid SRM # 4990-B) must be divided by 1.3 to estimate the fraction of contemporary (biogenic) carbon. When the biogenic source spans a number of years, the situation is less straightforward. If a 60 year-old log is burned in a fireplace, for example, its average radiocarbon contribution is enhanced by an additional 9 percent due to the wood formed during the period of major nuclear testing [24]. (One must integrate the input function, Figure 1, over the life of the vegetation taking into account also the rather small correction for radioactive decay.) Unlike most chemical species, however, radiocarbon directly tracks the biospheric source emissions, and the isotope ratio is extremely resistant to changes during transport, from source to receptor site.

Most of the subtle, yet critical sources of error in the low-level counting of radiocarbon have been discussed previously [14,21]. To assure reliability we now routinely monitor six parameters during counting periods; and our measurements generally encompass five (hierarchical) levels of quality control.

New information concerning two other factors, developed within the past year, bears special mention. These are the blank and isotopic heterogeneity. Until recently sufficient

material and information concerning the blank was lacking. Blank quartz-fiber filters obtained recently from R. K. Stevens, of the U.S. EPA, however, gave us sufficient filter-blank carbon to carry out a radiocarbon determination. The result, that the blank was indistinguishable from contemporary carbon, must be considered when measuring samples having less than a few milligrams of carbon.

Isotopic heterogeneity, variation of the isotopic ratio among different chemical and/or size fractions of the ambient sample, is exactly analogous to the problem of non-contemporaneity in radiocarbon dating [25]. That is, although the overall radiocarbon concentration may be meaningful in terms of the average biogenic source contribution (or age), significant information loss takes place unless measurements are made on the individual fractions. As will be discussed in the next section, we have observed particle size and volatility-related isotopic heterogeneity in carbonaceous particulate samples; therefore, the relative mix of biogenic and fossil source contributions must differ among the different fractions, and conclusions based upon just the average isotopic composition (TSP) may be relatively weak or ambiguous. A corollary to these observations is that quantitative chemical recoveries (from particles to pure CO_2 counting gas) are mandatory; otherwise even the estimated average isotopic composition may be biased due to selective chemical losses.

EXPERIMENTAL RESULTS -- CONTEMPORARY CARBON IN URBAN AND RURAL AEROSOLS

1. The isotopic dimension; chemical and physical selectivity. Initially, mini-radiocarbon measurements were applied in a simple dichotomous manner to determine whether urban and rural ambient aerosols were typically "anthropogenic" (fossil) or "natural" (biogenic, vegetative) in origin; the results were not surprising [14]. More recently, it has become important to assay radiocarbon in samples from specific episodes which implied serious health consequences (especially involving fine carbonaceous particles) or where significant contemporary carbon emissions, from wood burning or vegetative emissions, were presumed present. Under these circumstances it has become necessary not just to assay ^{14}C in the Total Suspended Particulate matter (TSP), but also to examine individual chemical or size fractions. In addition to this "serial selectivity", "parallel" measurements of other chemical or physical characteristics of the samples in question have served two important purposes: (a) validation of the isotopic conclusions (or the converse, the Chemical Mass Balance [CMB] conclusions), and (b) complementarity (orthogonality) needed for extracting more source information than either approach alone could provide.

The first, quality control, application has been and will continue to be of major importance in the development and validation of new methods; its value rests especially on the uniqueness of the radiocarbon tracer, and on the complete independence (with respect to underlying assumptions and methods)

of the alternative (isotopic, chemical) techniques. The second aspect, which implies complete integration of the isotopic dimensions with the chemical characterization, provides the most powerful use of the isotopic data, and it should lead to one of the more reliable and precise approaches to future efforts in receptor modeling [26,27]. The summary in Table 4 of one rural and three urban ambient aerosol investigations, all completed within the last two years, illustrates both of these aspects.

Is is noteworthy that the percent of contemporary carbon observed in these investigations covered the full range from 10 ± 3 percent to 107 ± 15 percent. (Both of the extremes represented periods of severe particulate pollution, but from very different sources!) A general observation from these studies is that contemporary sources do contribute significant amounts of particulate carbon to the ambient aerosol from vegetative emissions during the summer (Los Angeles, rural Utah), and from wood-burning in the winter (Portland, Denver). Continuing severe pollution episodes in Los Angeles and Denver ("Denver brown cloud") were the geneses for two of the investigations, and the remaining two were connected with special situations involving contemporary (Portland, field and slash burning) and fossil (Utah, oil shale tracts) carbon. Of particular importance is the nature of the supporting data. As shown in the fourth column of Table 4, serial or parallel information on particle size, emission/dispersion modeling,

and inorganic or organic composition were intimately involved in the overall efforts at source reconciliation.

2. Patterns of results and conclusions

The isotopic data served as a truly independent dimension in the urban studies, in that they were more or less formally combined with chemical, meteorological and emission data to infer sources of the carbonaceous particles. Emission, chemical and radiocarbon data collected for Denver samples, for example, were consistent with the conclusion (for the sampling period in the winter of 1978) that wood-burning was responsible for about one-fifth of the carbonaceous aerosol and two-fifths of the visibility-reducing elemental carbon [28,29]. Qualitative support for the 54 percent contemporary carbon in the Los Angeles study was given by observations of significant amounts of primary or secondary organic species characteristic of fossil sources (a large hump of branched cyclic compounds in the GC trace of the hydrocarbon fraction, polycyclic aromatic hydrocarbons, and dicarboxylic acids) on the one hand, and species reflecting vegetative emissions ($\delta^{13}C$, odd carbon-numbered high molecular weight n-alkanes, predominantly even carbon-numbered fatty acids, 2-ketones, camphor) on the other. It should be noted that individual size fractions were examined in the Los Angeles study, and that wind patterns at the location of the receptor site (City of Hope hospital, Duarte, in the foothills of the San Gabriel Mountains) favored impacts from both intense urban smog and forest emissions (carried by night-time winds) [30].

The investigations in Portland and Utah provided important opportunities for semi-quantitative tests of consistency between isotopic and chemical data. Table 5 lists results (and Poisson standard deviations) for ^{14}C-inferred contemporary carbon derived from vegetative burning in Portland and vegetative emissions in Utah. Paralleling the radiocarbon results are independent estimates based on inorganic chemical mass balance (CMB) in Portland [24] and organic chemical "pattern recognition" (CPR) in Utah [31]. The general pattern of results is quite satisfactory, but two special comments are in order. That is, the CMB estimates (of biogenic carbon) were rather indirect, involving several assumptions, so that the assignment of uncertainties was extremely difficult. (Overall consistency between the ^{14}C and CMB estimates would admit an average (CMB) standard deviation of about 9 percent.) The CPR uncertainties (Utah samples) reflected measurement error only; sampling and model errors would, of course, increase the uncertainty intervals. It is interesting to note that K/Fe ratios (Portland) were qualitatively consistent with the radiocarbon data, but were subject to large fluctuations.

Finally, let us briefly examine patterns associated with the Utah and Denver results. Figures 2 and 3 show: the pyrolysis-mass spectra for the fossil and three vegetative components contributing to the ambient sample in Utah, and the resulting separation of these components as shown in non-linear

two-space using pattern recognition technqiues. An overview of the Denver study is given in Table 6, and a three dimensional projection of the pattern of selected results (TSP) appears in Figure 4. This figure shows contemporary carbon as a function of three variables: degree of pollution, percent of volatile ("organic") carbon, and chemical fraction (total carbon, "elemental" carbon)*. General conclusions which may be drawn from this overall pattern of results are (a) that the radiocarbon blank must not be ignored, (b) contemporary carbon, comprising up to about 40 percent of the carbonaceous material, is a significant component -- presumably due to residential wood burning -- in the winter-time Denver "brown cloud", and (c) the fossil component is more pronounced: in the elemental carbon fraction, with increasing pollution, and with decreasing volatility.

Three of the major assumptions/limitations in the isotopic inferences mentioned in the previous section deserve special comment with respect to the Denver results. First, the average age of the wood burned was not taken into account in deriving the results as shown in Figure 4. The maximum likely effect would be a relative shift of about 9 percent toward fossil carbon.

---

* The terms organic and elemental are used here in an operational sense. The "elemental" fraction, defined as being non-volatile, may include high molecular weight compounds as well as amorphous or graphitic carbon [28,29].

Second, the effect of the blank, which corresponded to about 0.7 mg-C, has been taken into account. Fortunately, the corrections were small compared to the Poisson counting errors, since the correction involves assumptions concerning the chemical and isotopic compositions and variability in the total mass of the carbon blank [19]. For the samples (Fig. 4) having the smallest and largest blank contributions -- sample "P" with 23.9 mg-C and sample "U" with 9.8 mg-C -- the adjustment to the percent of contemporary carbon was just -1.5 percent and -3.3 percent, respectively.

The third limitation relates to chemical yield. If the recovery (as CO_2, counting gas) is non-quantitative, isotopic heterogeneity can lead to bias for the estimated *average* percent contemporary carbon; and low yields greatly increase the error-propagation uncertainties when the volatile carbon component is deduced from the two (total, elemental) measured components. For example, the pair of samples, "WD", had estimated recoveries of 87 percent (total) and 101 percent (non-volatile), and contemporary carbon compositions of 26 ± 5 percent and 14 ± 5 percent, respectively. The derived contemporary carbon estimate for the volatile component was 56 ± 26 percent. Obviously, quantitative recovery and direct measurement of ^{14}C in the volatile component are desirable for future studies.

SUMMARY

Radiocarbon has been demonstrated to be a unique and robust tracer for contemporary carbon in atmospheric particles. Utilization of this isotope, together with selective sampling plus measurements of $\delta^{13}C$ and inorganic and organic chemical composition has indicated the importance of a number of specific vegetative sources contributing to urban and rural ambient particles. Semi-quantitative confirmation of the radiocarbon conclusions has been derived from chemical mass balance (inorganic species, emission ratios) and chemical pattern recognition (organic species).

Rapid progress has occurred in the measurement of radiocarbon, in that (a) small (5-10 mg-C) samples may be measured using mini-gas proportional counters with a method which has been developed with a high degree of internal control and is nearly routine in applicability, and (b) the eventual capability for micro (10-20 μg-C) samples has been demonstrated using direct atom counting with a tandem accelerator.

Assay of contemporary carbon, which has been carried out for the first time on a complete blank and on different chemical fractions of small samples of atmospheric particles, has indicated isotopic heterogeneity -- viz., the organic and elemental carbon fractions of ambient particles have been shown to depend to differing extents on biogenic carbon sources. These observations, obtained from measurements of "Denver Brown Cloud" particles, are analogous to the contemporary carbon

(isotopic) heterogeneity which we observed in different size fractions of particles collected both in Denver and in Portland, Oregon. For the particles sampled in these studies, the contemporary carbon fraction -- presumably from vegetative burning -- tended to be concentrated in the organic carbon fraction and in the fine particle fraction. The overall contemporary carbon fraction depended greatly on locale and conditions, ranging from 10 ± 3 percent (Denver) to 107 ± 15 percent (Portland).

Elemental carbon, already important because of its impact on climate, health and visibility, is of special interest for radiocarbon measurements. This is because the composition of such a single chemical species can only be characterized using isotopes, because it has a very low blank, and because it is a chemically robust tracer for combustion sources. Finally, elemental carbon represents the ideal chemical form for the technique having greatest sensitivity -- accelerator atom counting.

As isotopic measurements of greater sensitivity (smaller sample size) or improved precision become practicable, it will be increasingly important to pay attention to three critical factors: the blank, recovery (and isotopic heterogeneity), and assumed vegetative age. Uncertainties connected with the blank are negligible for elemental carbon and slightly smaller than current Poisson counting errors for total carbon. Isotopic heterogeneity means that low chemical yields will result in

biased contemporary carbon estimates, and important information loss will occur if individual chemical and size fractions are not separately analyzed. Vegetation age, if inadequately corrected for, can introduce uncertainties up to about 10 percent, due to the injection of bomb radiocarbon during the last two decades.

The next steps to be taken in the application of carbon isotopes to the investigation of the life cycle of carbonaceous particles will include sampling at remote sites and advances in measurement methodology. The latter will include isotopic enrichment and multiple counter arrays plus exploration of precision and sensitivity improvements using a dedicated radiocarbon accelerator. Also, further utilization of chemical and size selectivity are planned, together with full integration of the isotopic and chemical data in the source deconvolution process. For these purposes, efforts will be made to further characterize a particulate standard reference material, and to provide a standard data set for receptor modeling.

ACKNOWLEDGMENT

The urban and rural studies reviewed in this manuscript, and to be published in full elsewhere, took place in cooperation with the following scientists: Portland -- J. A. Cooper (Oregon Graduate Center), Los Angeles -- I. R. Kaplan (Global Geochemistry, Inc.), Utah -- K. J. Voorhees (Colorado School of Mines), and Denver -- R. J. Countess, G. T. Wolff and D. P. Stroup (General Motors Research Laboratory). R. K. Stevens (USEPA) supplied the blank ("B", Fig. 4). G. A. Klouda and R. E. Continetti of NBS were largely responsible for the experimental radiocarbon measurements. Grateful acknowledgment is expressed to all of these colleagues. Partial support for this research was provided by the Office of Environmental Measurements, U. S. National Bureau of Standards, and the Energy-Environment Program (EPA-IAG-D6-E684), U. S. Environmental Protection Agency.

Table 1. Carbon Isotope Concentrations Characterizing Different Sources[a],[b]

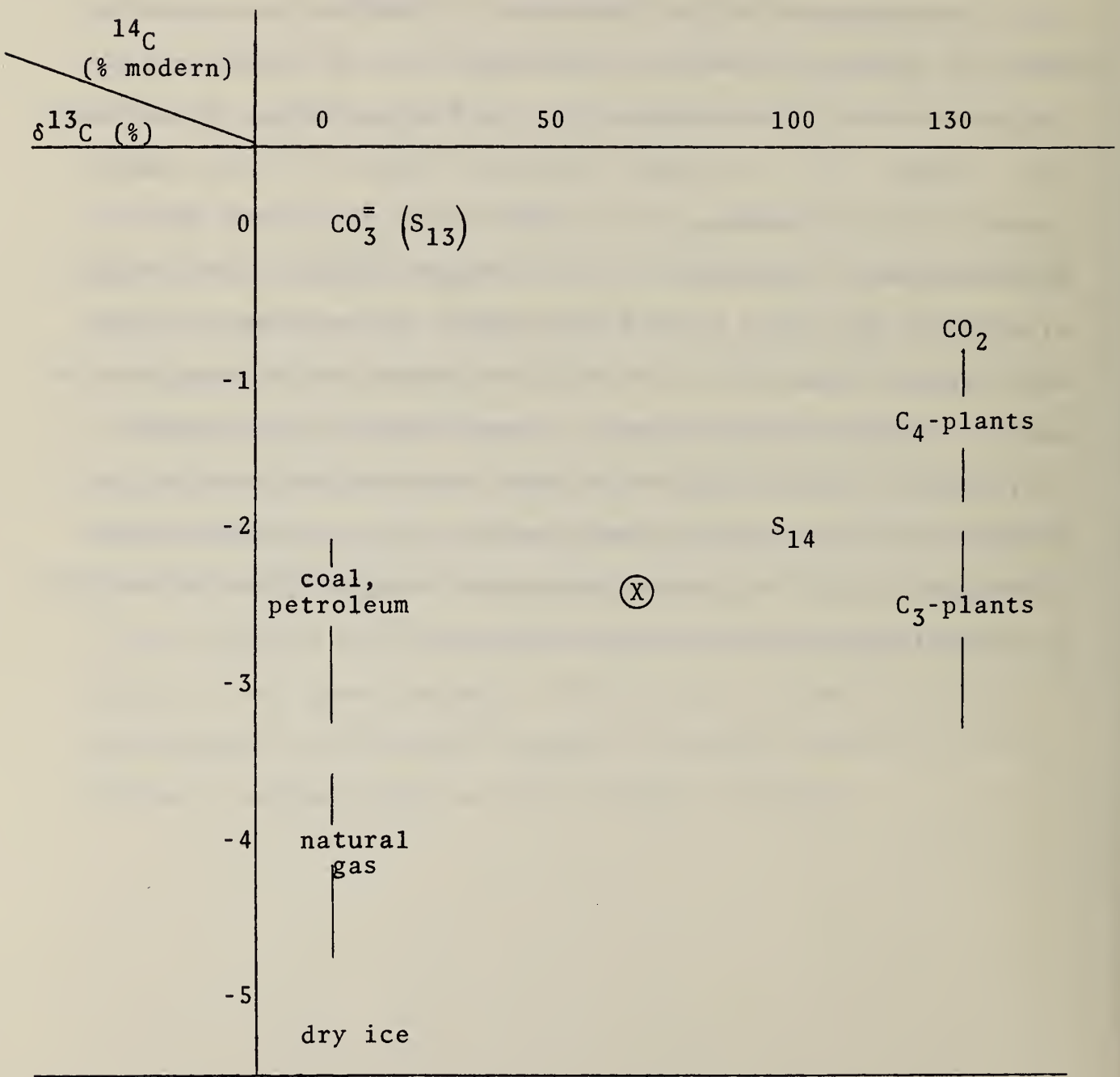

(a) $^{14}C/^{12}C$ relative to the radiocarbon standard, S_{14} (100%≡0.95 x NBS Oxalic Acid), [23]; and $^{13}C/^{12}C$ deviations (%) from the PDB standard, S_{13}, [10]. Note that contemporary (∿1979) C-14 is about 30% higher than "modern standard" (pre-nuclear era, C-14.

(b) C_4, C_3 plants represent the two major photosynthetic classes, [12]. Point (X) represents a Los Angeles aerosol sample whose isotopic composition is consistent with 54% temperate (C_3) vegetative emissions and 46% fossil fuel [30].

Table 2. Radiocarbon Measurement -- Evolution, Sensitivity

(See text for references and explanation of symbols)

	Mass (form)	Precision	Notes
Radiocarbon Dating (1960);	10 g (gas, liquid)	0.5% ($\tilde{}$40 yr)	Minimal Chemistry
Small Sample Decay Counting (1976):			
Liquid Scintillation	100 mg (C_6H_6)	2%	Individual Chemical, Size Fractions
Gas Proportional	10 mg (CO_2)*	5%	
Accelerator Atom Counting (1977)	10 μg (C)**	3%	Exploratory; 1st Dedicated Machine (1981)

$$\text{Number of Counts} = \begin{cases} AE\Delta t = (0.18\ \text{min}^{-1})(0.8)(2880\ \text{min}) = 415^{*} \\ AE'\tau = (95\ \text{yr}^{-1})(0.001)(8270\ \text{yr}) = 786^{**} \end{cases}$$

Table 3. Cautions and Assumptions

Model Validity

Radiocarbon:

* two-source assumption (soil-carbon, nuclear energy, gasohol)
* ^{14}C-variations (solar, bomb, Suess effects)
* vegetation age (firewood)

Receptor:

* all sources identified
* accurate, reproducible profiles at receptor site

Sample and Sample Preparation Limitations

* the blank
* large particle contamination (spores, insect parts, ...)
* chemical stability, reliable separations (recovery, charring)

Counting Difficulties

* isotopic heterogeneity (non-quantitative recovery)
* background fluctuations (sunspots, barometric pressure)
* radon contamination
* electronegative contamination (efficiency)
* spurious pulses

Table 4. Recent Particulate Studies

Locale	Carbon Sources	Percent Contemporary	Supporting Data	Reference
Portland, OR	Field, slash and wood burning	57. to 107.	Known impact, particle size, inorganic composition (Chemical Mass Balance)	24
Los Angeles	Urban fossil fuel and vegetative emissions	∿54.	Particle size, dispersion data, $\delta^{13}C$, organic composition	30
Rural Utah	Vegetative emissions and oil shale dust	∿64.	Pyrolysis--mass spectrometry (Chemical Pattern Recognition)	31
Denver	Urban fossil fuel and wood burning	10. to 55.	Organic/elemental fractions, inorganic composition, emission data and modeling, coarse/fine fractions	28

Table 5. Quantitative Consistency

(percent contemporary carbon)

Portland[a]		Utah[b]	
^{14}C	CMB, Emission Ratios (inorganic)	^{14}C	CPR, Py-MS (organic)
107 ± 15 (field)	99	64 ± 4 (sage)	64 ± 2
111 ± 19 (slash)	85	64 ± 4 (pine)	11 ± 2
83 ± 16 (slash)	78	64 ± 4 (juniper)	_
79 ± 12 (slash)	97	fossil (shale)	24 ± 2
57 ± 12 (wood)	79		

(a) Fine particle fraction (≤2.5 μm), corrected for wood age (ref. [24]). (CMB = Chemical Mass Balance.)

(b) Ref. [31]. Chemical Pattern Recognition (CPR). Figures represent the derived percent contributions from the indicated sources.

Table 6. Denver Samples (Overview)

Conditions:

Sunny, cloudy, -20 °C to +10 °C
Clear, weekend, weekday, polluted
[7. to 43. μg-C/m^3]

Fractions:

Total, non-volatile, fine

Percent Volatile:

25. to 70.

Percent Recovery (CO_2):

70 to 108

Mass (carbon):

5.6 mg to 23.9 mg
[Blank = 0.7 mg; ~8. μg/cm^2]

Percent Contemporary:

10 ± 3 to 55 ± 13

References

[1] Covert, D. A., Charlson, R. J., Rasmussen, R., and Harrison, H., "Atmospheric Chemistry and Air Quality", Review of Geophysics and Space Physics, 13, 765, (1975).

[2] Kneip, T. J., Lioy, P. J., Eds., "Aerosols: anthropogenic and natural sources and transport." Annals N.Y. Acad. Sci., 338, 1-618, (1980).

[3] Bolin, B., "The impact of production and use of energy on the global climate", Ann. Rev. Energy, 2, 197 (1977).

[4] Cooper, J. A., Watson, J. G., and Huntzicker, J. J., "Summary of the Portland aerosol characterization study", Paper No. 79-24.4, 72nd Air Pollution Control Association Meeting, Cincinnati, Ohio, June 1979.

[5] Courtney, W. J., Tesch, J. W., Russwurm, G. M., Stevens, R. K., Dzubay, T. G., and Lewis, C. W., "Characterization of the Denver aerosol between December, 1978 and December 1979", Paper No. 80.58-1, 73rd Air Pollution Control Association Meeting, Montreal, Canada, June 1980.

[6] Rahn, K. A., Brosset, C., Ottar, B., and Patterson, E. M., "Black and White Episodes, Chemical Evolution of Eurasian Air Masses, and Long-Range Transport of Carbon to the Arctic", Particulate Carbon: Atmospheric Life Cycle, GMR Symposium (Warren, October 1980).

[7] National Research Council. Controlling Airborne Particles. National Academy of Sciences: Washington, D. C., 1980.

[8] Geophysics Study Committee, Energy and Climate, NRC Geophysics Research Board, National Academy of Sciences, Washington, D.C. 1977.

[9] Novakov, T., Ed., Proc. Conf. Carbonaceous Particles in the Atmosphere, LBL-9037 (Lawrence Berkeley Laboratory) 1978.

[10] Craig, H., Geochim. Cosmochim. Acta, 3, 53 (1953).

[11] Calder, J. A., and Parker, P. L., Stable isotope ratios as indices of petrochemical pollution of aquatic systems, Env. Sci. Tech., 7, 535 (1968).

[12] Troughton, J. H., "Carbon Isotope Fractionation by Plants", Proceedings of the Eighth International Radiocarbon Dating Conference, Lower Hutt, New Zealand, Vol. 2, 421, 1972.

[13] Currie, L. A., and Murphy, R. B., "Origin and residence times of atmospheric pollutants: Application of ^{14}C", in Methods and Standards for Environmental Measurement, W. H. Kirchoff, Ed., NBS Spec. Pub. 464, National Bureau of Standards, Washington, D.C., p. 439, Nov. 1977.

[14] Currie, L. A., Kunen, S. M., Voorhees, K. J., Murphy, R. B., and Koch, W. F., "Analysis of Carbonaceous Particulates and Characterization of Their Sources by Low-Level Radiocarbon Counting and Pyrolysis/Gas Chromatography/Mass Spectrometry," Conference on Carbonaceous Particles in the Atmosphere, University of California, Berkeley, 1978.

[15] Muller, R. A., "Radioisotope dating with a cyclotron," Science, 196, 489 (1977).

[16] Gove, H., Ed., Proceedings of the First Conference on Radiocarbon Dating with Accelerators, University of Rochester, 1978.

[17] Currie, L. A., Klouda, G. A., Elmore, D., Ferraro, R., and Gove, H., "Accelerator Mass Spectrometry and Electromagnetic Isotope Separation for the Determination of Natural Radiocarbon at the Microgram Level," (in preparation).

[18] Rubin, M., "Sample Preparation for Van de Graaff Accelerator Dating," in L. A. Currie, Ed., Nuclear and Chemical Dating Techniques, American Chemical Society Symposium Series, 1981.

[19] Stevens, R. K., McClenny, W. A., Dzubay, T. G., Mason, M. A., and Courtney, W. J., "Analytical Methods to Measure Carbonaceous Content of Aerosols," Particulate Carbon: Atmospheric Life Cycle, GMR Symposium, Warren, Oct. 1980.

[20] Libby, W. F., Radiocarbon Dating, University of Chicago Press: Chicago, 1952.

[21] Currie, L. A., Noakes, J., and Breiter, D., "Measurement of Small Radiocarbon Samples: Power of Alternative Methods for Tracing Atmospheric Hydrocarbons," Ninth International Radiocarbon Conference, University of California, Los Angeles and San Diego, 1976.

[22] Swanson, J., Fairhall, A., and Currie, L. A., "Carbon Isotope Analysis of Sedimentary Polycyclic Aromatic Hydrocarbons," (in preparation).

[23] Olsson, I. U., Ed., Radiocarbon Variations and Absolute Chronology, Proceedings of the 12th Nobel Symposium held at the Institute of Physics at Uppsala University, Wiley-Interscience, New York, 1970; and Damon, P. E., Lerman, J. C., and Long, A., "Temporal Fluctuations of Atmospheric C-14: Causal Factors and Implications", Annual Review of Earth and Planetary Science, 6, 457 (1978).

[24] Cooper, J. A., Currie, L. A., and Klouda, G. A., "Assessment of Contemporary Carbon Combustion Source Contributions to Urban Air Particulate Levels Using C-14 Measurements," to be published in Env. Sci. & Tech., 1981.

[25] Schultz, H., Currie, L. A., Matson, F. R., and Miller, W. W., "Pretreatment of Wood and Char Samples," Radiocarbon, 5, 342 (1963).

[26] Watson, J. G., Edit., Proc. Receptor Modeling Workshop, Quail Roost, N. C., Feb. 1980.

[27] Gordon, G. E., "Receptor Models," Env. Sci. & Tech., 14, 792 (1980).

[28] Currie, L. A., Countess, R. J., Klouda, G. A., G. T. Wolff, and Stroup, D., "The Contribution of Contemporary Carbon to the 'Denver Brown Cloud'," (in preparation).

[29] Wolff, G. T., Countess, R. J., Groblicki, P. J., Ferman, M. A., Cadle, S. H., and Muhlbaier, J. L., "Visibility-Reducing Species in the Denver 'Brown Cloud'. Part II. Sources and Temporal Patterns," GMR-3394, 1980. See also Ref. 5, and

Heisler, S. L., Henry, R. C., Watson, J. G., and Hidy, G. M. "The 1978 Denver Winter Haze Study", Motor Vehicle Manufacturers Association, Detroit, Michigan, 1980.

[30] Kaplan, I. R., Currie, L. A. and Klouda, G. A., "Isotopic and Chemical Tracers for Organic Pollutants in the Southern California Air Basin," (in preparation).

[31] Voorhees, K. J., Kunen, S. M., Durfee, S. L., Currie, L. A., and Klouda, G. A., "The Determination of Source Contribution of Organic Matter in Atmospheric Particulates by Pyrolysis/Mass Spectrometry and ^{14}C Analysis," to be published in Analytical Chemistry, 1981.

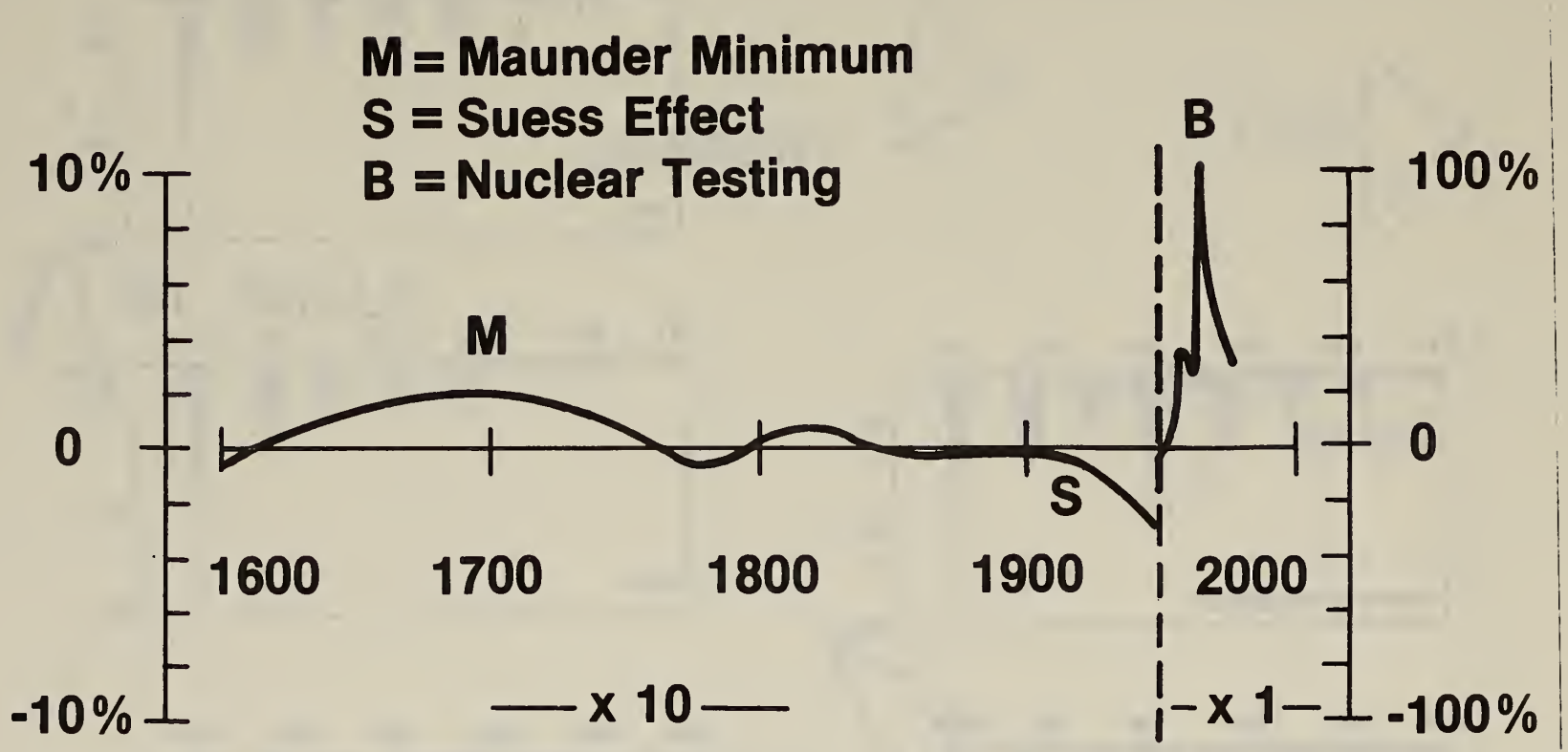

Figure 1. Natural Radiocarbon Variations. Percentage deviations from steady-state radiocarbon concentration in biosphere. Scale is expanded by a factor of ten before 1950. Major excursions marked "M", "S", and "B" correspond to: the Maunder minimum in solar activity (and the Little Ice Age), the Suess Effect (fossil CO_2 dilution) and the Bomb effect (atmospheric nuclear testing). See reference [23] for further discussion.

Pyrolysis — Mass Spectrometry Data

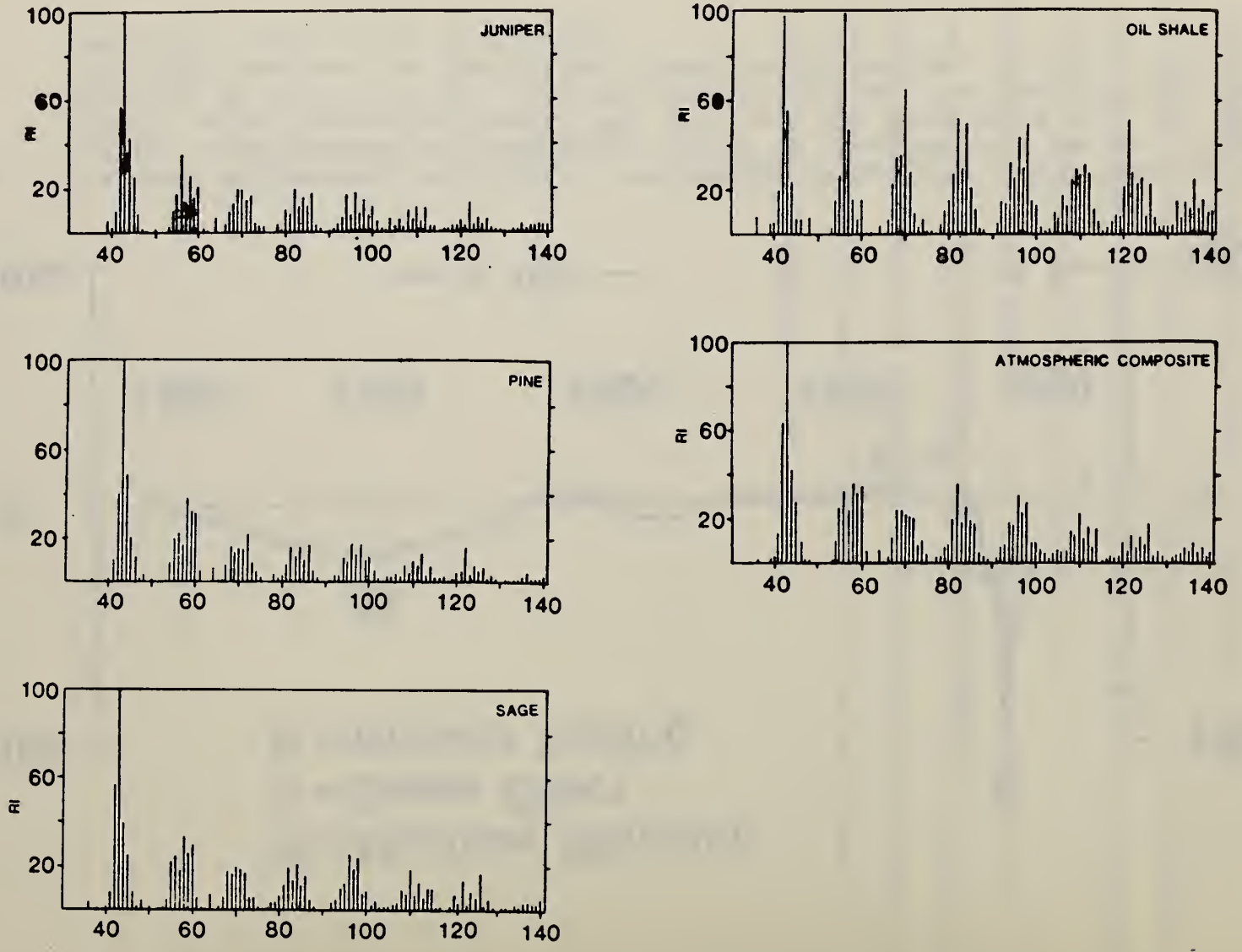

Figure 2. Summary of Pyrolysis-Mass Spectra (Py-MS) for Source Samples and Ambient Atmospheric Particulate Sample Collected in Utah Oil Shale Tract [31].

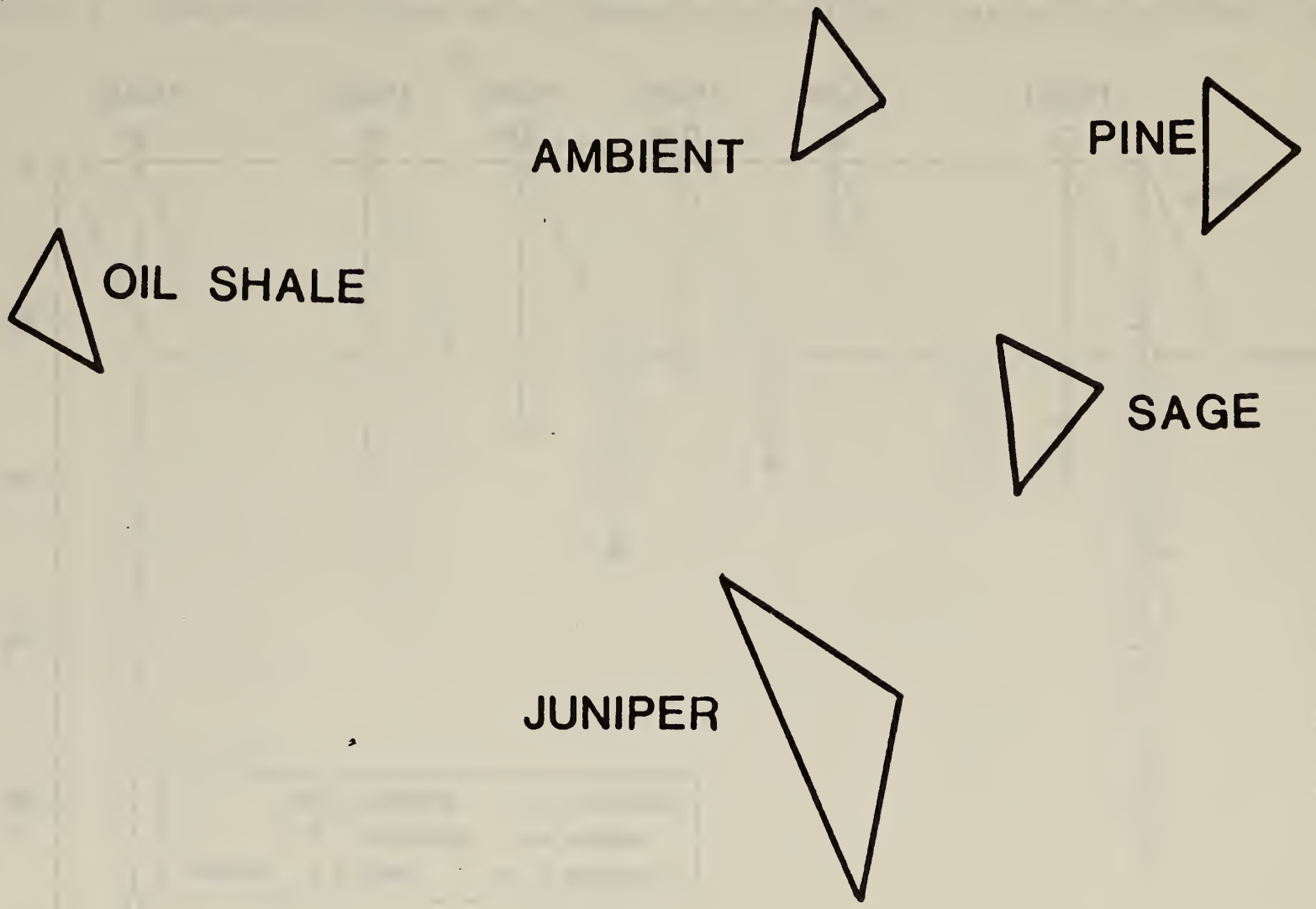

Figure 3. Non-Linear Map of Py-MS Data Summarized in Figure 2 [31].

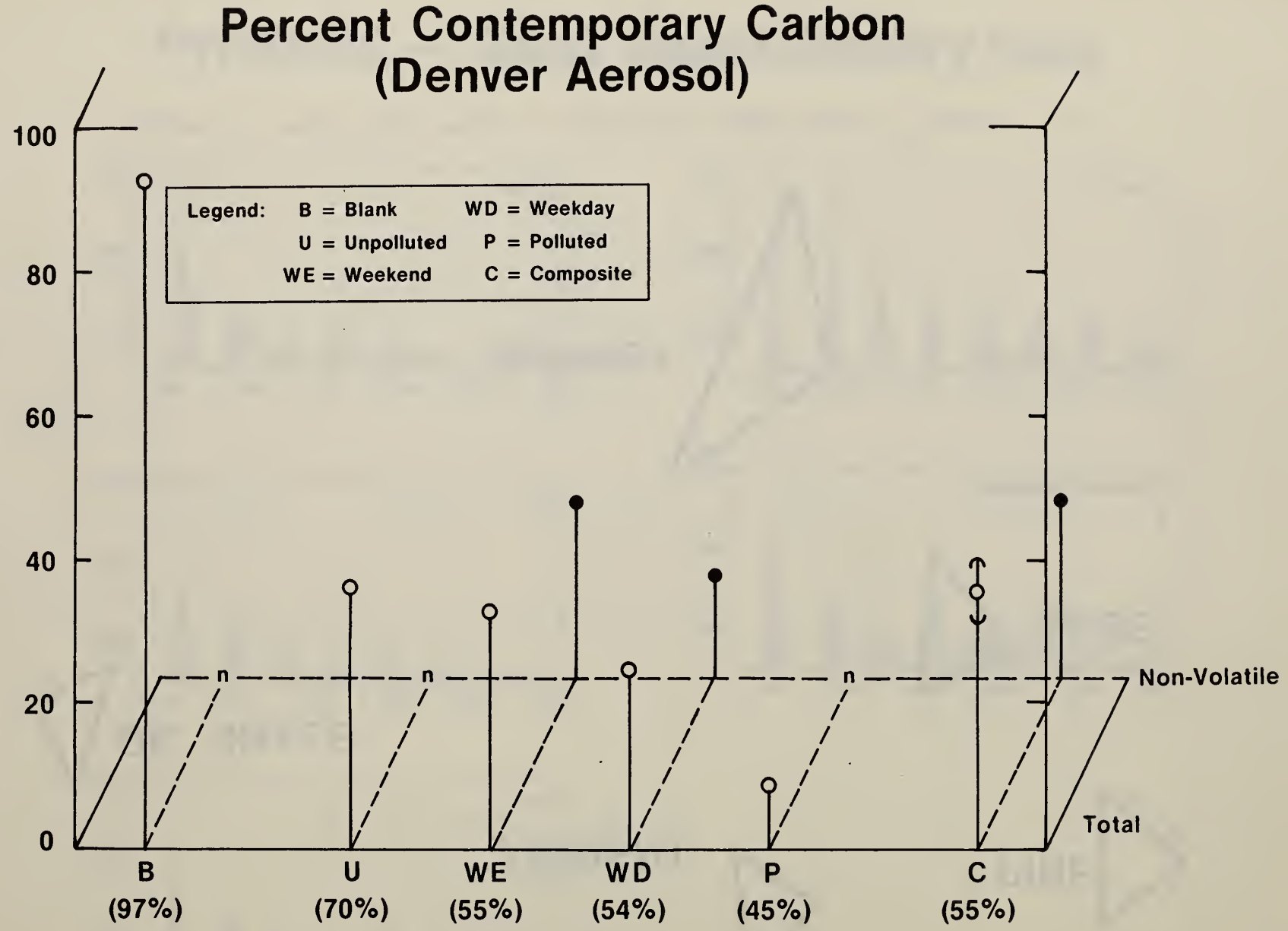

Figure 4. Contemporary Carbon in the Denver Aerosol (TSP). Percent contemporary is given as an (ordered) function of increasing pollution (for 4 samples, U-P), for two volatility fractions (total and "non-volatile" carbon). An independent, composite Denver sample (C) also is shown, as well as a quartz filter blank (non-Denver) supplied by R. K. Stevens. The Poisson error is indicated for sample-C and percent volatility is shown at the bottom of the figure.

APPENDIX 2

Evaluation of the CARS - Capillary Waveguide Detection System for HPLC

John J. Blaha and John C. Schaefer

INTRODUCTION

The work reported here was an attempt to utilize the capillary waveguide cell for Coherent Anti-Stokes Raman Spectroscopy (CARS) to determine lower limits of detection for polycyclic aromatic hydrocarbons and to establish the applicability of the technique as a detector for HPLC.

In previous characterizations of organic materials (benzene and toluene) conducted with CARS, the capillary waveguide sample cell was examined and found to increase the detectability of the CARS signal by approximately two orders of magnitude compared to the 1 cm path length cuvette normally used (1). The capillary waveguide was found to be most efficient with a very small internal diameter and a very long pathlength. For the tests, a 50 μm diameter by 30 cm long capillary tube was used to obtain the 100-fold signal enhancement and thus to lower the detection limits by non-resonant CARS to about 10^{-4}M. Resonance enhanced CARS (wherein the w_1 beam approaches an allowed electric dipole transition) shows a lowering of the limits of detection to the micromolar concentration level. If the extra enhancement of the capillary waveguide could be applied to the resonant enhanced CARS signal, detection limits of approximately 10^{-7} or less might be achieved. This would make the CARS technique comparable to fluorescence in detection limits and offer the added factor of molecular specificity to an analysis. This was the basis for this work.

EXPERIMENTAL

The experimental set-up is identical to that used in the initial testing of the capillary waveguide (Figure 1 in Ref. 1). The capillary waveguide was modified to fit in an adjustable holder and to allow a syringe pump to be attached so that the conditions of a flowing cell could be examined.

Two polycyclic organic materials (chrysene in benzene and perylene in toluene) were examined. Solutions of each in their respective solvents were prepared and then placed in the capillary waveguide for testing. These materials were also examined with a 1 cm cuvette cell. The description of results will be based on the perylene in toluene system.

Studies were conducted with both non-resonant and resonant-enhanced conditions. To determine the appropriate wavelength for the pump laser, λ_1, in each case, UV - VIS absorption spectra of the solutions were obtained. These are presented in figures 1 and 2. For the non-resonant enhanced scans, λ_1 was selected to be 510 nm. For the perylene solution λ_1 was chosen to be 450 nm for resonant enhancement and for chrysene λ_1 was chosen to be 337 nm.

RESULTS

Perylene could easily be observed in toluene at concentrations down to 10^{-4} under non-resonant conditions with the capillary waveguide. No such spectra could be found at this concentration when a cuvette was used as a sample cell. This demonstrates the enhancement potential of the capillary waveguide cell.

No spectral features of perylene could be observed for 10^{-4}M concentrations when resonant conditions were applied. In addition, no toluene peaks could be discerned either. The 1002 cm^{-1} toluene band would be expected to be the strongest band in the spectrum so its absence indicates the absorption of the signal by the solution. To investigate this possibility a 10^{-5}M solution of perylene in toluene was prepared and examined in the waveguide. Under non-resonant conditions, the bands at 1002 and 1035 cm^{-1} in figure 3 and at 1204 cm^{-1} in figure 4 of toluene are readily observed. However, when resonant conditions are applied the features are entirely obscured indicating that the CARS signal has been absorbed by the sample.

When resonant conditions are used, λ_1 is at 450 nm and the CARS signal varies in the region between 425 and 435 nm. In this region the absorption of the light by perylene is 10 fold greater for the CARS signal than for this λ_1 beam. Considering that the enhancement of the capillary waveguide is produced by multiple passes of the lasers through the sample solution (up to 130 passes for this cell), the total absorption of the signal by perylene is so great that no signal reaches the detector. Thus resonant enhanced CARS is not possible with a capillary waveguide.

We also examined the possibility of using coherent Stokes scattering to eliminate the absorption problem. Here, fluorescence proved to be too intense to permit any but the strongest features to be observed (figures 5 and 6 for coherent Stokes and figure 7 for normal Raman scattering; note in this figure the indication of the reported Raman bands on the intense fluorescence profile).

To eliminate the fluorescence interference, CARS must be used. To eliminate the absorption of the signal by the sample and thus obtain detection limits at the 10^{-7}M level, a single pass cell with a very short path length is necessary. This has already been tried and found to be an excellent cell by Carreria et al. (2). By using a melting point capillary

cell of I.D. 1.6 mm, detection limits for many organic materials have been reported at 10^{-6} to 10^{-7}M levels. This approach appears to be best suited for continuing study in the use of CARS as a detection system for HPLC.

REFERENCES

1. J. C. Schaefer and J. Chabay, "Generation of Enhanced Coherent Anti-Stokes Raman Spectroscopy Signals in Liquid-Filled Waveguides", Optics Letters 4, 227-229 (1979).

2. L. A. Carreria and L. B. Rogers, "New Liquid Chromatographic Detection System For Environmental Pollutants," EPA research report EPA-600/4-80-015, February 1980, 55 pages.

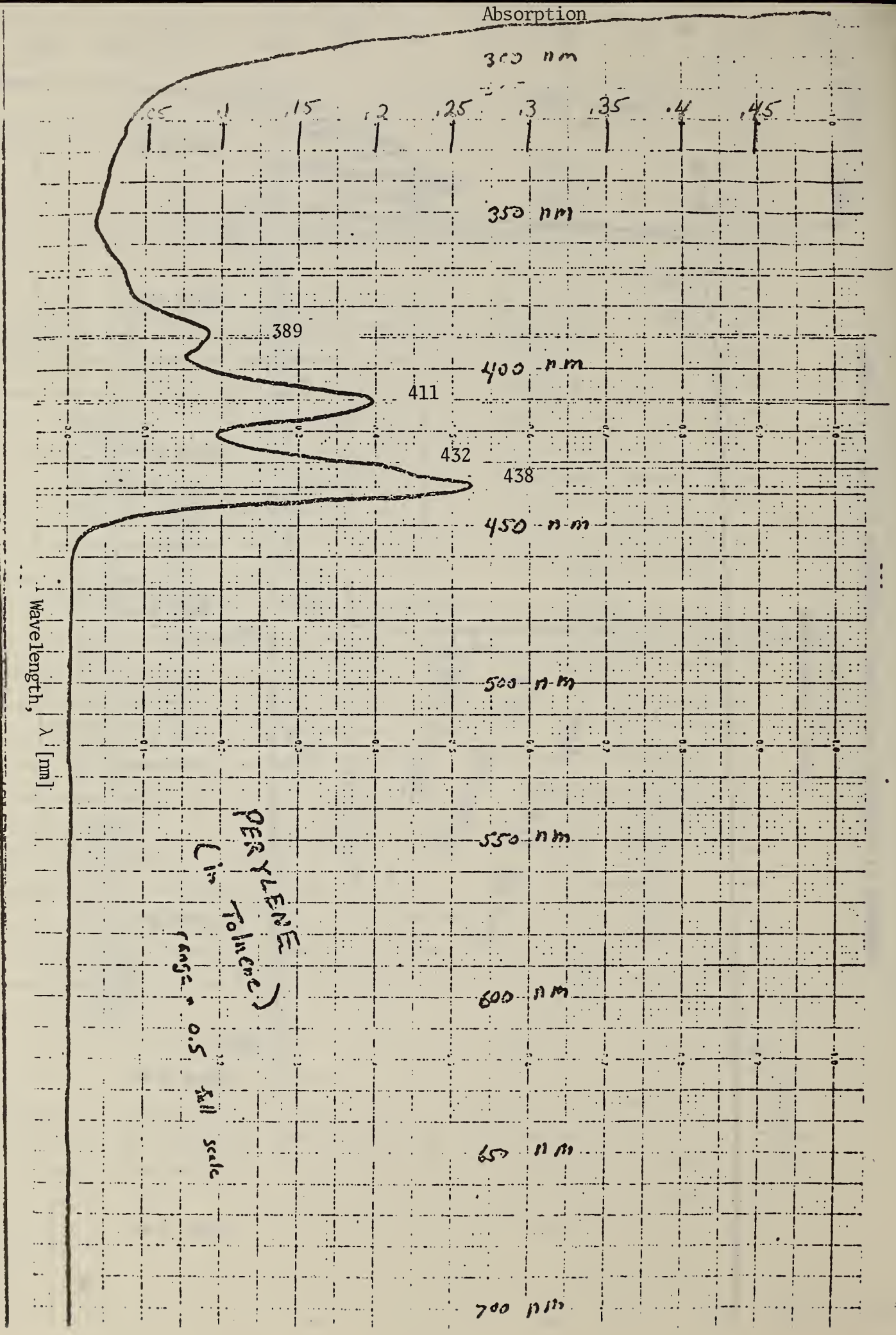
Absorption
300 nm
.05
.1
.15
.2
.25
.3
.35
.4
.45
350 nm
389
400 nm
411
432
438
450 nm
500 nm
550 nm
600 nm
650 nm
700 nm
Wavelength, λ [nm]
PERYLENE
(in Toluene)
range = 0.5 full scale

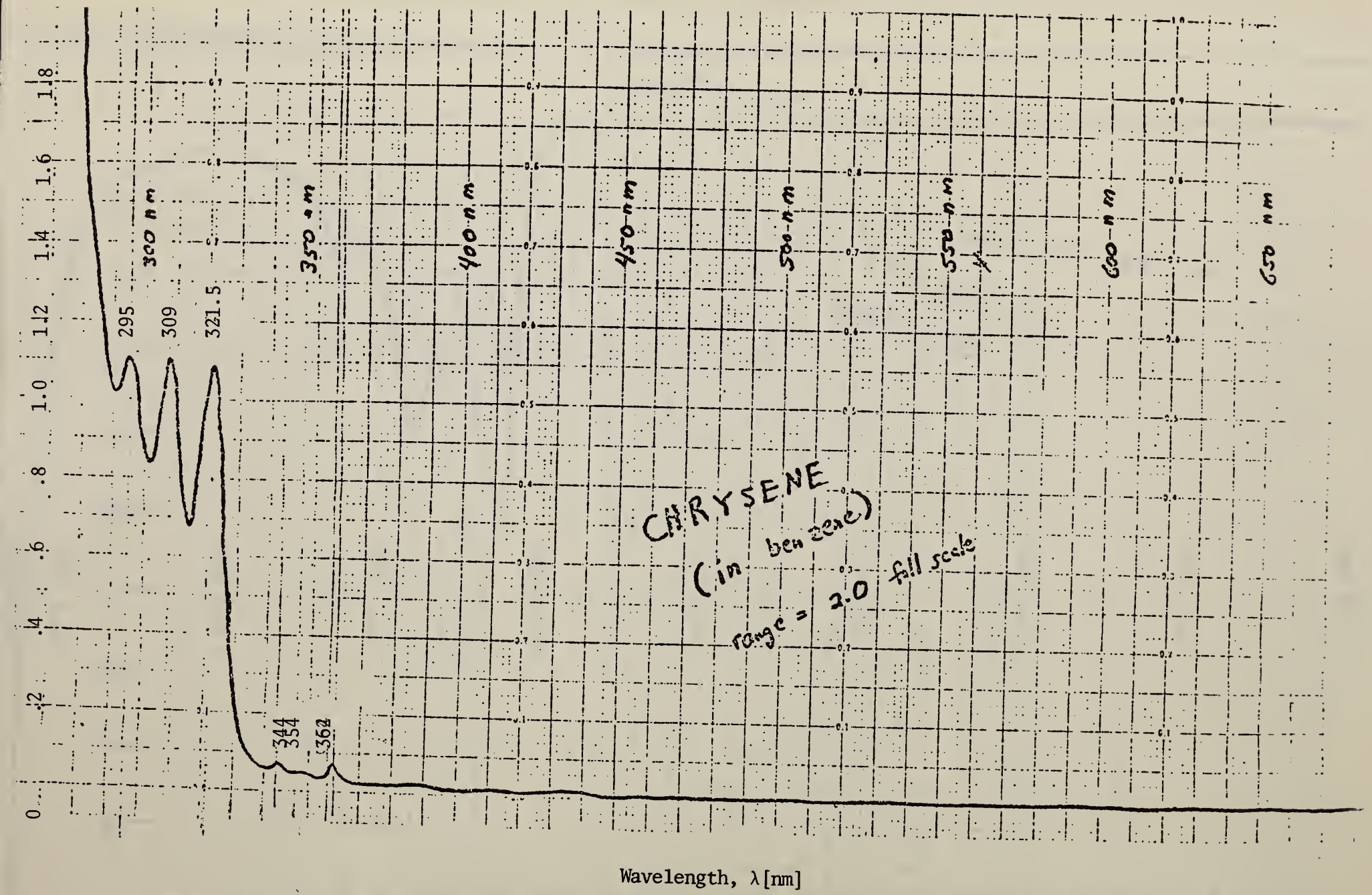

Figure 1. UV-Vis absorption spectra of chrysene in benzene

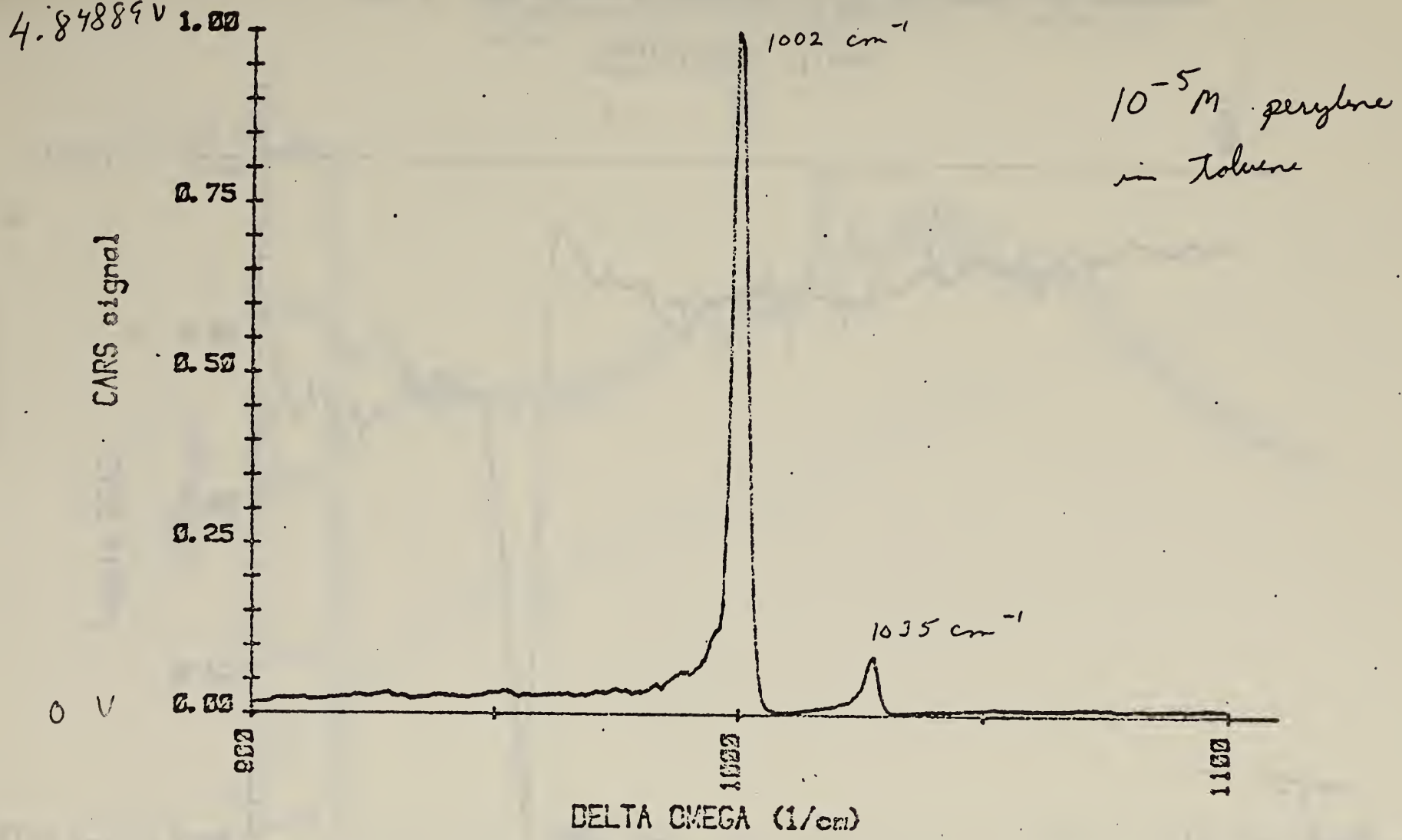

Figure 3. CARS spectra of perylene (10^{-5}M) in toluene. λ_1 constant = 510.000; λ_2 increasing; Ardol laser produces λ_1 36 pulses per point: 10 pulses per second; λ step size = 0.010nm

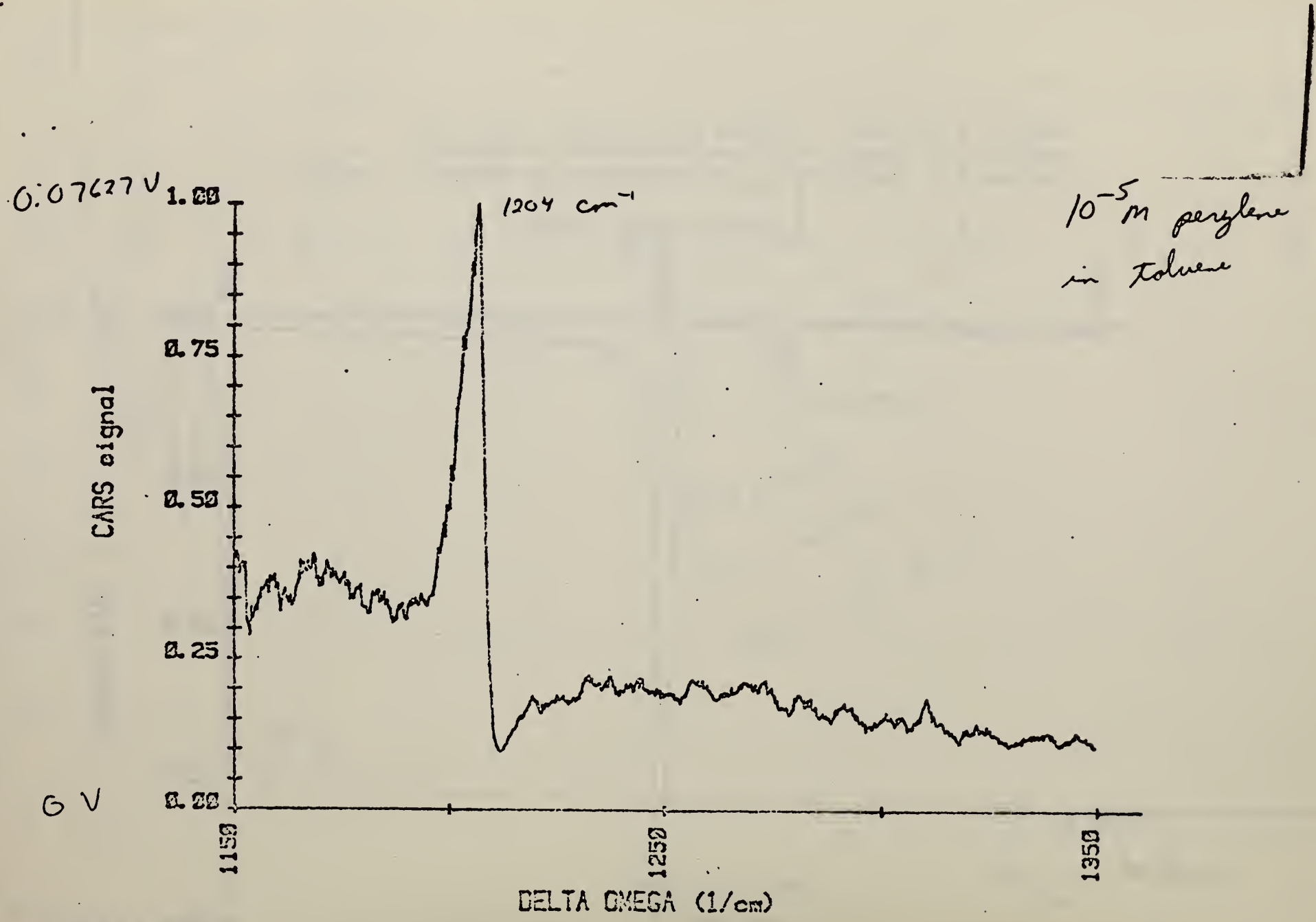

Fig. 4. CARS spectra of perylene (10^{-5}M) in toluene. λ_1 constant = 510.000; λ_2 increasing; Ardel laser produces λ_1 36 pulses per point: 10 pulses per second; λ_2 step size = 0.010 nm.

Fig. 5. Coherent Stokes Raman Scattering (CSRS) of 10^{-5}M perylene in toluene. λ_1 constant = 510.000, λ_2 increasing: Ardel laser produces λ_1 36 pulses per point: 10 pulses per second: λ_2 step size = 0.010 nm

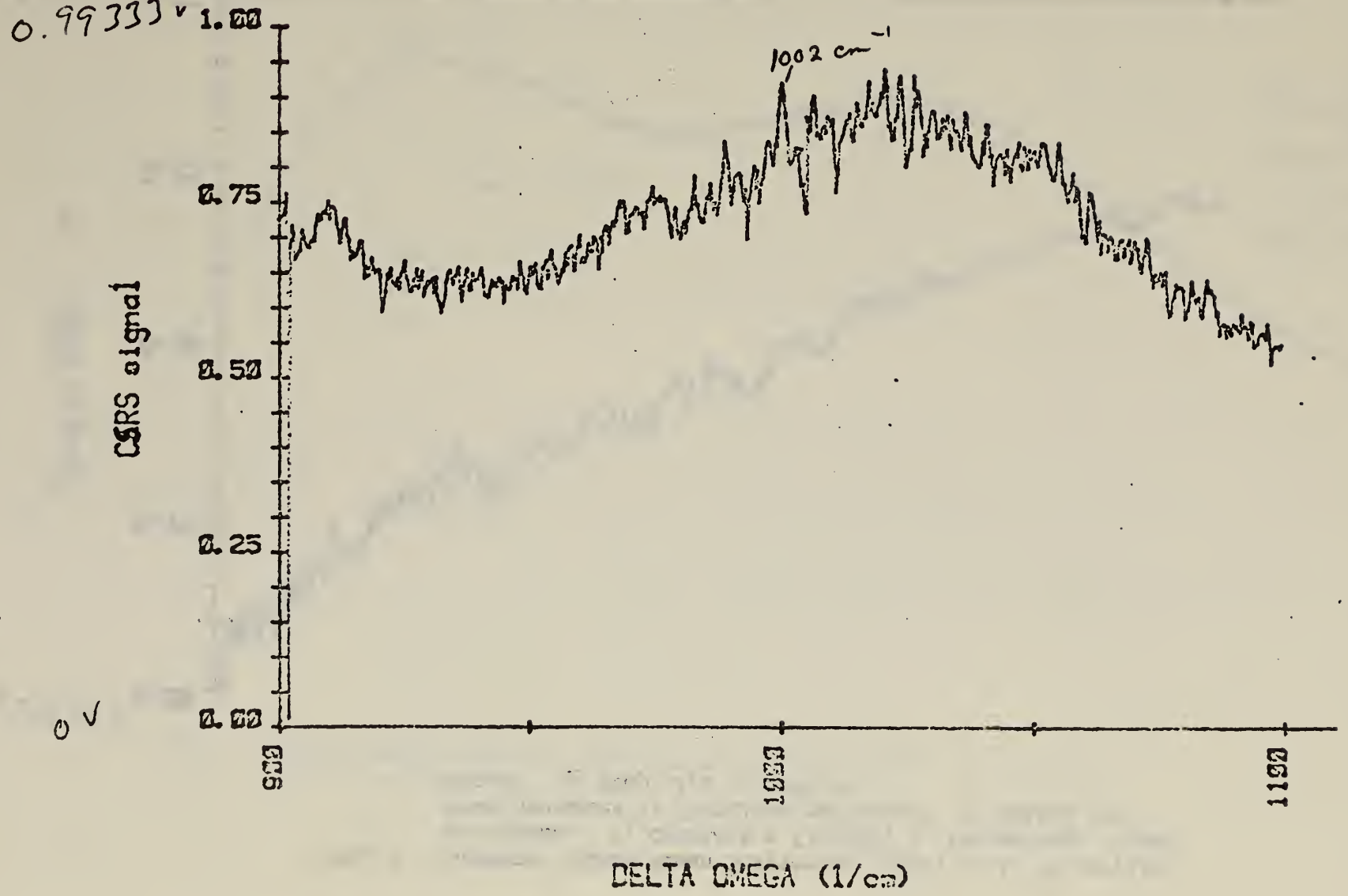

Fig. 6. Coherent Stokes Raman Scattering (CSRS) of 10^{-5}M perylene in toluene. λ_1 constant = 510.000, λ_2 increasing: Ardel laser produces λ_1 36 pulses per point: 10 pulses per second: λ_2 step size = 0.010 nm.

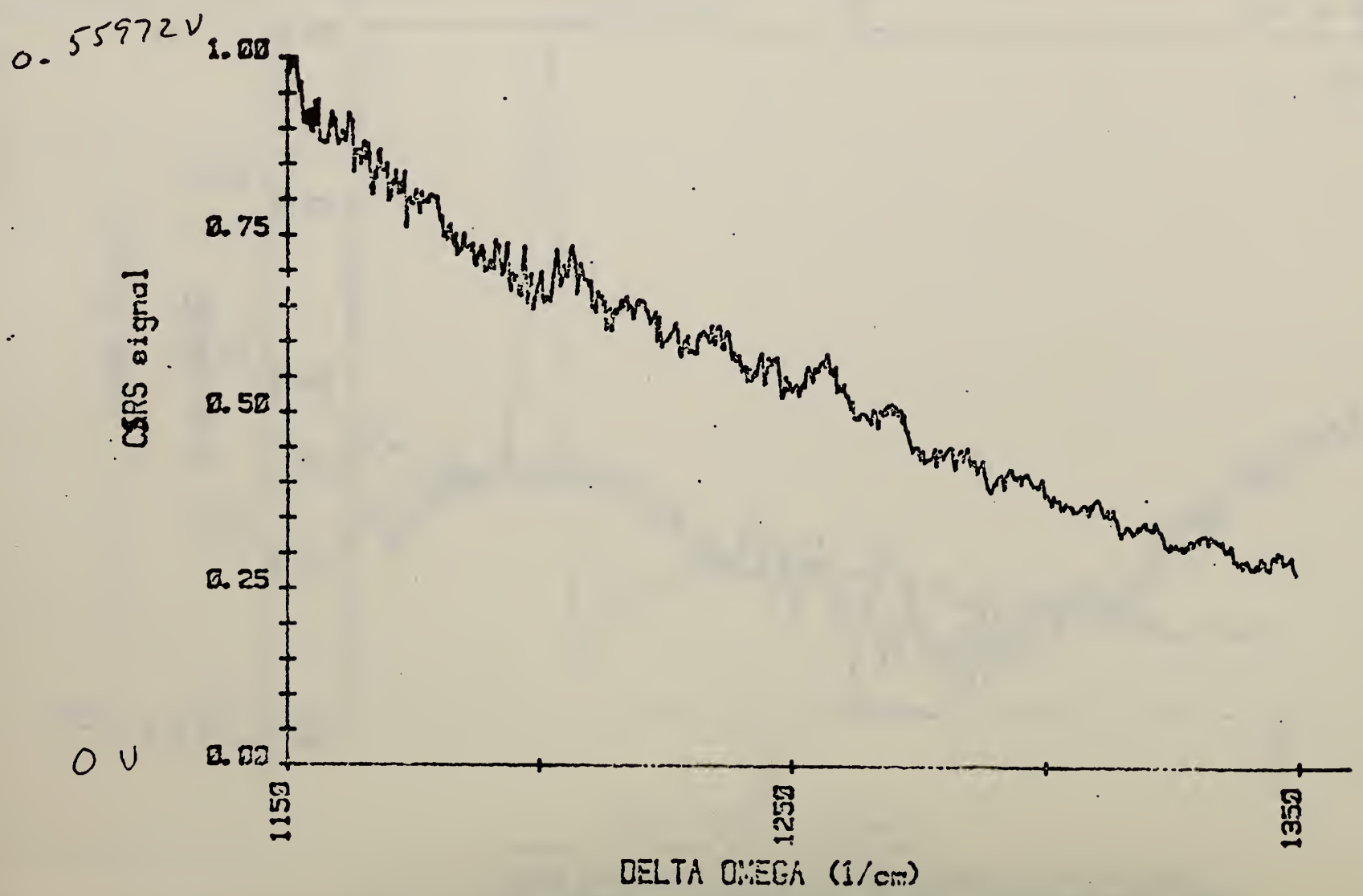

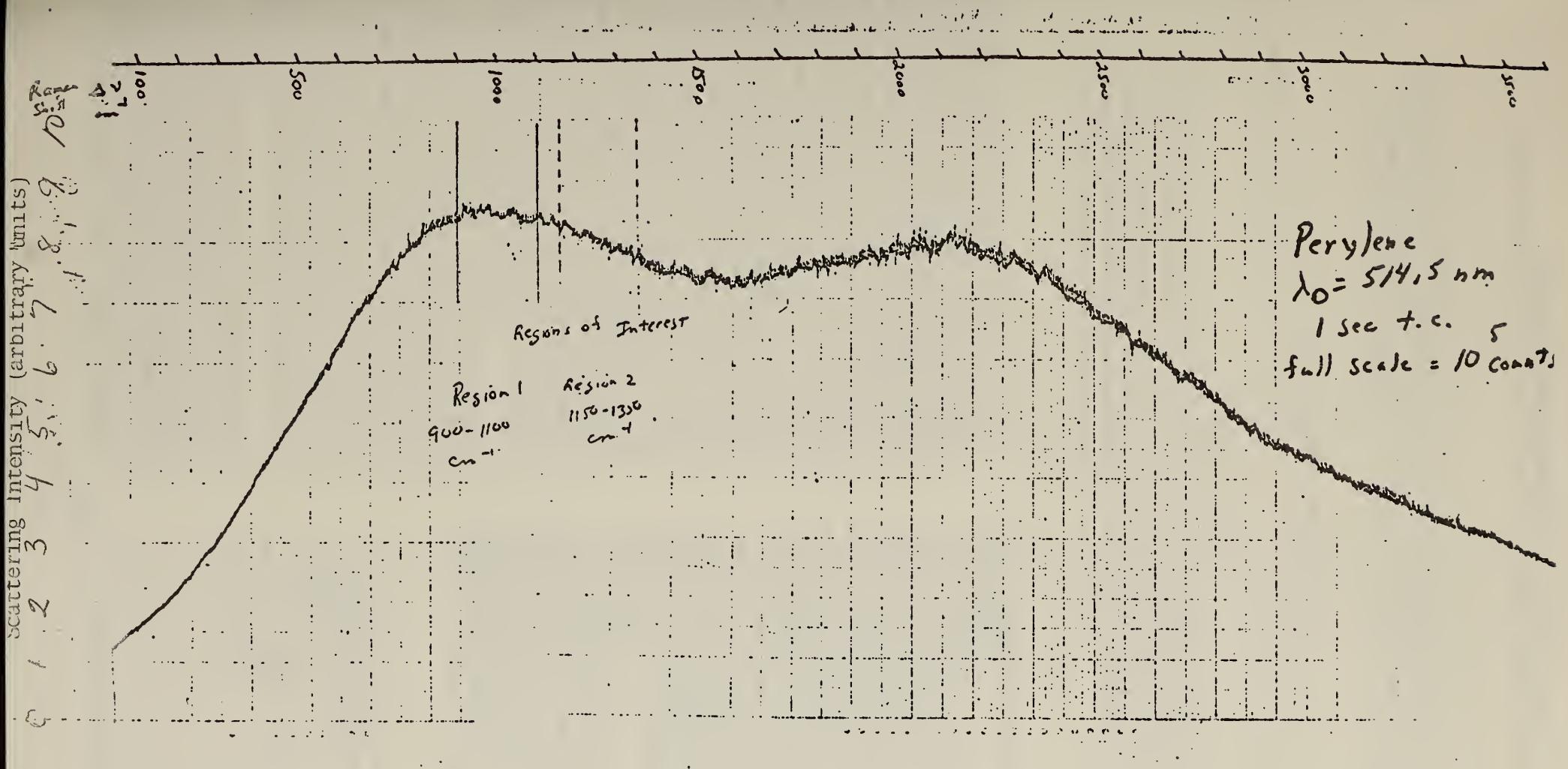

Fig. 7. Normal Raman scattering spectra of perylene (10^{-5}M) in toluene. (λ_0 = 514.5 nm)

Reprinted from OPTICS LETTERS, Vol. 4, page 227, August 1979

Generation of enhanced coherent anti-Stokes Raman spectroscopy signals in liquid-filled waveguides

John C. Schaefer and Ilan Chabay

National Measurement Laboratory, Center for Analytical Chemistry, National Bureau of Standards, Washington, D.C. 20234

Received April 2, 1979

We have demonstrated enhancement of coherent anti-Stokes Raman spectroscopy signals in liquid benzene contained in dielectric waveguide capillaries with angular phase-matching conditions. Enhancement factors as high as 130 were observed relative to a single crossing. These were measured for capillaries of various cross sections as a function of length. The maximum enhancement we observed was in a 50-μm × 50-μm × 292-mm capillary with a sample volume of 0.75 μl. Signals increased steadily with capillary length and showed the same dependence on pump-beam crossing angle (phase-matching conditions) as in bulk samples.

We report here the use of optical waveguides to enhance the coherent anti-Stokes Raman spectroscopy (CARS)[1] signal of a liquid sample. Optical waveguides have been employed previously to enhance spontaneous Raman spectra[2–5] and coherent Raman spectra of gases and solid fibers.[6–8] Our experiments differ from the gas-phase experiments in that the nonnegligible frequency dispersion of a liquid sample requires that the two incident pump beams cross at a certain angle, which depends on the pump frequencies. At this phase-matching angle (generally, a few degrees) momentum-conservation relationships among the pump and signal photons are satisfied, and maximum signal is generated. The use of mode dispersion to allow collinear, phase-matched three-wave mixing as reported for solid waveguides by Stolen *et al.*[3] is possible only at a limited number of wavelengths, making spectroscopy impractical. Angular phase matching is possible for any two pump wavelengths but does have the disadvantage that the volume probed is limited to the intersection of the two focused pump beams. The purpose of these experiments was to increase the intensity of CARS spectra from liquids by increasing the interaction volume while maintaining angular phase matching.

Waveguide enhancement of CARS signals in liquids was demonstrated by measuring the signal that is due to the 992-cm^{-1} symmetric stretch mode of benzene for a single crossing in a bulk sample and comparing it with the signal obtained from benzene in hollow waveguides. Pyrex and quartz capillaries of various lengths, cross-sectional areas, and geometries were tested. A square Pyrex capillary with dimensions 50 μm × 50 μm × 292 mm (~0.75-μl volume) produced a signal that was greater than the bulk signal by more than 2 orders of magnitude.

The experimental arrangement was functionally the same as that described previously.[1] The effective *f* number for crossing with the 160-mm crossing lens (L_2) was *f*/16, whereas that for each pump beam separately was *f*/40. For bulk samples, the crossing point was located within a 1-cm path-length cuvette filled with spectro-grade benzene. In the waveguide experiments, the crossing point was located at the entrance aperture of the capillary.

Two collecting lenses were placed between the cell and the spectrometer. The pump beams and the CARS signal were recollimated by the first lens, which was identical to the crossing lens. The focus of this lens could be placed at the crossing point when a bulk sample was run or at the exit aperture of the capillary when a waveguide was being used. The recollimated beams were focused onto the 0.5-mm-wide slit of a small double monochromator (JY DH-10) by the second lens, whose *f* number was chosen to match that of the monochromator (*f*/3.5). The lens was used at *f*/8. CARS signals were detected by a photomultiplier tube and measured with a Molectron LP20 photometer. A mirror could be introduced just upstream of the monochromator, allowing the power in the pump beams to be measured by a photodiode.

The waveguide cell is shown in Fig. 1. It consisted of a cylindrical Pyrex cell of the appropriate length having a long narrow waist and reservoirs at each end. These reservoirs were capped with end windows made from microscope slide covers. The capillary itself was mounted so that it was supported at its ends by a slightly larger Pyrex jacket. The jacket was supported over most of its length by the narrow waist of the cell.

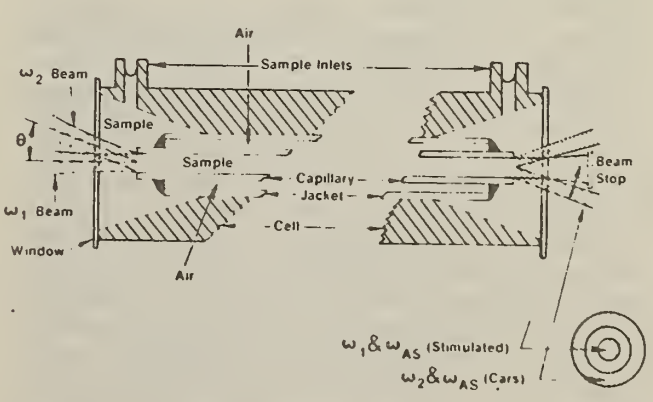

Fig. 1. Capillary cell, showing pump and CARS beams.

The capillary extended to within a few millimeters of the cell windows. The cell was mounted on a two-axis gimbal mount, placed on X,Y,Z translation stages, allowing complete adjustment of position and alignment of the capillary.

The capillaries used in these experiments were purchased from Vitro Dynamics Company. One type was made of Pyrex and had a square cross section. These were available in lengths up to 300 mm. A second variety was made of quartz with a circular cross section and was available only in lengths to 100 mm. Inner dimensions of these capillaries were comparable to the size of the beam waists at their foci. Capillaries were tested whose inner dimensions were 50, 65, 75, 100, and 200 μm. For all the capillaries, the numerical aperture was assumed to be determined by the largest angle for which total internal reflection occurs in benzene. This angle was calculated to be about 17°, corresponding to a numerical aperture of 0.30.

The experiments were done in the following manner. A cuvette was centered at the crossing point, and pump powers were measured for the pump beams. The CARS signal at $2\omega_1 - \omega_2$ was optimized by moving only the two collection lenses. The cuvette was then replaced with a capillary cell that was aligned with the ω_1 beam. The collimating lens was moved downstream to refocus the pump and signal beams onto the monochromator slit, and minor adjustments of the collection lenses were made to reoptimize the CARS signal. The crossing angle was set to generate the maximum CARS signal in the cuvette for a particular $\omega_1 - \omega_2$. Dependence of signal on crossing angle was measured for a 75-μm × 75-μm × 92-mm capillary and was the same as for the cuvette.

Measurement of the enhancement was made by direct comparison of the CARS signal from benzene in the capillary with that from the cuvette with no change in the input beams or detection sensitivity. Only the signal-collection optics and capillary alignment were tweaked. The value of each capillary measurement was divided by the cuvette signal measured immediately before. These results are shown in Fig. 2 for the 50-μm-square capillaries and the 65-μm-diameter round capillaries. Thus the enhancement factor of 130 for the 50-μm-square by 292-mm capillary shown in Fig. 2 is totally independent of the transmitted pump-beam powers (43% of the incident power for the ω_1 beam and 25% for the ω_2 beam).

Variations in capillary alignment, signal collection efficiency, and the degree to which the capillary was obstructed by particles could all combine to reduce or even eliminate the CARS signal in a given experiment, as is evident in Fig. 2. Cuvette signals, on the other hand, were constant to within 20% and correlated with variation in pump powers. In spite of the variations in the capillary results, however, the results as a whole show consistent, significant enhancement and definite trends with respect to dimensions. As a function of length, enhancement increased steadily up to 300 mm. Spectra can be generated in the waveguide in spite of the variations in signal since pump wavelengths can be changed without adjustment of capillary alignment or collection optics. Spectroscopic results will be described in a future article.

The spatial distribution of pump and CARS signals

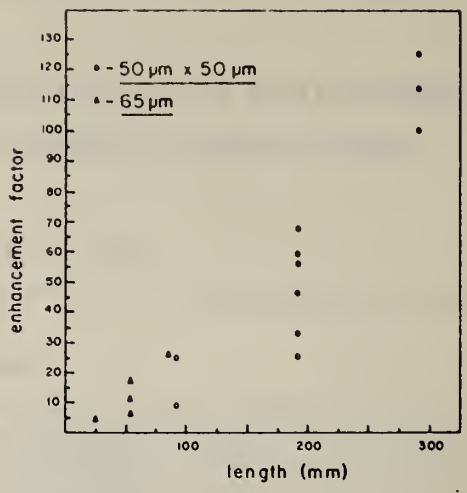

Fig. 2. Waveguide enhancement compared to a single crossing in a cuvette as a function of capillary length for 50-μm-square Pyrex capillaries and 65-μm-diameter round quartz capillaries.

from the capillary was determined by photographing the output pattern. The two pump beams formed separate images, showing maxima and apparent nodes that were reproducible from one photograph to another. The ω_1 pump beam was aligned with the capillary axis and formed a central spot. The output pattern of a round capillary is shown schematically in Fig. 1. For a square capillary, the ω_2 beam formed two vertical bands about the central ω_1 maximum. Each band at ω_2 had vertical and horizontal nodes. From the distance between ω_2 maxima and the center of the pattern, it is estimated that the light at ω_2 emerges from the capillary at an angle of ~1.8° relative to the ω_1 axis. This is consistent with the entrance crossing angle (2° in air) within the accuracy of the measurement.

The CARS signal was also photographed with a narrow-band interference filter used at the CARS frequency. When both pump beams were present, three maxima occurred, a central spot with a vertical band on either side. The patterns observed when the pump beams were present individually indicated that the central spot was due to stimulated emission at $\omega_1 + 992$ cm^{-1} (the anti-Stokes frequency) and the bands on either side were CARS signal. It is significant that phase matching by angular displacement was maintained throughout the length of the capillary. Spatial filtering can be used to improve the signal-to-noise ratio just as in the bulk measurement.

For convenience, all the results were measured using pump beams attenuated by approximately 1 order of magnitude below the powers that could normally be used with a sample contained in a cuvette. At pump powers 1.3 orders of magnitude higher than those used, bubble formation within the capillaries interfered with production and measurement of CARS signals.

Enhancement showed an overall inverse dependence on capillary cross-sectional area. To model this dependence, we employed the expression given by DeWitt *et al.*[9] for anti-Stokes power in the plane-wave limit,

$$P(\omega_{AS}) = \frac{4\pi^2\omega_{AS}^2}{cn_{AS}} |3\chi^{(3)}|^2 \frac{[P(\omega_1)]^2[P(\omega_2)]}{A^2} L^2,$$

where L is the length and A the cross-sectional area of the interaction region. We normalized the results for various-diameter capillaries to remove the dependence of signal on pump power and cross-sectional area. One would expect this normalization to yield identical dependences of normalized CARS output power on length for all the capillaries. Results indicated that this simple picture is not adequate to describe the data accurately.

The dependence of CARS power on length for a single crossing can be inferred from a comparison of the confocal beam parameter, b, the interaction length, L, and the waveguide radius, a.[7] For our experiments the plane-wave approximation is appropriate, and CARS power will increase as the square of the interaction length. This square dependence will also apply to the 50-μm capillary since the capillary's inner dimension is close to the optimum waveguide radius for beams with $b \cong 10$ mm. Our data do not allow a clear distinction to be made between quadratic and linear dependence on length, although the 50-μm capillary appeared to indicate quadratic dependence.

The number of phase-matched crossings per unit length was found to depend critically on the alignment of the pump beams with respect to the capillary axis. The maximum number of phase-matched crossings occurs when one beam is aligned with the capillary axis and the other beam intersects this axis at the crossing angle. When both beams are tilted in the same direction with respect to the capillary axis, more crossings occur, but there are fewer crossings at the correct phase-matching angle. The number of phase-matched crossings for a symmetrical alignment is one half of the maximum value. The enhancement measured for the symmetric case was indeed significantly less than that for the optimum alignment used to obtain all the reported data.

We have demonstrated a capillary cell that enhances the CARS signal by more than 2 orders of magnitude with a liquid sample volume of $\sim$0.75 μl. A cell can be designed in which the sample could be made to flow through the capillary. Such a cell could be connected directly to a liquid chromatograph to provide continuous, nondestructive chemical analysis of the output of the chromatograph.[10] Mixing of contiguous eluent fractions would be minimized in a longitudinal capillary cell, and signal is increased by 2 orders of magnitude with the same pump powers. Effective sample volumes in a longitudinal waveguide cell and a transverse melting point capillary are approximately equal. The waveguide cell may also prove valuable in studies of vibrational and electronic excited states produced in the capillary and probed by CARS.

The waveguide properties of the capillary require that the index of refraction of the sample be greater than that of the waveguide material. If silica capillaries must be used, this is a serious limitation since it precludes the study of aqueous solutions. The development of a low-index capillary or the use of metal or metal-coated capillaries could remove this restriction and allow almost any sample to be used.

We are grateful to Instruments S.A. for the loan of the double monochromator and scan control used in these experiments. We would like to thank Hank DeLeonibus for expert assistance in constructing cells and Gregory Rosasco for valuable discussions.

References

1. I. Chabay, G. K. Klauminzer, and B. S. Hudson, Appl. Phys. Lett. 28, 27–29 (1976).
2. R. H. Stolen, E. P. Ippen, and A. R. Tynes, Appl. Phys. Lett. 20, 62–64 (1972).
3. G. E. Walrafen and J. Stone, Appl. Spectrosc. 29, 337–344 (1975).
4. P. Rabinowitz, A. Kaldor, R. Brickman, and W. Schmidt, Appl. Opt. 15, 2005–2006 (1976).
5. G. E. Walrafen and J. Stone, Appl. Spectrosc. 26, 585–589 (1972).
6. R. H. Stolen, J. E. Bjorkholm, and A. Ashkin, Appl. Phys. Lett. 24, 308–310 (1974).
7. R. B. Miles, G. Laufer, and G. C. Bjorklund, Appl. Phys. Lett. 30, 417–419 (1977).
8. J. Stone, J. Chem. Phys. 69, 4349–4356 (1978).
9. R. N. DeWitt, A. B. Harvey, and W. M. Tolles, Naval Research Laboratory Memorandum Report 3260 (1976), p. 21.
10. L. B. Rogers, J. D. Stuart, L. P. Goss, T. B. Malloy, Jr., and L. A. Carreira, Anal. Chem. 49, 959–962 (1977).

APPENDIX 3

[Reprinted from the Journal of Physical Chemistry, 84, 1611 (1980).]

Low Reynolds Number Fluid Flow Induced by Settling Aerosol and Detected by the Particle Doppler Shift Spectrometer

Robert A. Fletcher, David S. Bright, and Ilan Chabay

Published in Journal of Physical Chemistry, June 12, 1980, pp. 1611–1614, by the American Chemical Society

Low Reynolds Number Fluid Flow Induced by Settling Aerosol and Detected by the Particle Doppler Shift Spectrometer

Robert A. Fletcher,* David S. Bright, and Ilan Chabay

Gas and Particulate Science Division, Center for Analytical Chemistry, National Bureau of Standards, Washington D.C. 20234
(Received September 28, 1979)

Publication costs assisted by the National Bureau of Standards

Air flow generated by gravitationally settling 5–15-μm diameter droplets has been observed. The magnitude of the flow phenomenon is derived from measurements of the particle settling velocities by using the particle Doppler shift spectrometer (PDSS). The PDSS can determine particle velocity and size with high accuracy due to the inherent internal calibration characteristic of the instrument. The magnitude of the fluid flow velocity is dependent on the particle number concentration. Experimental evidence verifying the flow pattern is presented.

Introduction

Each settling particle in a cloud drags some of the air medium with it which effectively increases the settling velocity of neighboring particles. The net effect is to increase the apparent settling velocity of a cloud of particles. In a closed system, such as our PDSS optical scattering chamber, the downward flow of the medium, which results from the settling particles, must be compensated by an equal, but oppositely directed flow. If only part of the chamber is filled with settling particles, an air circulation pattern will be set up as shown in Figure 1a. This occurs because the return flow will be along the path of least resistance which is the path void of particles. If particles homogeneously fill the tube as in Figure 1b, there will be no apparent settling velocity increase due to interaction of the return flow with the aerosol. This description follows that of Happel and Brenner.[1]

An alternative way to describe this particle-induced fluid motion is to examine the net flow in a small sample volume element. For case 1b, the net flow will be zero for a small volume element taken anywhere in the chamber. While for case 1a, if a volume element is taken in the particle stream, a net downward flow will be observed. Likewise, outside the particle column, there will be a upward flow. In both cases, the net flow through any cross-sectional slice of the tube is zero.

We present the first experimental measure of settling-aerosol-induced fluid flow in the low Reynolds number regime. The fluid velocity measurements are made by measuring the settling velocity of clouds of 5–15-μm diameter dioctyl phthalate (DOP) particles which are gravitationally settling in a small closed vessel filled with air. The particle Doppler shift spectrometer (PDSS) is used to detect and measure the particle-induced fluid motion. The fluid motion is observed as a small velocity increment to the particle settling velocity which is calculated from Stokes law. Measurements of such small velocities are primarily due to the internal calibration capability of the PDSS.

The PDSS measures particle settling velocity directly. From the gravitational settling velocity, the aerodynamic size can be determined. The PDSS is capable of determining particle diameter to an accuracy of 0.05 μm (Bright et al.)[2] as a result of an internal calibrating procedure based on the fact that the light scattering intensity is a rapidly varying function of particle diameter over the size range of 5–15 μm.

The Experimental Section contains a description of the PDSS and experimental conditions. In the Results section, the data reduction technique and experimental results are presented. The Discussion section summarizes the work and offers possible applications of the results.

Experimental Section

A schematic of the experiment is shown in Figure 2. Pure DOP aerosol is generated by a medicinal atomizer modified to generate large (5–15-μm diameter) aerosol. The atomizer is driven by a positive pressure air stream that is precisely flow controlled. Dilution air flowing past the atomizer entrains the aerosol stream and determines the final particle concentration. The aerosol is then passed through a charge neutralizer and then is sampled in a 1.3

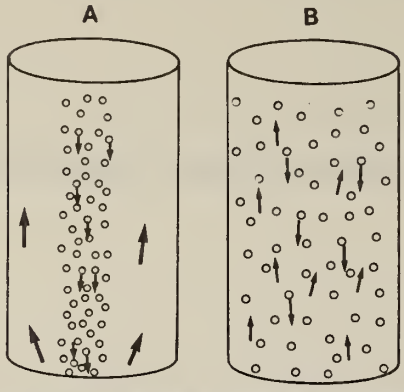

Figure 1. Description by Happel and Brenner of the particle-induced air flow pattern. Case a segregates the return flow to the outside region of the cylinder (region void of particles) while case b integrates the return flow into the cloud.

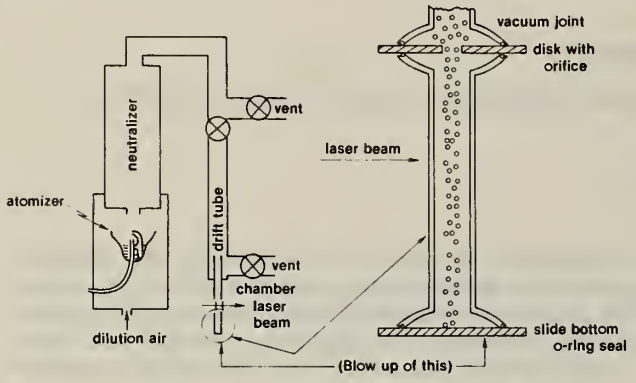

Figure 2. Schematic view of the experimental arrangement.

m long by 0.022 m diameter drift tube. The drift tube is jacketed by a larger diameter tube to allow stable air density layering to occur for the 1–2 °C/m vertical thermal gradient in the laboratory. The drift tube is valved to isolate the aerosol sample from the laboratory environment. The optical scattering chamber is located below the drift tube.

The aerosol clouds used in these experiments contain 5–15-μm diameter DOP particles in number concentrations of 100–1000/cm^3. The aerosol cloud settles through an air medium which is at 25 °C and 1 atm (10^2 kPa) pressure. The Reynolds number for flow past particles of this size range is on the order of 10^{-2}–10^{-3}. The particles are allowed to freely settle under only gravitational influence and the opposing Stokes drag force.

The PDSS has been described in full.[3,4] Briefly, a horizontal laser beam is directed through the settling particle stream. As the particles pass through the beam, they scatter light most strongly in the forward direction. By virtue of the particle motion, the scattered light frequency is Doppler shifted. This frequency shift can be detected by mixing the frequency shifted radiation with unshifted scattered radiation from a stationary source (the chamber window) onto the photomultiplier tube. The frequency shift is related to the particle velocity. The photomultiplier tube output is filtered, amplified, fast Fourier transformed, and displayed as relative scattered light intensity vs. frequency, from which the Doppler frequency shift may be determined.

The PDSS can be used to size single particles or determine the size of individual particles in an aerosol cloud. For a wide size distribution (5–15 μm diameter) of spherical particles the summation of the spectra generates a predictable pattern. The summation spectrum contains local

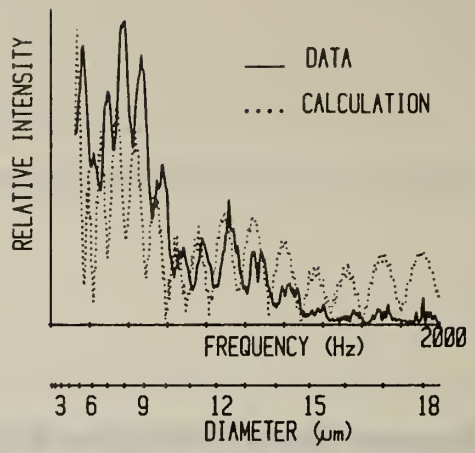

Figure 3. Relative light scattering intensity as a function of Doppler shift frequency compared to theoretical scattering curve. The solid line is the data for DOP aerosol. The dashed line is the exact theoretical calculation. The positions of the data extrema are shifted to the right as a result of the air flow. The shift is measured in terms of the frequency change, Δf, which is subsequently converted to settling velocity.

maxima and minima "features" which reflect the resonant scattering properties of spheres as described by the Mie scattering theory (see Figure 3). Approximately 20 of the features produced are used in the data reduction technique discussed later.

The laser probes the aerosol cloud in the optical scattering cell, which is located directly below the drift tube as shown in Figure 2. The cell is a straight glass cylinder of 9-mm i.d. with microscope slide windows attached for optical purposes. A disk containing a 2–8-mm orifice which serves as an aperture for the particle stream is located above the scattering chamber (Figure 2). Verification of the return, upward directed fluid flow requires a disk of special design. One half of the cell's cross sectional area is open to admit particles, the other side is closed with the exception of a small particle admitting orifice. This design allows us to examine the influence of a large particle stream upon a much smaller one. The bottom of the scattering cell is sealed with a microscope slide which is removeable. Particles collected on this slide can be counted with a microscope to determine the sample number concentration. The seals above and below the scattering window region are made with vacuum o-ring glass joints to ensure isolation of the sample and yet give flexibility in chamber orientation and aperture (disk) alignment.

Results

The experiments demonstrate that the circulation pattern illustrated in Figure 1a is present and that the induced fluid flow velocity depends on particle concentration. The fluid velocity is the difference between the experimentally measured particle settling velocity, v, and the corresponding settling velocity, v_s, calculated from Stokes law. Stokes law is applicable for a single particle settling in a still fluid.

The velocity shift is experimentally observed as a shift of the entire experimental curve to the right of the calculated curve. The frequency difference, Δf, is obtained by subtracting the center position of each experimental extrema from its corresponding calculated position.[2] The frequency difference is converted to velocity difference, $v - v_s$, by

$$v - v_s = \Delta f \lambda / \sin \theta$$

where λ is the wavelength of the laser line in air, v is the

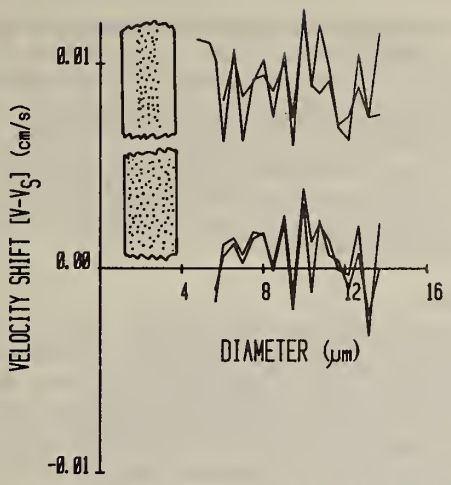

Figure 4. Velocity shift as a function of particle diameter for four sets of data. The upper curves show a positive velocity shift for the aerosol column. When the same scattering chamber is used without the orifice in place (two lower curves), there is no shift. The orifice geometries are indicated on the left of their respective data curves.

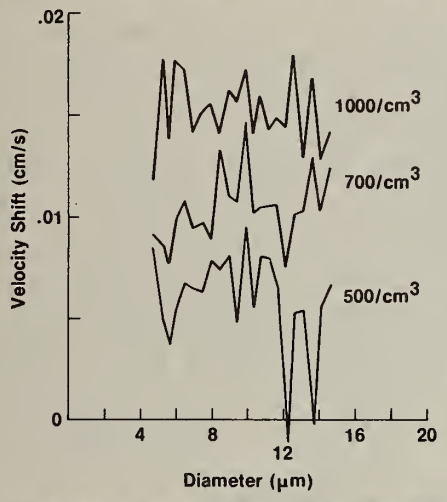

Figure 5. Velocity shift vs. particle diameter for three particle number concentrations. This plot show the dependence of air flow velocity on the particle number concentration.

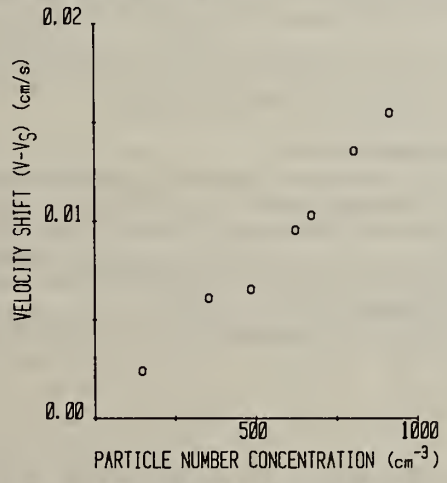

Figure 6. Velocity shift plotted as a function of aerosol particle concentration. Each point is an average of the velocity shift found for the first 15 Mie extrema.

experimentally observed velocity, v_s is the calculated settling velocity via Stokes law, and θ is the angle between the incident laser beam and the detector (typically 5–7°). The results are plotted in Figures 4–8 as velocity shift

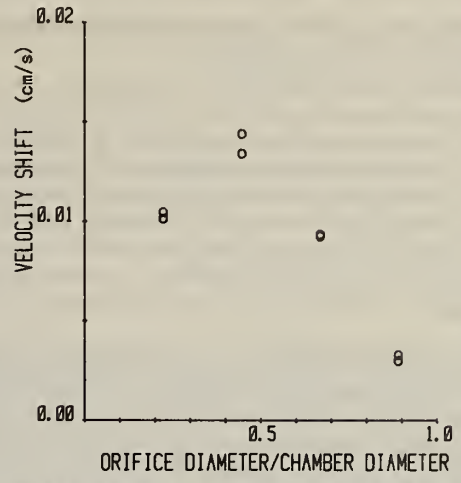

Figure 7. The fluid velocity dependence on the particle admitting orifice size. The orifice is located above the scattering cell.

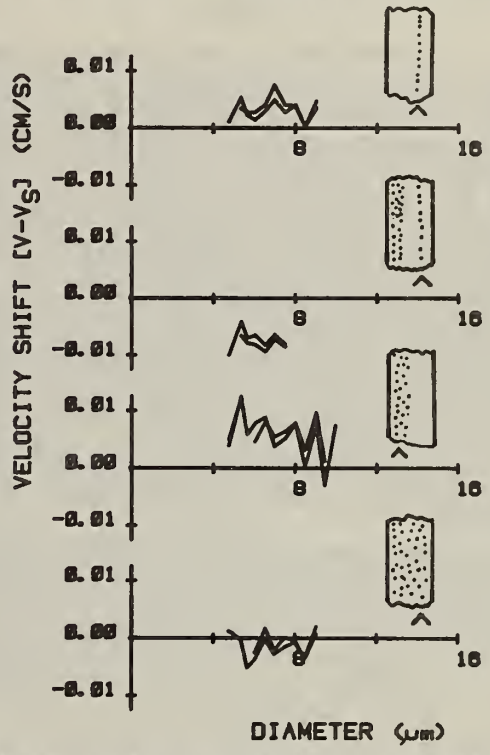

Figure 8. Demonstration of return fluid flow. The various particle void geometries and the resultant velocity shifts of the particles are illustrated in parts a–d. A positive velocity shift is observed in cases a and c where a return flow path is present. A negative velocity shift is observed for the small column of particles because it is located in the return path of the fluid flow induced by the large column of settling particles. This velocity shift demonstrates the existence of the return flow. When the return flow is integrated in the volume of the particle column (d) no velocity shift is observed.

(fluid velocity, $v - v_s$) vs. extrema position where the extrema position have been converted to particle diameter by using Stokes law.

The demonstration of the particle-induced fluid flow is illustrated in Figure 4. The upper two curves show the condition illustrated by Figure 1a, where the column of aerosol produces a downward air flow in the aerosol column and an upward air flow outside the aerosol column, i.e., in the region void of particles. The result show pronounced positive velocity shifts. The bottom two curves are for the case when the entire cross section of the chamber is filled with particles, illustrated in Figure 1b, and show that in this case there is no velocity shift indicating there is no

net microscopic flow. The duplicate data sets show the reproducibility of the experiment.

The particle-induced fluid flow circulation increases with increase in particle concentration. The velocity shifts for three particle concentrations are shown in Figure 5. A summary of velocity shift as a function of particle concentration is presented in Figure 6 where each single shift point is an unweighted average of the velocity shift for the first 15 feature positions at a given particle concentration. A 4-mm diameter collimating orifice is used throughout and the particle concentrations are determined by microscopy.

An order of magnitude calculation is in good agreement with the experimental results. When applying the Navier–Stokes equation in the creep flow regime, the acceleration and inertial terms may be neglected.[5] Balancing the viscous diffusion force against the Stokes particle driving force, F, and replacing $\partial/\partial r$ by $1/R$, we can estimate the vertical fluid (air) velocity, u_z, by

$$u_z|_{max} \sim nFR^2/\eta$$

Here, n is the particle number concentration, η is the fluid viscosity, and R is the radial dimension of the particle column. If we assume an average particle size of 8-μm diameter which has a settling velocity of 0.19 cm/s, a particle number concentration of 1000/cm^3, and $R \sim 0.1$ cm, then $u_z|_{max}$ is on the order of 0.01 cm/s. The experimental results in Figure 6 confirm both the linear dependence on particle number concentration and the general magnitude of the result to within a factor of 2.

The velocity shift as a function of the orifice size (Figure 2) normalized by the chamber size is shown in Figure 7. Below 4 mm, an increase in orifice size causes an increase in the velocity shift. This is reasonable because more particles are put into the system to drive the fluid. As the orifice diameter is increased above 4 mm, the boundary of the particle column and the vessel restrict the return flow resulting in the observed gradual decrease in the velocity shift.

The existence of return flow in the particle-void regions, i.e., outside of a collimated particle stream (Figure 1a) is demonstrated in the following experiment. The fluid velocities are very small, on the order of 0.001–0.01 cm/s, and thus difficult to measure by ordinary means. It is possible, however, to observe the return fluid flow resulting from a column of settling particles by measuring its effect on the velocity of a small column of particles settling in the return fluid flow. The smaller column is used as a probe to sense the fluid flow generated by the larger particle column.

The existence of the return flow is demonstrated by comparing the particle velocities for four geometries as presented in Figure 8a–d. The settling velocity of the particles in the small particle column (Figure 8a) shows a positive shift, as expected for particles settling in a closed system where the return upward fluid flow can occur outside the particle stream. The introduction of the large particle column (Figure 8b) produces a negative velocity shift in the small particle column. This apparent velocity reduction is due to the interaction of the downward velocity field of the small particle column and the upward return flow induced by the large particle column. Measurement of the large particle column velocity reveals the expected positive velocity shift (Figure 8c) for the same reason as in Figure 8a. When the collimators are removed, we see no shift (Figure 8d).

Conclusions

This work presents two main results: one, the experimental observation and quantification of particle-induced steady-state fluid flow phenomenon and, two, demonstrations of the unique capacity of the particle Doppler shift spectrometer to measure small velocities when used in a manner such that the internal size calibration capability can be utilized.

To our knowledge, this is the first experimental measurement of particle-induced fluid flow from cloud droplet size aerosol (5–15 μm) gravitationally settling in air. The results of these experiments may be useful for particle cloud modeling. The role of particle-induced fluid flow in a cloud will for the most part be secondary to thermal convective forces,[6] however, the particle-induced circulation velocities are particle number concentration dependent and thus may become significant at high number concentrations. This work also suggests that a few percent error can result in particle size determinations when using only Stokes law for particle clouds settling in closed containers that have regions void of particles. The ability to measure air flow velocity–particle concentration dependence provides a means of determining the quality of a specific PDSS scattering chamber. The absence of particle concentration dependence implies that a chamber is satisfactory and thus will allow us, by knowing that the calibration is correct, to use solely the aerodynamic properties of the particles to a much higher degree of accuracy. Conversely, in a chamber where circulation occurs, we can estimate particle number concentrations by measuring the velocity shift.

This work also shows the capability of the particle Dopple shift spectrometer to make extremely small velocity measurements in real time. Some of the velocities reported are on the order of 10 μm/s. We will apply these techniques and the unique sensitivity and accuracy of the PDSS to further studies of fluid behavior in the low Reynolds number, low velocity regime.

References and Notes

(1) J. Happel and H. Brenner, "Low Reynolds Number Hydrodynamics", Prentice-Hall, Englewood Cliffs, N.J., 1965, p 371.
(2) D. S. Bright, R. A. Fletcher, and I. Chabay, *J. Phys. Chem.*, this issue.
(3) I. Chabay and D. S. Bright, *J. Colloid Interface Sci.*, **63**, 304 (1977).
(4) J. P. Gollub, I. Chabay, and W. H. Flygare, *Appl. Opt.*, **12**, 2838 (1973).
(5) J. Happel and H. Brenner, ref 1, p 41.
(6) N. H. Fletcher, "The Physics of Rainclouds", University Press, New York, 1969.

Particle Doppler Shift Spectrometry. Accurate Size Determinations of 5–15-μm Aerosol

David S. Bright,* Robert A. Fletcher, and Ilan Chabay

Gas and Particle Science Division, Center for Analytical Chemistry, National Bureau of Standards, Washington, D.C. 20234
(Received September 28, 1979)

Publication costs assisted by the National Bureau of Standards

We have improved the particle Doppler shift spectrometer (PDSS) to determine the diameter of 5–15-μm droplets to high accuracy (±0.05 μm). The diameter is calculated from Stokes law and the gravitational settling velocity which is obtained by measuring the Doppler shift of laser light scattered at a single angle. This scattered light also shows intensity variations with diameter as predicted by Lorenz–Mie light scattering theory. Characteristic features of the plot of scattered light intensity vs. droplet diameter are used as size calibration markers. The features are a function of only the index of refraction of the aerosol material and the wavelength of the light. Our results show better agreement with Stokes law without the slip correction than with the correction.

Introduction

Particle size measurement has many important applications. For example, particle size measurements will likely be involved in the monitoring of industrial crushing or grinding processes and quality control of paints, cements, or other powders is likely to involve particle size measurement.[1-3] The implementation of industrial hygiene standards and the study of air pollution[4] also involve particle size measurements. Most particle sizing and size measurement instruments cannot be calibrated from first principles and require calibration by a laboratory generated aerosol. For example, the widely used optical particle counters[5-7] which measure particle size as a function of the light intensity scattered off single particles must be calibrated by using some type of aerosol standard. Most aerosol generators in turn require size measurement of the aerosol by an accurate method[8] in order to be useful as a calibrating standard.

The particle Doppler shift spectrometer (PDSS) has been already applied in the calibration of an optical particle counter[9] by determining the diameter of the monodisperse calibrating aerosols. In this paper we will establish the accuracy of the PDSS technique and demonstrate its utility.

Golub, Chabay, and Flygare[10] first used a laser Doppler shift technique to measure droplet growth. A variation of the more commonly used dual-beam laser Doppler velocimetry technique, this single beam heterodyne technique involved beating Doppler shifted laser light scattered from particles against reference laser light scattered from the chamber window, which is the heterodyne source. This technique measured many droplets in the laser beam at once, since the individual signal packets of each droplet could be separated with respect to the heterodyne frequencies. The frequency information gave the settling velocities and thus the droplet diameters. The same authors suggested using the Mie intensity features in the data as sized calibration markers, and they qualitatively employed one such marker.[11]

Using this same technique with the PDSS, Bright and Chabay[12] then reported using five to ten Mie size markers. Here we report the following developments: (a) improved precision of the PDSS; (b) a quantative measurement of improved accuracy by using up to 20 Mie features as size markers; (c) the experimental conditions necessary to obtain this accuracy, and; (d) an experimental verification of Stokes law without the slip correction factor.[13]

Experimental Section

The PDSS is shown schematically in Figure 1, where a horizontal laser beam, polarized horizontally, passes through a vertical tube (A) in which the particles settle under gravity. The optics now include a 20-cm focal length lens with a 10-μm pinhole at the focal point. This allows observation of the particles for the full 2-mm height of the beam while limiting the observation angle to within 3 mdeg of θ, i.e., 6 ± 0.003°. Any averaging of light scattering over this angle range is negligible; light scattering and Doppler calculations are performed for precisely 6°. The optics are mounted on a tiltable table which can be lowered to θ = 0° for alignment. Alignment of the pinhole is the most critical step. The tilt of the table, which has been checked with gauge blocks and a sine-bar, is within less than 0.01° of 6°. A 0.01° error is compared with other sources of error in Figure 5. The maximum effect expected from the observation angle error is small.

Light is scattered into the detector (see Figure 1) both from the particles and from the windows on tube A. The light from the windows is the heterodyne source. The heterodyne frequency[12,14] for a particle is $F = \bar{V}\cdot\bar{K}$ or, since $|\bar{K}_s| \simeq |\bar{K}_0| = 2\pi/\lambda$ and $\bar{K} = \bar{K}_0 - \bar{K}_s$ then

$$F = \frac{V}{\lambda} \sin \theta \qquad (1)$$

where $\bar{K}$ is the scattering vector, $\bar{K}_0$ and $\bar{K}_s$ are the initial and scattered momentum vectors, θ is the scattering angle, λ the wavelength of the laser line in air through which the particle falls, 514.5 nm, and $V = |\bar{V}|$ is the velocity of the particle.

A single particle falling through the beam with Stokes velocity V produces a photomultiplier current signal having modulation frequency F and amplitude envelope proportional to the product of the intensity of the light scattered by the particle and the time the packet is observed. The resolution of the PDSS is shown by the representative single-particle peaks in Figure 2. The limits of resolution are a function of the following parameters:

(a) Resolution of the 400-channel FFT (fast Fourier transform) spectrum analyzer. This is 5 Hz for the 2000-Hz range.

(b) Broadening due to Brownian motion. The full width at half-maximum is $2D|\bar{K}|^2/2\pi$,[12,14] where D is the diffusion coefficient of the particle.[13,15] This width is less than 3 Hz for 5-μm diameter DOP (dioctyl phthalate) spheres, and is even less for larger spheres.

Published in Journal of Physical Chemistry, June 12, 1980, pp. 1607–1611, by the American Chemical Society

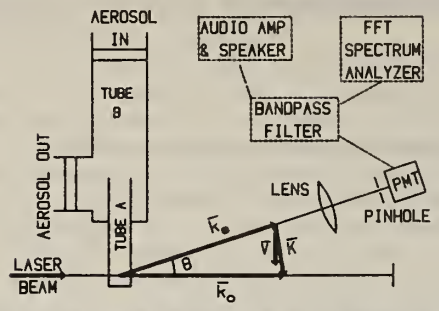

Figure 1. Schematic of apparatus. Aerosol is passed through tube B (1 m × 22 mm). Valves are closed, sealing the tube A–tube B system. Data are collected for 5 min with the FFT spectrum analyzer as the particles settle into tube A (20 cm × 9 mm) and through the beam. Microscope slide sections are inserted into the walls of tube A for windows for the laser light. The lens–pinhole–PMT (photomultiplier tube) system rests on a tiltable platform inclined at the scattering angle θ (6°) and collects light scattered at angle θ from the full length of the beam intersecting tube A. The loudspeaker is routinely used to monitor experimental conditions.

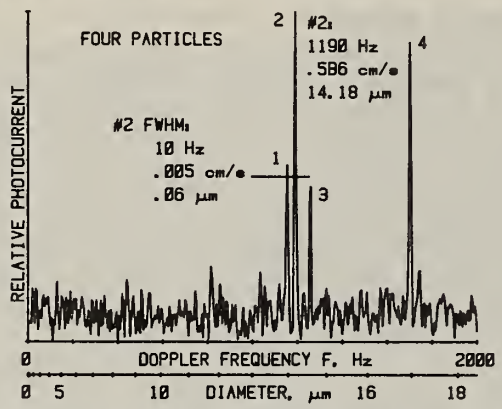

Figure 2. Example of resolution of PDSS. Frequency spectrum of a 0.2-s time window, during which four particles were falling through the beam. Data reported in this paper are 5 min of such spectra, averaged in the frequency domain. The full width at half-maximum of peak 2 is 10 Hz, corresponding to 0.005 cm/s or, from Stokes law, 0.06 μm.

(c) Truncation error. The error associated with a FFT frequency measurement is inversely proportional to the time of the measurement. The minimum amount of time the fastest particles (18 μm, V = 1 cm/s) are in the beam is about 0.2 s, which is also the sampling window of the FFT. This resolution is then limited by the 5-Hz channel widths of the FFT analyzer.

For shorter portions of wave packets, the corresponding peaks on the frequency spectrum are broader than 5 Hz and are of low amplitude. These low amplitudes result from the short duration of the packets or because the particles are in the edge of the beam. These broad peaks contribute a small amount to the background noise.

The Doppler frequencies are audibly distinguishable especially at the beginning of a run when only a few larger particles are in the beam. Small leaks, streaming of the air near the beam, or excessively dirty windows can be detected conveniently and quickly after some practice by listening to these Doppler signals. This serves as a diagnostic which allows us to avoid making a complete run only to find the Mie structure (Figure 3) buried in noise and artifacts.

Of all the geometries tried for scattering chambers, the best is a tube with windows made of pieces of microscope slides set into the walls. Thermal shielding is not necessary, especially since a stabilizing thermal gradient of about 1 °C/m fortuitously exists in the room. However, thermal convection cells do spontaneously occur for chambers with

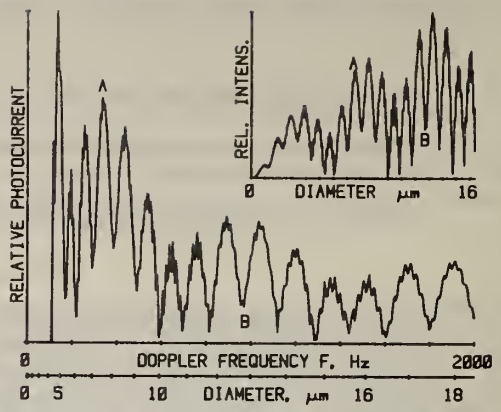

Figure 3. Mie features in the light scattering calculations. The inset shows Lorentz–Mie light scattering calculations plotted vs. diameter for DOP at 25 °C (index of refraction = 1.48970, λ = 514.5 nm, θ = 6 °). In the main figure, for direct comparison with the data, the light scattering calculations are plotted vs. the Doppler frequency F (calculated from the diameter, Stokes law, and the density, ρ = 0.9797 at 25 °C). The intensity is scaled by $1/F$. Two corresponding features are labeled as A and B.

any horizontal dimension greater than that of the 9 or 10 mm diameter tube (tube A, Figure 1). Another subtle factor is important in the design of the chamber. If there are regions void of particles near the scattering region, air flow will be induced in the scattering region by the motion of the falling particles. This streaming invalidates diameter measurements by Stokes law because it results in a settling velocity greater than the aerosol gravitational settling velocity. This is easily detected on the PDSS.[16] To avoid this phenomenon, the chamber must be filled homogeneously with the falling aerosol, which is achieved by the relatively simple design of tube A. The windows are set into the wall to match the inner diameter as closely as possible, protruding slightly into the aerosol stream rather than leaving small gaps that would not be filled with the falling aerosol. The tubes are set as closely as possible to vertical.

We have chosen dioctyl phthalate (DOP) aerosol for our experiments because it has the following characteristics: (a) It has a low vapor pressure; the particles do not change size significantly during the measurement time of less than 1 s.[18,19] (b) It is optically nonabsorbing at 514.5 nm. (c) Its physical characteristics have been accurately measured here at the National Bureau of Standards. At 25 °C and 514.5 nm, the index of refraction is 1.48970 and the density is 0.9797 g/m^3.

The DOP aerosol is generated by using a glass medicinal atomizer modified by removing the curved tube where the larger droplets normally impact and run back to the liquid reservoir. This modification extends the upper size limit of the generated aerosol. The air supply to the atomizer is carefully regulated and filtered. The aerosol, after dilution with filtered air, is transported through tube B (see Figure 1). For a measurement, valves at both ends of tube B are closed, trapping some aerosol in the tube, and the aerosol in the sample then to settles through tube A. The 20-cm settling space in tube A above the scattering region allows only those particles greater than 4 μm to reach the laser beam during a 5-min run. The maximum concentration of particles during any part of a run is several hundred per cm^3. If the large number of very small particles generated by the atomizer drifted into the scattering region, the light scattered from these particles would mask the heterodyne signal from the beam spots on the windows which serve as the heterodyne sources. This homodyning would obliterate the Mie structure in the data.

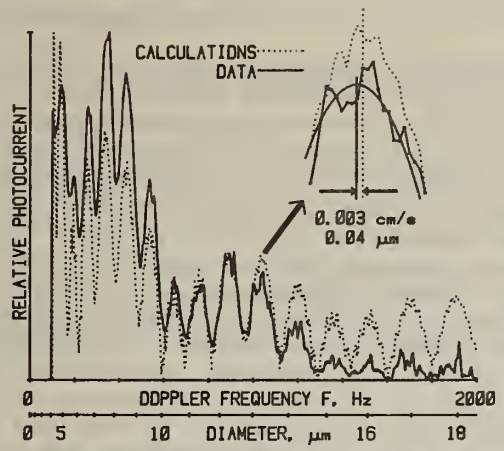

Figure 4. Velocity shift measurement example. The calculated photocurrent vs. diameter curve of Figure 3 (dotted) is superimposed on data (solid) to illustrate how the differences in the feature positions (abscissa only) are measured. The inset shows this peak, with a shift of −0.003 cm/s is one such feature. The vertical lines mark the centers of the parabolas fitted to a selected region of points of the data and the calculations. The segment of points fitted with a parabola is shown only for the data. The shift of −0.003 cm/s corresponds to a diameter measurement error of −0.04 μm.

Theory

Setting Velocity. In still air, spheres with diameter d settle with terminal or Stokes velocity

$$V_s = \frac{\rho g d^2}{18\eta} \tag{2}$$

where $g = 0.9802$ m/s^2 is the acceleration of gravity, ρ is the density of the sphere minus the density of air, and $\eta = 1.832 \times 10^5$ Pa·s (1.832×10^4 P) is the viscosity of air at 1.01×10^5 Pa (760 mmHg) and 25 °C. For larger particles, a Reynold's number correction becomes necessary. For example, the velocity correction[13] for 30-μm particles of unit density is 0.7%. Extrapolation of Davies'[13] empirical formula to diameters less than 30 μm shows the correction for the size range discussed here to be less than 0.09% and to be proportional to d^3. For particles below the 5–15-mm size range a slip correction is used.[13] The slip correction in air for particles larger than 2 μm is of the form $V = SV_s$ where

$$S = 1 + \frac{1.257l}{0.5d} \tag{3}$$

and where l is the mean free path of air molecules, 6.53×10^{-6} cm, at atmospheric pressure. Extrapolation of this empirical formula beyond the particle sized originally measured,[20] of about 2 μm, then shows that the velocity correction from the slip factor increases linearly with diameter:

$$V - V_s = SV_s - V_s = \frac{\rho g(1.257)2l}{18\eta} d$$

In the 5–15-μm size range, the velocity correction is respectively 3–1% of the overall settling velocity. The PDSS technique has sufficient accuracy to test for this correction, as will be shown.

Mie Features and Calibration. Lorentz–Mie light scattering calculations[21,22] show the relative scattered light intensity at a fixed angle to oscillate rapidly with increasing diameter for transparent or weakly absorbing spheres (Figure 3, inset). Features such as peaks or valleys occur at specific diameters.[11] To make Lorentz–Mie scattering

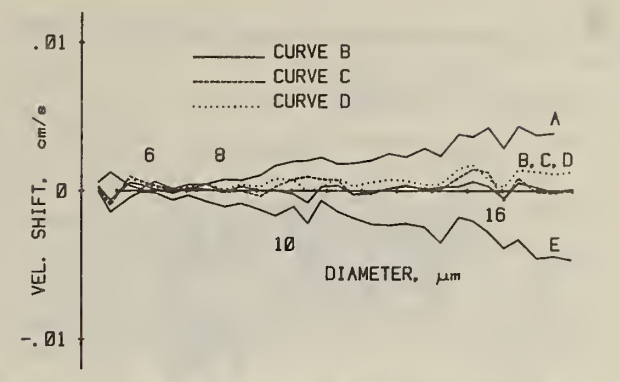

Figure 5. Error analysis. These five calculated curves show shifts of feature positions from positions of the correctly calculated curve, for the following reasons: A. Temperature shift of 2.5 °C. (Experimental temperature changes were less than 0.5 °C.) B. Additional light scattered through 174° = 180° − 6° due to 9% of the beam returning back through the aerosol from each surface the second window. C. Aerosol density change of +0.57% and index of refraction change of −0.1%. This mimics a run with near zero shifts. Changes of index and density by the right ratio to exactly offset each other are improbable. For example, they do not occur with temperature changes, as seen from curve A. D. Scattering angle change, $\theta = 6.01°$. E. Index of refraction change of 0.1% only.

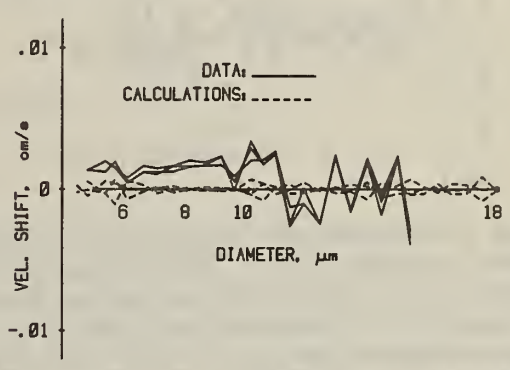

Figure 6. Sensitivity of the velocity shift measurements to the measurement procedure. Three separate determinations of shift were performed on one data curve from one measurement (solid lines) and on one curve from Mie calculations (dotted lines). The measurement procedure involves choosing initial feature positions by hand and gives a small degree of variability. Feature positions of the data are not measured above 15 μm because there are too few particles to define the features there.

calculations, one must know the wavelength of the incident light and the index of refraction of the particles. DOP particles meet these requirements: DOP is a clear liquid and the index and density of the bulk material are well characterized. After the light scattering calculations are suitably scaled (Figure 3), they resemble PDSS data for a reasonably flat distribution of particles as seen in Figure 4. The comparison of data with the scaled theoretical calculations corresponds to the comparison of the measured Doppler settling velocities (solid vertical line, Figure 4, inset) with the theoretically calculated velocities from the feature diameters using Stokes law (dotted vertical line, Figure 4, inset). The measured velocity minus the calculated velocity, i.e., the velocity shift, is determined as illustrated in Figure 4 and is measured at a number of diameters throughout the size range as shown in Figures 5–8. In practice, an initial feature position is marked on a plot of the data, and then digitized to locate the center of the segment data points used for the parabola fit. This fit (Figure 4) then determines the feature position more accurately. For both theoretical calculations and experimental data analysis, the width of the segment of each curve that works well with the parabola fit is a constant

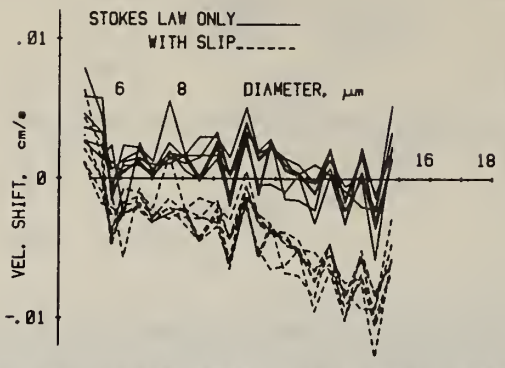

Figure 7. Effect of the slip correction. Shifts of data from seven runs and several chambers were measured with respect to calculations employing the slip correction (dotted lines) and with respect to calculations using Stokes law only (solid lines).

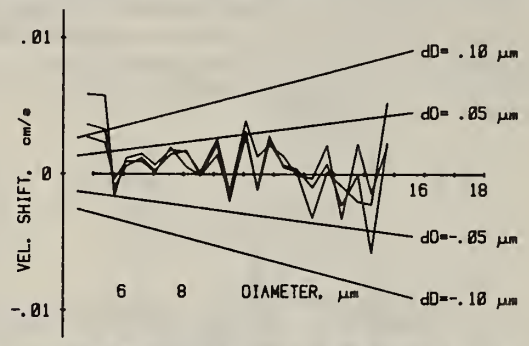

Figure 8. Typical calibration data. These curves show shift vs. diameter for three runs from one chamber. The shifts reflect the differences between the settling velocities measured by the Doppler shift and the settling velocities calculated from the optical diameter (abscissa) by using Stokes law only. Slanted lines show the shifts corresponding to the indicated diameter changes as a function of diameter. This relates the error in diameter determination to the scatter in the shift measurements.

fraction of the total segment between adjacent features. Figure 4 illustrates the determination of velocity shifts. A feature is not used if there are insufficient particles to give a measurable peak (or valley).

Changes in temperature shift the features (Figure 5, curve A) because of temperature dependence of the index of refraction and density of the particles and the viscosity of air. The apparent velocity shifts are small for the experimental temperature deviations of 0.5 °C or less.

Since the diameter is related to the Doppler frequency by eq 1 and 2, a calibration measurement is a verification of these equations, especially of the value of the density–viscosity ratio. If the shifts for a measurement are all near zero and if the index of refraction is correct, then the ratio must be accurate. The sensitivity of the calculated feature positions to changes in either the ratio or the index of refraction is shown by examples in Figure 5. Also illustrated in Figure 5 is the mathematically possible but experimentally unlikely instance of compensation of errors in the two above parameters. In cases such as this, where the fractional error in the ratio is −6 times that in the index of refraction, all shifts are expected to be near zero. Experimentally, such changes in the parameters are not expected because the droplets were made from pure DOP in contact with glass only.

There is some additional light scattered into the PMT from the particles at an angle of 174°. The windows of tube A are almost perpendicular to the beam, and 9% of the light going through the second window is reflected back into the aerosol from each surface. The Doppler frequency associated with this light is the same as with the 6° scattered light; this additional reflected light potentially could distort the Mie features and shift their positions. Curve B of Figure 5 shows that these shifts are minimal. Reflected light is ignored in all other calculations.

The repeatability of feature position measurements is illustrated in Figure 6. The slight amount of scatter for any one feature is due to the manual stage of the measurement process, and the larger scatter from feature to feature is due to the statistical nature of the data.

The accuracy with which the PDSS can measure velocities suggests that other effects on velocity might become experimentally observable such as hydrodynamic particle–particle or particle–wall interactions. For the diameters in use, however, the chamber should give a wall effect[23] one order of magnitude below that presently detectable. Particle–particle interactions should not be significant. Although theoretical predictions of such interactions for randomly sized droplets are not available, calculations for monodispersed droplets are.[23] The particle concentration in the chamber was never above several hundred cm^{-3}. When the number-averaged sized droplets with this concentration is used, these calculations predict the magnitude of this effect to be again an order of magnitude below that presently detectable.

Results

The noise level or variability of the PDSS shift measurements is illustrated by the solid curves in Figures 7 and 8. This variability is small enough to allow measurement of the slip phenomenon. The dotted curves of Figure 7 show the differences between the measured velocities and the calculated velocities when the slip-corrected Stokes law is used, i.e., eq 2 and 3. The slip correction overpredicts the settling velocities (the downward trend of the dotted curves) while stokes law, eq 2, provides best agreement with the data (the near zero shifts of the solid curves). Thus any slip phenomenon is much less than predicted. Equation 3 is not valid for this size range at atmospheric pressure.

Finally, the accuracy of the PDSS is shown by the small magnitudes of the velocity shifts. The slanted lines that form a varying diameter scale in Figure 8 shows the deviations in diameter via eq 2 that result from the velocity shifts. From runs such as these, diameter measurements of 5–15-μm DOP aerosol are calibrated to within 0.05 μm.

Conclusions

The internal calibration of the PDSS has been demonstrated for spherical particles. Velocity shifts average less than 0.002 cm/s. Most of the diameters from the settling velocities and the nonslip-corrected Stokes law match the optical diameters to within ±0.05 μμ. In the 5–15-μm size range, we believe this to be the most accurate real time size measurement of droplet diameter.

We have used the PDSS for calibrating an optical particle counter[9] and for measuring small air flows induced by a settling particle stream.[16]

We plan to use the PDSS for calibrating other instruments and monodisperse aerosol generators, for investigating the aerodynamic and light scattering properties of aerosols, for measuring the deviations from Stokes law due to slip for small particles in a partial vacuum, and for measuring the deviation from Stokes law due to turbulence for larger particles.

References and Notes

(1) S. Berg, *Powder Technol.*, **10**, 1 (1974).
(2) R. Davies, *Am. Lab.*, **10**, 97 (1978).
(3) J. W. Sadowski and E. Byckling, *Powder Technol.*, **20**, 273 (1978).
(4) K. T. Whitby and R. A. Vomela, *Environ. Sci. Technol.*, **1**, 801 (1967).

(5) D. Y. H. Pui and B. Y. H. Liu, "TsI Quarterly", TSI Inc., St. Paul, MN, May/June 1979.
(6) D. D. Cooke and M. Kerker, *Appl. Opt.*, **14**, 734 (1975).
(7) B. Y. H. Liu, R. N. Berglund, and J. K. Agarwal, *Atm. Environ.*, **8**, 717 (1974).
(8) K. T. Whitby, D. A. Lundgren, and C. M. Peterson, *Int. J. Air Water Pollut.*, **9**, 263 (1965).
(9) R. A. Fletcher, G. Mulholland, I. Chabay, and D. S. Bright, *J. Aerosol Sci.*, in press.
(10) J. P. Gollub, I. Chabay, and W. H. Flygare, *Appl. Opt.*, **12**, 2838 (1973).
(11) J. P. Gollub, I. Chabay, and W. H. Flygare, *J. Chem. Phys.*, **61**, 2139 (1974).
(12) I. Chabay and D. S. Bright, *J. Colloid Interface Sci.*, **63**, 304 (1978).
(13) C. N. Davies, *Proc. R. Soc. London*, **57**, 18 (1945).
(14) H. Z. Cummins and H. L. Swinney, *Prog. Otp.*, **8**, 135, 155, 157 (1970).
(15) S. K. Freidlander "Smoke, Dust and Haze: Fundamentals of Aerosol Behavior", Wiley, New York, 1977, Chapter 2.
(16) R. A. Fletcher, D. S. Bright, and I. Chabay, *J. Phys. Chem.*, this issue.
(17) B. Y. H. Liu, V. A. Marple, and H. Yazdani, *Enviorn. Sci. Technol.*, **3**, 381 (1969).
(18) R. Chang and E. J. Davis, *J. Colloid Interface Sci.*, **54**, 352 (1976).
(19) E. J. Davis and A. K. Ray, *J. Aerosol Sci.*, **9**, 411 (1978).
(20) R. A. Millikan, *Phys. Rev.*, **22**, 1 (1923).
(21) M. Kerker, "The Scattering of Light and Other Electromagnetic Radiation", Academic Press, New York, 1969.
(22) J. V. Dave, "Subroutines for Computing the Parameters of Electromagnetic Radiation Scattered by a Sphere", Report No. 320-3237, IBM Scientific Center, Palo Alto, CA, May, 1968.
(23) J. Happel and H. Brenner, "Low Reynolds Number Hydrodynamics with Special Applications to Particulate Media", Prentice-Hall, Englewood Cliffs, N.J., 1965.

AIR FLOWS INDUCED BY SPARSE CLOUDS OF DROPLETS

by

David S. Bright, Robert A. Fletcher and Howard R. Baum

Submitted to Journal of Fluid Mechanics

Experimental Variables

a	droplet diameter
r	distance from axis of chamber
R	inner radius of chamber
R_0	radius of droplet column
$U_d(a)$	Doppler velocity of droplets downward past chamber windows
$U_s(a)$	Stokes velocity of droplets, calculated using optically measured diameters
$u(r)$	air velocity induced by droplets, $u(r) = U_s(a) - U_d(a)$
$\bar{U} = \int_0^{R_0} u(r)dr$	measured air velocity = u(r) averaged across droplet column (positive downward)
$F(a)$	force on 1 cm^3 air by one droplet = $6\pi\mu a U_s(a)$
n	droplet number density, $\#/cm^3$
μ	viscosity of air
ρ	density of droplets

Dimensionless Variables

$k = R_0/R$	dimensionless radius of particle column
$\eta = r/R$	dimensionless distance from axis of chamber
$U'(\eta) = \mu u(a)/R^2 nF$	dimensionless air velocity

I. Abstract

Very slow air flows (.01 cm/s), induced by a column of 5 - 15 μm diameter droplets settling in a 9 mm diameter chamber were measured with a laser light velocimeter apparatus. We measured the air flow velocity as the difference between the Doppler-measured Stokes settling velocity of individual droplets and the settling velocity calculated from simultaneous optical measurements of droplet diameter. Experimental conditions included a wide range of droplet sizes, relatively slow air motion, and many droplets being in the laser beam at the same time.

We describe the interaction of the particles with the air in terms of a simple two-fluid model with an exact solution of the Navier-Stokes equation.

II. Introduction

The theory of suspensions is currently in a state of active development. Many models employ particle-particle interactions via the fluid medium, Happel (1965) and Fuchs (1964). Batchelor (1972), in particular, has performed a series of studies based on the analysis of pairs of randomly placed spheres. The recognition that the particle-fluid interaction cannot be calculated by treating the particles as a fixed array has led to a variety of other approaches, Nagatani (1978), and to a statistical theory of suspensions. A recent review of this work is given by Herczynski and Pienkowska (1980).

Although statistical approaches have led to greatly increased understanding of the collective interactions between particles, they are difficult to apply to experimental macroscopic flow problems. Here, we introduce the "two-fluid" model to analyze our experiments. This model assumes that the positions of droplets at different locations are completely uncorrelated, allowing the droplets to be described by a number density only. While providing less detailed information than Batchelor's approach, the model does permit direct computation of the fluid flow induced by the settling droplets.

The two-fluid model agreed well with this experiment: We measured the velocities of slow air flow caused by settling aerosol droplets. The 5 to 20 μm diameter droplets settled by gravity down the center of a closed glass tube. When there was an annular droplet free region surrounding the column of droplets, the air moved down the center of the tube and returned back up

the annular region surrounding the column. When the cross section of the tube was uniformly filled with droplets, no air motion was detected. The air velocity was determined in a unique and accurate manner based on laser Doppler velocimetry and on the Lorentz-Mie light scattering of spheres. The air motion determined to within 0.002 cm/s, ranged from approximately 0.002 cm/s to 0.015 cm/s and varied linearly with droplet number concentration.

III. Theory

To model the particle induced air flow, we make the following assumptions:

1) There is an inner cylindrical droplet-air fluid phase inside a coaxial air annulus which is the second fluid phase (figure 1). Each phase may be described by mass and momentum transport equations. In the droplet phase, coagulation and diffusion may be ignored.

2) The mean droplet velocity relative to the air, of magnitude $U_s(a)$, is directed vertically downward. The droplets have reached a steady state and are no longer accelerating.

3) The tube in which the measurements are made is sufficiently long for all quantities near the measurement volume to be taken as independent of distance along the tube.

Under these conditions the size distribution n(r,a) is given by:

$$n(r,a) = \tilde{n}_0(a) \quad 0 \leq r \leq R_0$$
$$= 0 \qquad R_0 < r < R$$

and $U_s(a)$ is given by Stoke's law:

$$\frac{4}{3}\rho_p a^3 g = 6\pi a \mu U_s(a) \equiv F(a). \tag{1}$$

Here, r is the radial distance from the centerline of the measurement tube, R_0 is the radius of the droplet stream (figure 1), R is the tube radius, ρ_p is the droplet density, μ is the viscosity of the air, g is the gravitational acceleration, $\tilde{n}_0(a)$ is the spatially averaged droplet number density, and F(a) is the force exerted on the air by one droplet. The air phase mass and momentum balances are given by:

$$\int_0^R u(r)\, r dr = 0$$

$$\frac{1}{r}\frac{d}{dr}\left(r\mu\frac{du}{dr}\right) = \frac{dp}{dz} + \int_0^\infty n(r,a)\,\tilde{F}(a)da \qquad (2)$$

where u(r) is the air velocity and $\frac{dp}{dz}$ is the unknown pressure gradient, taken to be independent of z. Equation (2) must be integrated subject to the following boundary conditions:

$$u(r=R) = 0$$

$$\frac{du}{dr}(r=0) = 0 \qquad (3)$$

Moreover, at $r = R_0$, the velocity u(r) and shear stress μdu/dr must be continuous. Since the viscosity μ is constant (recall μ is the viscosity of the air and not of the suspension), this reduces to a requirement that μdu/dr be continuous at droplet stream boundary R_0. Note that the inertial acceleration terms vanish identically in this geometry without approximation. This fact, together with assumption (2) means that equations (1) and (2) are an exact set of equations for this two-fluid model.

These equations can be readily integrated to yield:

$$U' = -\frac{k^2}{4} - \frac{k^2}{2}\log(k) - \frac{\eta^2}{4}(1 - k^2)^2;$$

$$0 \leq \eta \leq k.$$

$$U' = -\frac{k^2}{4}(2 - k^2)(1 - \eta^2) - \frac{k^2}{2}\log(\eta);$$

$$k \leq \eta \leq 1. \qquad (4)$$

where dimensionless forms for u(r), r and R_0 are respectively

$$U' \equiv \frac{\mu u(r)}{R^2 n_0 F}, \qquad \frac{r}{R} \equiv \eta, \quad \text{and} \quad \frac{R_0}{R} \equiv k, \text{ and where}$$

$$n_0 F \equiv \int_0^\infty \tilde{n}_0(a)\, F(a)\, da \,. \tag{5}$$

The results are plotted in dimensionless form in figure 2. Positive values of u(r) denote downward motion. The upwelling on the side is needed to ensure an air mmass balance since the tube is blocked off at the bottom. Note that there is no induced flow if the tube is uniformly filled with droplets. The absolute motion of the droplets relative to the laboratory, U_d, is then given by:

$$U_d(a) = U_s(a) + u(r). \tag{6}$$

It is this formula which is tested against the experiments to which we now turn.

IV. Experimental

Dioctylphthalate (DOP) droplets were generated with a medicinal atomizer. The atomizer air flow rate controlled the number density of the droplets, but did not appreciably affect the relative size distribution. The atomizer was modified to remove the impaction surface that ordinarily collects most of the droplets above two to three micrometers in diameter. The cloud of droplets then passed through a krypton-85 neutralizer, and then through tube B (figure 3). For a velocity measurement, the valves were closed for 500 s and the droplets were allowed to fall through tube A, the orifice and the laser beam, and then allowed to settle onto the microscope slide. Immediately after the measurement, the microscope slide was removed, droplets were counted, and both tubes were flushed with air. The droplets ranged in diameter from about 5 μm, those large enough to reach the laser beam during the 500 s measurement period, to about 15 μm.

The radius of the stream of droplets, R_0, was fixed by the radius of the orifice (see figures 1 and 3). R_0 was assumed to be constant throughout the height of the chamber (tube B) because the droplets formed a clear image of the orifice on the slide after settling over 15 cm.

The motion that the droplets induced in the air was measured by a laser light scattering technique, Bright, Fletcher & Chabay (1980) and Fletcher, Bright & Chabay (1980). Briefly, the falling velocities of the droplets were measured relative to the chamber windows by a single beam laser Doppler velocimetry technique (figure 3). Data was collected for the entire width of the

droplet stream that was intersected by the laser beam (figure 1). The velocity of the air was the excess of the falling velocities over the Stokes velocities calculated using the optically measured diameters. The diameters were measured by light scattering measurements done concurrently with the velocity measurements. The light scattering size measurements were performed on a collection of droplets as follows: Data for a broad size distribution of droplets, such as generated here, appeared as a curve of light intensity vs. droplet velocity, U_d, with about twenty peaks and valleys or features. This was because the 500 second summation of data averaged out the much narrower signal peaks of the individual droplets, but retained the broader variations of intensity vs. size due to the properties of light scattered from spheres. In other words, the features corresponded to droplet diameters that scatter the laser light most or least strongly at the 6 degree scattering angle (figure 3). The features were matched along the velocity axis with similar features in a calculated curve, Kerker (1969), of Lorentz-Mie light scattering intensity vs. Stokes settling velocity for droplets of known index of refraction and density. The index of refraction and density of the bulk DOP liquid were measured by standard techniques at NBS.

The velocities for these feature diameters were $U_d(a)$ and $U_s(a)$ for the data and Lorentz-Mie-Stokes calculations respectively. In air moving up or down, the velocity of the air, $u(r) = U_d(a)-U_s(a)$, is the velocity of each data feature with respect to the corresponding Lorentz-Mie-Stokes feature.

The air velocities reported were the averages of velocity measurements for the twenty or so feature diameters between 5 and 15 μm. The Doppler velocities, $U_d(a)$, were measured to a precision of better than 0.002 cm/s and the diameters to a precision of better than 0.03 μm, allowing a determination of air velocities from 0.002 to 0.015 cm/s even though $U_d(a)$ and $U_s(a)$ were in the range of 0.1 to 0.7 cm/s.

Absolute concentrations of the droplets could not be determined from the light scattering data due to an undetermined amount of background shot noise that would change with very minute shifts in chamber orientation. However, the data did provide an estimate of the relative size distribution, from which a mass mean diameter was determined, and from which the force term, $n_o F$ was calculated.

Total droplet concentrations were determined from microscope slide counts. The slides with oil repelling surfaces collected the settling particles for the 500 s measurement.

V. Results

The predictions of the two-fluid model agree well with the data from two experiments, as shown in figures 4 and 5. For these experiments the air velocity $u(\hat{r})$, integrated along the laser beam was:

$$\bar{U} = \int_0^{R_0} u(r)\, dr \ .$$

In figure 4, the induced flow is maximized for a droplet stream of about one half chamber diameter. Here, the droplet stream radius, R_0, is varied by changing the orifice, while the droplet concentration is not changed. When the droplet concentration is changed with R_0 constant, as in figure 5, the induced flow velocity is directly proportional to the force term, n_0F (equation 5). Because the relative size distributions were similar, the mass mean diameter varied by less than 4 percent. Thus, the force term, n_0F, and the flow velocity were proportional to the droplet concentration or slide count. The mass mean diameter was estimated from the light scattering data to be 12.8 μm. The droplet concentration was estimated from the slide counts of collected droplets and the volume of a cylinder with a base of the counted slide area and a height equal to the distance that a 12.8 μm droplet falls in 500 s.

The diameter and concentration estimates are crude and both parameters are in fact changing during the measurement period as the larger droplets settle out first. In spite of this, our calculated air velocities from the two-fluid model stay within 10 to 20 percent of the experimental measurements as shown in figures 4 and 5.

VI. Conclusions

We have demonstrated experimentally that an air column sparsely populated with droplets can be modeled as a homogeneous fluid. This was verified by measuring air velocities less than 150 μm/s using small droplets as probes. The index of refraction and density of the droplets must be known, but their radii need not be measured by other means. A distinctive feature of the two-fluid model is the linear dependence of the induced air velocity on droplet concentration.

References

BATCHELOR, G. K. 1972 Sedimentation in a dilute suspension of spheres. J. Fluid Mech. 52, 245.

BRIGHT, D. S., FLETCHER, R. A. & CHABAY, I. 1980 Particle Doppler shift spectrometry. Accurate size determinations of 5 - 15 μm aerosol. J. Phys. Chem. 84, 1607.

FLETCHER, R. A., BRIGHT, D. S. & CHABAY, I. 1980 Low Reynolds number fluid flow induced by settling aerosol and detected by particle Doppler shift spectrometry. J. Phys. Chem. 84, 1611.

FUCHS, N. A. 1964 The Mechanics of Aerosols. The McMillan Company, New York, p. 46.

HAPPEL, J. & BRENNER, H. 1965 Low Reynolds Number Hydrodynamics with Special Applications to Particulate Media. Prentice Hall, Englewood Cliffs, New Jersey.

HERCZYNSKI & PIENKOWSKA. 1980 Toward a statistical theory of suspension. Ann. Rev. Fluid Mech. 12, 237.

KERKER, M. 1969 The Scattering of Light and Other Electromagnetic Radiation. Academic Press, New York.

NAGATANI, T. 1978 Statistical theory of effective viscosity in a random suspension. J. Phy. Soc. Japan 47, No. 1, 320.

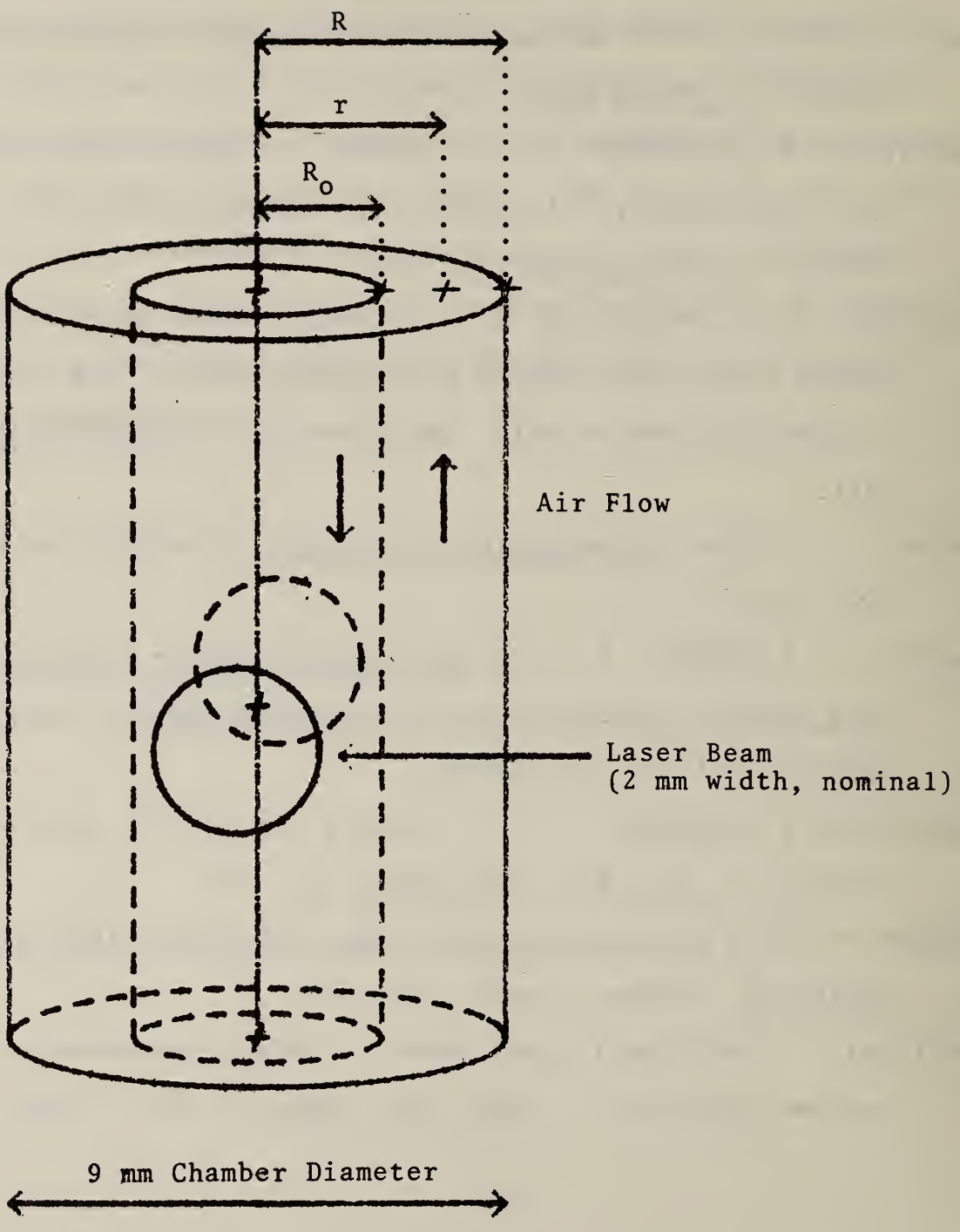

Figure 1. Geometry of the experiment: – schematic diagram of the measurement chamber and droplet stream.

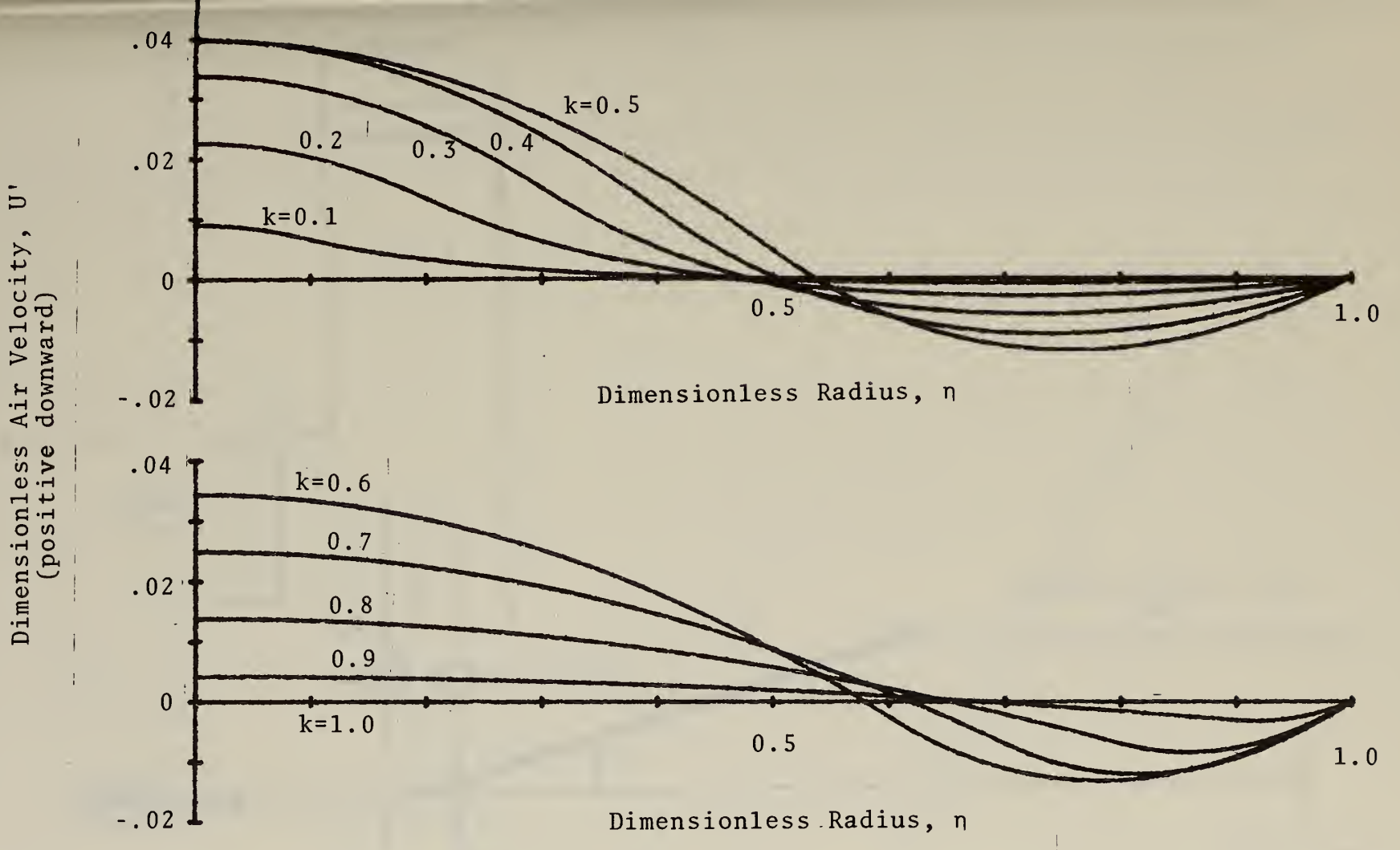

Figure 2. Two-fluid model prediction of the air flow across the chamber as a function of the size of the droplet stream. Note, for example, the conditions for where the droplet stream is half the diameter of the chamber (k=0.5): a. The downward air motion is maximized at the center (η=0). b. The air is motionless slightly outside the stream (η=0.54). and c. There is considerable upwelling of air in the annular shaped region between the chamber wall (η=1) and the edge of the stream (η=0.5).

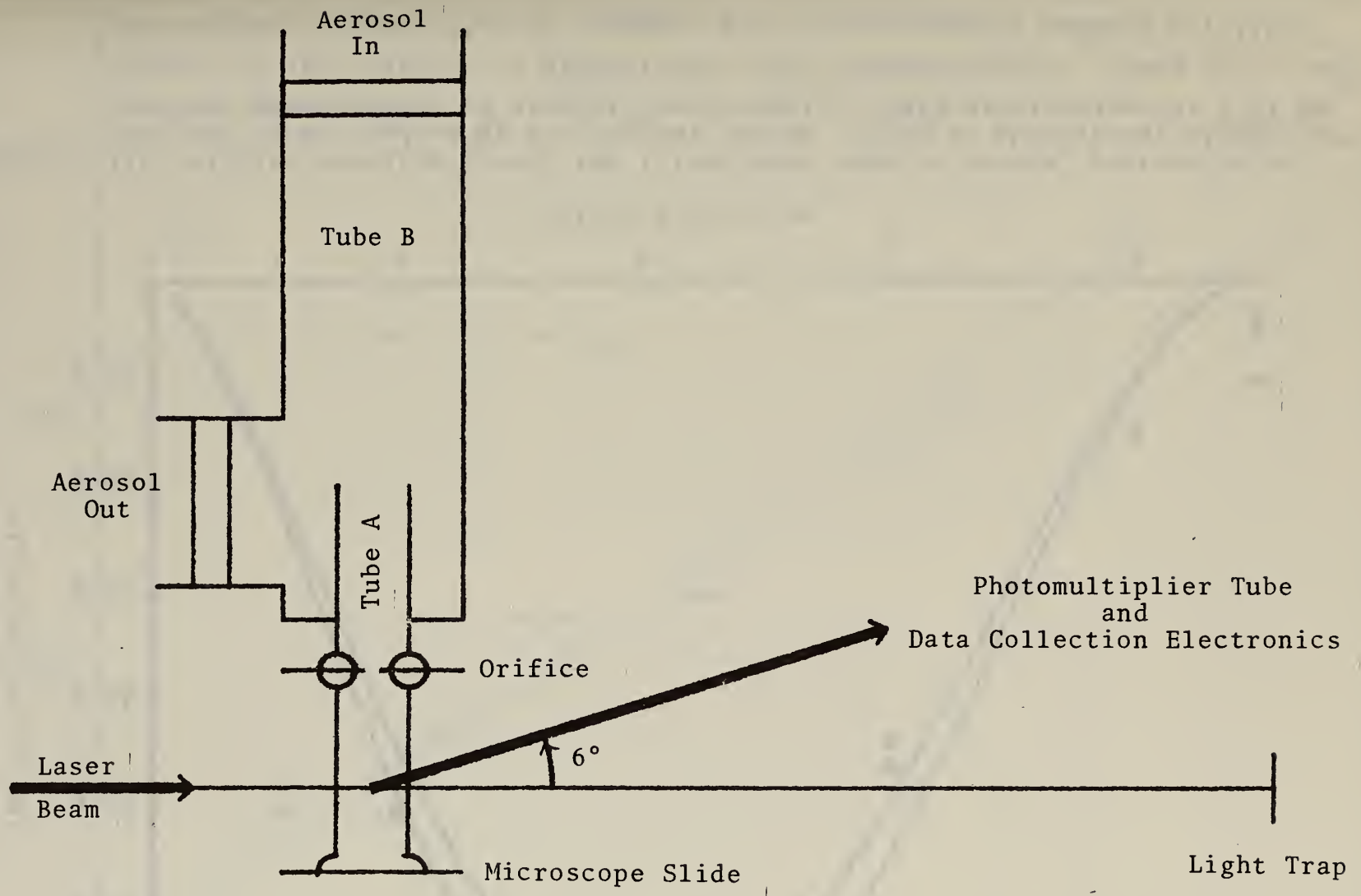

Figure 3. Schematic diagram of the experimental apparatus. Droplet diameters and falling velocities are measured from the laser light scattered at 6 degrees. Tube B is a reservoir for the droplets. Tube A is the 9 mm diameter measurement chamber. The orifice sets R_0, the radius of the droplet stream.

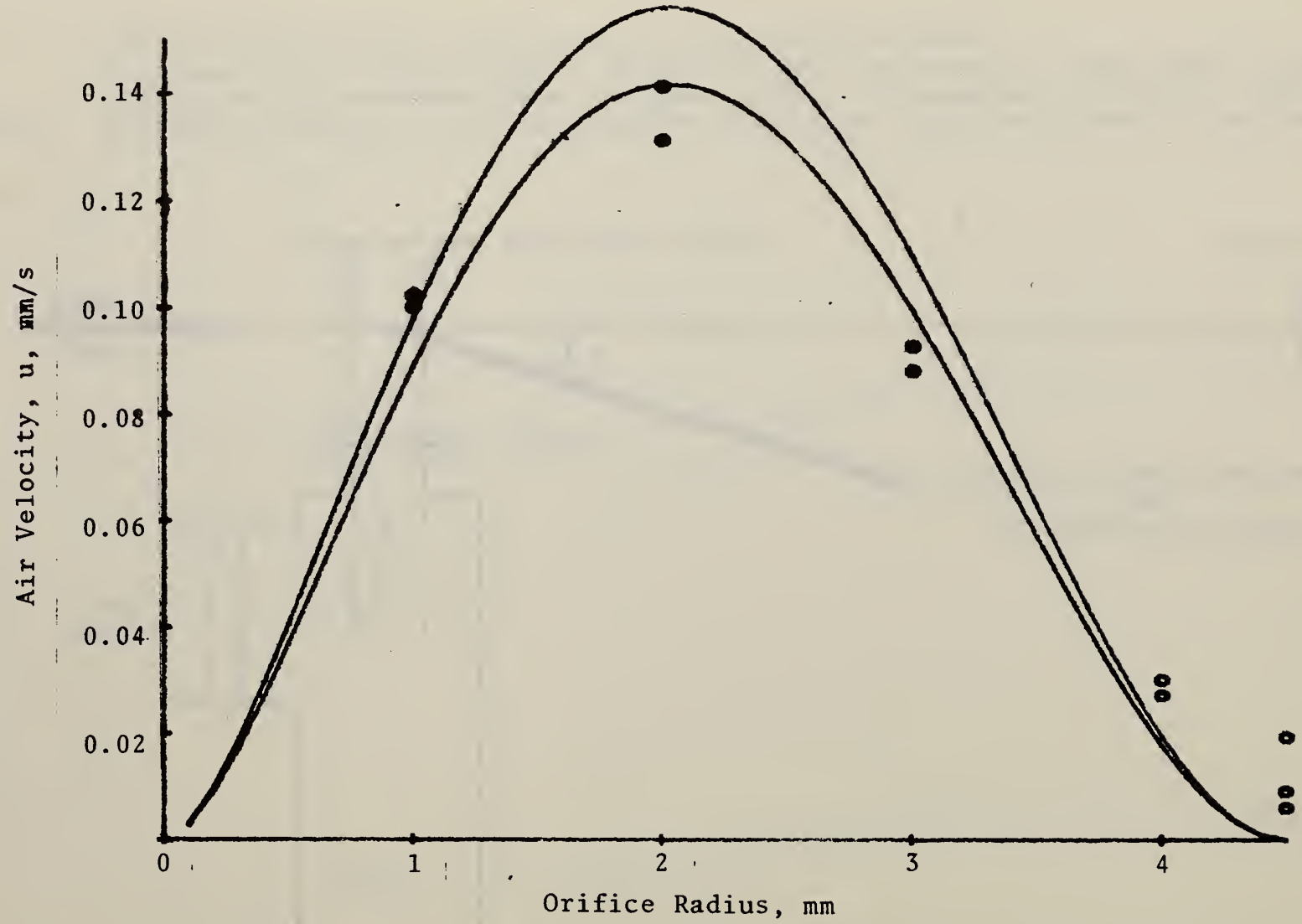

Figure 4. Air velocity averaged across the illuminated droplet stream, plotted as a function of the radius of the droplet stream. The two theoretical lines represent two measurements of droplet concentration. Data are lacking for R_0<1 mm because of the scarcity of droplets for such a small orifice. When R_0=4.5 mm, the droplet stream fills the chamber, and there is little induced air flow.

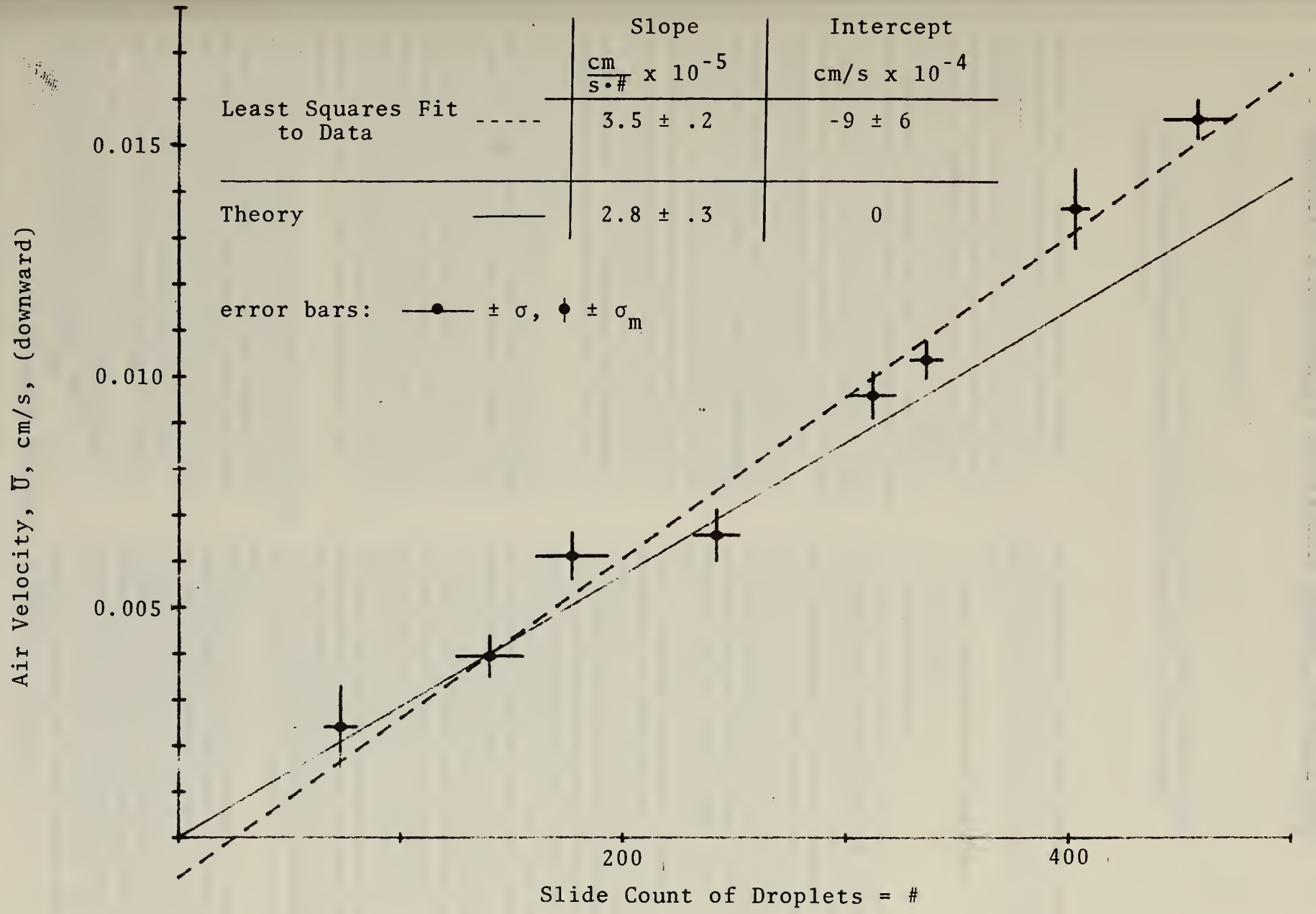

Figure 5. Averaged air velocity (as in figure 4), for R_0=2 mm, as a function of droplet count. The droplet count is a measure of droplet concentration because the relative droplet size distribution is nearly constant.

Matrix isolation Raman spectroscopy

D.S. KING, J.C. STEPHENSON

A new primary laboratory measurement is described for testing field standards and measurement techniques used to detect trace amounts of toxic organic substances in water.

Until this decade, the assessment of pollutant levels in water was based on measurements of such properties as total organic carbon or biochemical oxygen demand. Although it was realized that these tests did not take into account the toxic properties of specific chemicals, it was not until the discovery of specific toxic and carcinogenic substances in drinking water supplies in the early 1970's that programmes to identify and quantify routinely low concentrations of specific organic compounds were initiated. Now phrases such as 'consent decree pollutants' and 'priority pollutants' which reflect the legislative and regulatory mandates of the last few years are commonly heard in discussions of environmental assessment. In response to the need to identify and quantify low concentrations of organic compounds in environmental samples, a new arsenal of sophisticated analytical instruments is appearing in environmental laboratories. All use liquid or gas chromatography to separate the many compounds found in environmental samples. The individual components emerge sequentially from the chromatograph, swept along by the carrier gas or liquid. The technical challenge of the past ten years has been to develop methods to identify and measure the individual compounds in the few seconds during which they emerge from the chromatograph.

Several months ago, the authors initiated a programme, to develop a primary laboratory measurement method suitable for analysis of Standard Reference Materials (SRM's) or for referee-type measurements of trace toxic organics in water. This new method, involving laser Raman scattering from pollutants isolated in cryogenic matrices, should provide an alternative technique for the analysis of pollutants of the type on the EPA lists of regulated chemicals with a molecular specificity and sensitivity comparable to, or better than, existing techniques (eg, gas chromatography and mass spectrometry).

Any realistic approach to the identification and quantification of individual trace organic compounds in a complex sample must begin with the application of modern separation procedures, such as liquid or gas phase chromatography. However, even very efficient separation procedures may be unable to do more, in a realistic time frame, than to produce a series of fractions which themselves are rather complex mixtures. Therefore, any successful analytical procedure for the qualitative and quantitative analysis of complex mixtures of organics must incorporate a secondary and molecule-specific measurement method. Our approach involves three steps:

1. sample acquisition and initial separation,
2. matrix isolation,
3. spectroscopic analysis.

The total volatile pollutant content of the aqueous sample will be acquired by dynamic head-space sampling followed by concentration on a precolumn, and then separation on a gas chromatography (GC) column using argon as the carrier gas. The GC will separate the initial mixture into several fractions containing either a single or small number of physically or chemically similar molecular species. As the pollutants elute out the GC, a responsive valving system will be used to take cuts, or small sample amounts, of the effluent stream. These cuts will then be sprayed onto a cold finger, cryogenically maintained at 12 K. Both the organic pollutant and the argon carrier gas are frozen in a spot approximately 1 mm in diameter. The cold finger is rotated, in a step-like fashion, between sample cuts to maintain the initial separation achieved in the GC. Each sample containing only the compounds, if any, that emerged from the chromatograph during a specific one to three second period and now frozen, dilute in an argon matrix, is sequentially analyzed by matrix isolated laser Raman spectroscopy as it is stepped into view of a high resolution spectrometer. If chemical compounds are present in the region irradiated by the laser, they will re-emit light at wavelengths different from the wavelength of laser. This re-emitted Raman scattered light is characteristic of the compound(s). The intensity of the Raman scattered light is proportional to the amount of the compound present. As in the other detectors that have been developed for chromatographs, a small computer is needed to analyze the vast amount of data being generated and to present it in a form useable by the environmental analyst.

Matrix isolated laser Raman spectroscopy is used as the diagnostic means for several reasons: 1. Raman spectroscopy is a vibrational spectroscopy and as such provides a characteristic and reproducible 'fingerprint' that carries structural information to allow for the unambiguous identification of unknown contaminants; 2. All molecules have characteristic Raman spectra in an experimentally convenient spectral range; 3. The matrix substrate (in this case argon) is free of organic contaminants and has no spectral interferences; it is

The authors are at the Molecular Spectroscopy Division, B268 Physics Building, National Bureau of Standards, Washington D.C. 20234, USA. Paper received 6 December 1979

0030-3992/80/020097-02 $02.00

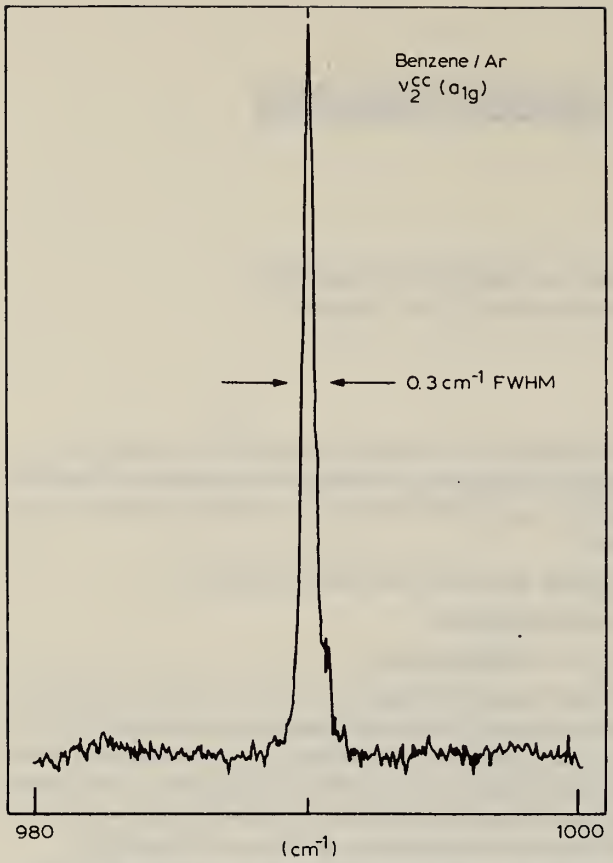

Fig. 1 Matrix isolated Raman spectrum of benzene. High resolution scan of the ν_2 mode of 5 n gram benzene isolated in argon at 11 K. The scan was acquired at 0.1 cm^{-1} resolution in 20 seconds.

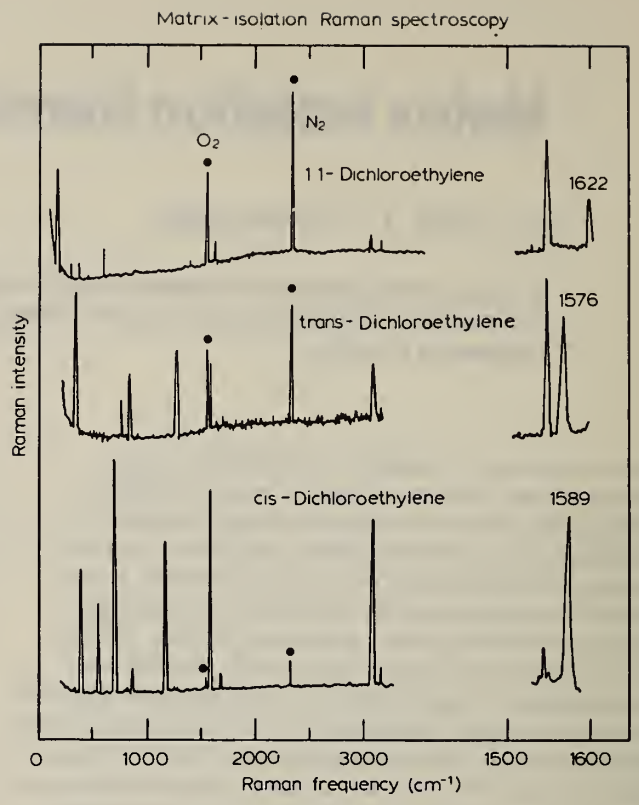

Fig. 2 Matrix isolated Raman spectra of three dichloroethylene isomers. The spectra were acquired at 5 cm^{-1} resolution in ten minutes. The dotted peaks are O_2 and N_2 'spiked' into the initial gas mixtures to aid in quantification. Also shown, to the right, is a closer look, at 1 cm^{-1} resolution, of the 1500–1600 cm^{-1} region.

transparent and allows the vibrational frequencies of the trapped pollutant to be readily compared to the gas phase values of known, pure compounds; 4. At the low temperatures used, all rotational motion is frozen out, and the spectral linewidths are very sharp, so sharp that the overlapping of bands observed in solution and in the gas phase is not a problem.

Although the engineering aspects of interfacing the technologies of sample acquisition, gas chromatography, and matrix preparation have not been fully implemented, matrix isolated Raman spectra have been obtained for laboratory samples of many of the toxic organics on the EPA's regulated list: benzene and substituted benzenes, halo-menthanes, ethylenes, and ethanes. Significantly, vibrational bandwidths were observed of about 1 cm^{-1} (see Fig. 1). By contrast, room temperature gas or liquid phase bandwidths are about 50 cm^{-1}; with such large bandwidths the spectral lines of many toxic and non-toxic compounds overlap, making analysis difficult or impossible. On the other hand, due to the narrowness of the spectral features in the low temperature matrix, spectra of these molecules are readily resolved; there is no difficulty in, for instance, analyzing mixtures of different molecular isomers (molecules with the same chemical formula but differing arrangements of the constituent atoms) such as cis, trans, and 1,1-dichloroethylene (see Fig. 2). With our present and far from optimum optics and low-power laser nanogram quantities of a wide variety of toxic organics can readily be detected.

Matrix isolated Raman spectroscopy may be favourably compared to the other techniques utilized in the analysis of low-level mixtures of complex organic species. Although similar in principle to infra-red absorption spectroscopy, Raman spectroscopy is inherently more sensitive (basically, in Raman spectroscopy one looks for small signals in the absence of any background while in infra-red absorption one looks for a small change in an otherwise very large continuum background). The Raman process is not prone to the interference problems that energy transfer introduces to fluorescence type measurements. Also, many regulated pollutants either do not fluoresce or they have electronic absorption spectra which are very broad or are in the experimentally difficult vacuum ultra-violet region. Although mass spectrometry has an equivalent sensitivity, it does not have the specificity of the Raman diagnostic (mass spectrometry cannot readily distinguish between similar species, such as isomers, even when one of these is regulated by the EPA while others are not).

The work to date has clearly demonstrated the feasibility of our technique for preparing and spectroscopically analyzing small quantities of complex organic molecules. It is now planned to use high-intensity pulsed laser Raman scattering, with gated electronics, to improve sensitivity and an optical multichannel analyzer with computer interfacing to reduce sampling time and to provide for rapid comparison of an 'unknown' spectrum to reference spectra. The feasibility of interfacing our sensitive detection apparatus to a liquid chromatograph for the analysis of non-volatile environmental and biological samples is currently under study. Although in its initial stages of development, this method, which is being developed with partial support by the U.S. Environmental Protection Agency, promises to be a major advance in the analysis of organic compounds.

APPENDIX 4

U.S. Department of Commerce
Juanita M. Kreps
Secretary

National Bureau of Standards
Ernest Ambler, Director

National Bureau of Standards Certificate

Standard Reference Material 2630

Nitric Oxide in Nitrogen

(Mobile-Source Emission Gas Standard)

(In Cooperation with the Motor Vehicle Manufacturers Association)

This Standard Reference Material is a mixture of nitric oxide in high purity nitrogen which is supplied in a high-pressure, compressed gas cylinder. The statistical uncertainty in each step of the preparation and analysis of this mixture has been carefully evaluated at the 95% confidence level. This Standard Reference Material should be used sparingly as a valuable primary standard to which daily working standards may be related.

CAUTION: Every precaution must be taken to avoid accidental contamination of the sample with atmospheric air during connection of the cylinder to any gas-handling system.

Nitric Oxide Concentration: ± μmol/mol (ppm)

Cylinder Number: Sample Number:

The concentration of nitric oxide is relative to all other constituents of the gas.

Each cylinder of gas is individually analyzed, but the concentration appearing on this certificate applies to all samples within the lot. The concentration of all samples in the lot fell within a limit of ± 0.3 percent of the average for the lot and all samples are considered identical within the stated limits of accuracy. The estimated upper limit of error of the nitric oxide concentration is ± 1.0% relative. This estimate is the 95% confidence interval based on allowances for known sources of possible error.

The research and development of this Standard Reference Material was supported by the Motor Vehicle Manufacturers Association of the United States, Inc. (MVMA), Detroit, Michigan.

The development and evaluation of the gravimetric primary standards used to certify this Standard Reference Material were performed at the National Bureau of Standards by MVMA Research Associates W. R. Miller and W. J. Thorn.

The overall direction and coordination of the technical measurements leading to certification were performed under the chairmanship of E.E. Hughes and H.L. Rook.

The technical and support aspects involved in the preparation, certification and issuance of this Standard Reference Material were coordinated through the Office of Standard Reference Materials by W.P. Reed.

Washington, D.C. 20234
May 2, 1979

George A. Uriano, Chief
Office of Standard Reference Materials

(over)

Analysis:

The nitric oxide content of this Standard Reference Material was determined by comparison with secondary standards that had been previously intercompared with a set of primary gravimetric standards. The method of intercomparison utilized the chemiluminescent reaction of nitric oxide with ozone.

The upper limit of the total uncertainty including both the imprecision of intercomparison and the inaccuracy of the gravimetric standards is less than 1.0% relative at the 95% confidence level.

At least 8% of the samples from the lot have been analyzed for nitrogen dioxide by a wet chemical method (a modified Saltzman technique). The maximum concentration of nitrogen dioxide did not exceed 0.5% relative to the nitric oxide in the samples analyzed.

Stability:

These samples are contained in aluminum cylinders. The stability is considered excellent and no losses of nitric oxide have been observed for similar samples contained in aluminum cylinders for periods of time greater than 2 years. The value appearing on this certificate is considered valid for 2 years from date of purchase. Periodic reanalyses of representative samples from this lot will be performed, and if significant changes are observed within a one year period the purchasers of other samples from the lot will be notified. Validation of the concentration of nitric oxide in cylinders that have been in the possession of the purchasers for more than one year can be made by the National Bureau of Standards at a nominal charge if more than 1000 psi remains in the cylinder.

Cylinder:

These gases are supplied in cylinders with a delivered volume of 0.85 m^3 (30 cubic feet) at STP. The cylinders conform to the DOT specification and are equipped with CGA 660 valves.

NOTE:

This cylinder is the property of the purchaser. If the user is unable to dispose of the cylinder it may be returned, prepaid, to the National Bureau of Standards for disposal.

U.S. Department of Commerce
Juanita M. Kreps
Secretary

National Bureau of Standards
Ernest Ambler, Director

National Bureau of Standards Certificate

Standard Reference Material 2631

Nitric Oxide in Nitrogen

(Mobile-Source Emission Gas Standard)

(In Cooperation with the Motor Vehicle Manufacturers Association)

This Standard Reference Material is a mixture of nitric oxide in high purity nitrogen which is supplied in a high-pressure, compressed gas cylinder. The statistical uncertainty in each step of the preparation and analysis of this mixture has been carefully evaluated at the 95% confidence level. This Standard Reference Material should be used sparingly as a valuable primary standard to which daily working standards may be related.

CAUTION: Every precaution must be taken to avoid accidental contamination of the sample with atmospheric air during connection of the cylinder to any gas-handling system.

Nitric Oxide Concentration:	±	μmol/mol (ppm)
Cylinder Number:	Sample Number	

The concentration of nitric oxide is relative to all other constituents of the gas.

Each cylinder of gas is individually analyzed, but the concentration appearing on this certificate applies to all samples within the lot. The concentration of all samples in the lot fell within a limit of ± 0.3 percent of the average for the lot and all samples are considered identical within the stated limits of accuracy. The estimated upper limit of error of the nitric oxide concentration is ± 1.0% relative. This estimate is the 95% confidence interval based on allowances for known sources of possible error.

The research and development of this Standard Reference Material was supported by the Motor Vehicle Manufacturers Association of the United States, Inc. (MVMA), Detroit, Michigan.

The development and evaluation of the gravimetric primary standards used to certify this Standard Reference Material were performed at the National Bureau of Standards by MVMA Research Associates W.R. Miller and W. J. Thorn.

The overall direction and coordination of the technical measurements leading to certification were performed under the chairmanship of E.E. Hughes and H.L. Rook.

The technical and support aspects involved in the preparation, certification, and issuance of this Standard Reference Material were coordinated through the Office of Standard Reference Materials by W.P. Reed.

Washington, D.C. 20234
May 2, 1979

George A. Uriano, Chief
Office of Standard Reference Materials

(over)

Analysis:

The nitric oxide content of this Standard Reference Material was determined by comparison with secondary standards that had been previously intercompared with a set of primary gravimetric standards. The method of intercomparison utilized the chemiluminescent reaction of nitric oxide with ozone.

The upper limit of the total uncertainty including both the imprecision of intercomparison and the inaccuracy of the gravimetric standards is less than 1.0% relative at the 95% confidence level.

At least 8% of the samples from the lot have been analyzed for nitrogen dioxide by a wet chemical method (a modified Saltzman technique). The maximum concentration of nitrogen dioxide did not exceed 0.5% relative to the nitric oxide in the samples analyzed.

Stability:

These samples are contained in aluminum cylinders. The stability is considered excellent and no losses of nitric oxide have been observed for similar samples contained in aluminum cylinders for periods of time greater than 2 years. The value appearing on this certificate is considered valid for 2 years from date of purchase. Periodic reanalyses of representative samples from this lot will be performed, and if significant changes are observed within a one year period the purchasers of other samples from the lot will be notified. Validation of the concentration of nitric oxide in cylinders that have been in the possession of the purchasers for more than one year can be made by the National Bureau of Standards at a nominal charge if more than 1000 psi remains in the cylinder.

Cylinder:

These gases are supplied in cylinders with a delivered volume of 0.85 m^3 (30 cubic feet) at STP. The cylinders conform to the DOT specification and are equipped with CGA 660 valves.

NOTE:

This cylinder is the property of the purchaser. If the user is unable to dispose of the cylinder it may be returned, prepaid, to the National Bureau of Standards for disposal.

U.S. Department of Commerce
Juanita M. Krepe
Secretary

National Bureau of Standards
Ernest Ambler, Director

National Bureau of Standards

Certificate of Analysis

Standard Reference Material 2673

Sulfate and Nitrate on Filter Media

This Standard Reference Material is intended for use in the evaluation of apparatus and methods used in the determination of atmospheric particulate sulfate and nitrate which have been collected on filters. It consists of a series of filter strips upon which sulfate and nitrate have been deposited in an essentially central location. The values certified correspond to the quantities of the substances leached from the filter strip without destruction of the filter matrix.

Sample Number	Sulfate content μg/filter		Nitrate content μg/filter	
	Average value	Tolerance limits	Average value	Tolerance limits
I	503	493 - 513	100	98 - 102
II	2002	1955 - 2049	1002	978 - 1026
III	6939	6635 - 7243	2513	2404 - 2622
Blank	2	0 - 6*	2	0 - 3*

* Range of measured values

The average value is the mean based on the analysis of 24 or 28 filters randomly selected from the lot. The tolerance limits are determined so that at the 95% confidence level they will contain the central 95% of the population of filter values. Details of the preparation, analysis, and statistical treatment of the data are given on the reverse side of the certificate.

This Standard Reference Material was prepared by B. I. Diamondstone. The analytical measurements were made by W. F. Koch. Statistical analysis of the data was provided by J. Orban. The overall direction and coordination of the preparation and analytical measurements leading to certification were performed in the Center for Analytical Chemistry under the chairmanship of J. K. Taylor.

The technical and support aspects involved in the preparation, certification, and issuance of this SRM were coordinated through the Office of Standard Reference Materials by W. P. Reed.

Washington, D.C. 20234
June 25, 1979

George A. Uriano, Chief
Office of Standard Reference Materials

(over)

Preparation

This SRM consists of strips cut from glass fiber filters, such as are commonly used for measurements of atmospheric particulates, using high volume samplers. Solutions containing known amounts of potassium sulfate and potassium nitrate were prepared, gravimetrically, and multiple aliquots of 25 μL were placed on the filter strips. Four aliquots were so transferred to each filter in the case of samples I and II, and five in the case of Sample III. The pipets were calibrated by weighing similar aliquots transferred into weighing bottles.

The filters were prepared in a clean room and allowed to air-dry before packaging in glassine envelopes. The filters were prepared in groups of 100 and the proper number of aliquots were dispensed into weighing bottles at the beginning and end of each sequence, to monitor the performance of the pipet.

Analytical Measurements

Twenty four samples were randomly selected from the production lot (28 in the case of sample III) for chemical measurement of their extractable sulfate and nitrate. Each filter strip was extracted with a standard eluent (see below) for 15 minutes in a 55 °C ultrasonic bath. The extracts were analyzed for sulfate and nitrate by ion chromatography. The eluent was a solution of 0.003 M $NaHCO_3$ and 0.0018 M Na_2CO_3. A 100 μL sample loop was used. Peak heights were compared with those obtained from accurately prepared standard solutions. Three standards were prepared for each concentration level so as to bracket the extracts.

The randomly selected filters were also analyzed in random order. No significant systematic errors were observed related to the order of preparation. Average values and the overall standard deviation, s_0, of individual measurements were calculated. This standard deviation includes measurement error and filter content error.

The standard deviation, s_f, due to filter content variability was computed from a sample of 12 or 14 weighed quantities delivered by the pipets during the preparation of the filters. The resulting tolerance interval for the sulfate/nitrate contents is of the form

$$\overline{X} \pm k\, s_f\,.$$

It is this tolerance interval that should be of greater interest to the participating laboratory since it gives practical bounds for the likely values of the sulfate or nitrate contents that might be found in a given filter.

The following table lists the values of s_0 and s_f for each set of filters. The measurement standard deviation, s_m, for NBS can be computed using the relation $s_0^2 = s_m^2 + s_f^2$

Set	Average (μg)	s_o	s_f
I SO_4	502.6	8.89	3.14
NO_3	100.3	2.56	.63
II SO_4	2001.7	29.30	14.88
NO_3	1001.7	15.92	7.44
III SO_4	6939.0	109.35	100.75
NO_3	2513.0	43.70	36.30

The average values calculated from the composition of the solutions and the quantitites delivered by the pipets are in general agreement with the analytical values. However, the values certified are those obtained by analysis.

Recommended Usage

The material is not homogeneously distributed on the filter; hence the sample must be used in its entirety for analysis. It is recommended that the filter be extracted at 55 °C in an ultrasonic bath, with water or other nonreactive solvents. The filter base should not be digested to put it into solution.

U.S. Department of Commerce
Juanita M. Kreps
Secretary

National Bureau of Standards
Ernest Ambler, Director

National Bureau of Standards

Certificate of Analysis

Standard Reference Material 2674

Lead on Filter Media

This Standard Reference Material is intended for use in the calibration of apparatus and the evaluation of methods used in the determination of atmospheric particulate lead which has been collected on filters. It consists of a series of filter strips upon which lead has been deposited in an essentially central location. The values certified correspond to the quantities of the substance leached from the filter strip without destruction of the filter matrix.

Sample No.	Lead Content, μg/filter	
	Average Value	Tolerance Limits
I	100	97 - 103
II	303	294 - 312
III	1505	1477 - 1533
Blank	1.4	0.7 - 2.1*

*Range of measured values

The average value is the mean based on the analysis of 26 or 28 filters randomly selected from the lot. The tolerance limits are determined so that at the 95% confidence level they will contain the central 95% of the population of filter values. Details of the preparation, analysis, and statistical treatment of the data are given on the reverse side of this certificate.

This Standard Reference Material was prepared by B. I. Diamondstone. The analytical measurements were made by E. J. Maienthal and M. S. Epstein of the Inorganic Analytical Research Division. Statistical analysis of the data was provided by J. Orban of the Statistical Engineering Division.

The overall direction and coordination of the preparation and analytical measurements leading to certification were performed in the Center for Analytical Chemistry under the charimanship of J. K. Taylor.

The technical and support aspects involved in the preparation, certification, and issuance of this SRM were coordinated through the Office of Standard Reference Materials by T. E. Gills.

Washington, D.C. 20234
December 18, 1979

George A. Uriano, Chief
Office of Standard Reference Materials

(over)

Preparation

This SRM consists of strips cut from glass fiber filters of the type normally used in high volume samplers for the measurement of atmospheric particulates. Solutions containing known amounts of lead nitrate were prepared gravimetrically, and aliquots of 25 μL were placed on the filter strips using micropipets. Four aliquots were transferred to each filter in the case of samples I and II and five in the case of sample III. The pipets were calibrated by weighing similar aliquots transferred into weighing bottles.

The filters were prepared in a clean room and allowed to air-dry before packaging into glassine envelopes. The filters were prepared in groups of 100 and the proper number of aliquots were dispensed into weighing bottles at the beginning and end of each sequence, to monitor the performance of the pipet.

Analytical Measurements

Twenty-eight filters were randomly selected from the production lot (26 in the case of Sample I) for chemical measurement of extractable lead. Selected filters were extracted with dilute nitric acid, using ultrasonic vibration to assist in the extraction. After the nitric acid extraction, the filters were thoroughly rinsed with distilled water to ensure complete extraction. The extracts were quantitatively diluted and analyzed by linear sweep voltammetry which had been calibrated with solution standards prepared from high purity lead.

The selected filters were analyzed in random order. No significant systematic errors were observed related to order of preparation. Average values were calculated together with the overall standard deviation, s_o, of individual measurements. This standard deviation includes measurement error and filter content error. The resulting confidence interval for the mean is of the form

$$\overline{X} \pm t\, s_o/\sqrt{n},$$

where s_o is based on $n - 1 = 27$ degrees of freedom.

A selected number of filters were also analyzed by atomic absorption. The results obtained were well within the tolerance limits given and were consistent with the certified values.

The standard deviation, s_f, due to filter content variability was computed from a sample of 12 or 14 weighed quantities delivered by the pipets during the preparation of the filters. The resulting tolerance interval for the lead content is of the form

$$\overline{X} \pm k\, s_f\,.$$

It is the tolerance interval that should be of greater interest to the participating laboratory since it gives practical bounds for the likely values of the lead content that might be found in a given filter.

The following table lists the values of s_o and s_f for each set of filters. The measurement standard deviation, s_m, for NBS can be computed using the relation $s_o^2 = s_m^2 + s_f^2$

Set	Average (μg)	s_o	s_f
I	99.7	1.59	0.89
II	302.9	5.37	3.00
III	1505.2	12.73	9.24

The average values calculated from the composition of the solutions and the quantities delivered by the pipets are in general agreement with the analytical values. However, the values certified are those obtained by the analysis.

Recommended Usage

The material is not homogeneously distributed on the filter, hence the sample must be used in its entirety for analysis. It is recommended that the filter be extracted at 45-50 °C in an ultrasonic bath, with dilute nitric acid (2 mL HNO_3 + 15 mL H_2O). After extraction the filters should be thoroughly rinsed with distilled water. The filter base should not be dissolved.

U.S. Department of Commerce
Juanita M. Kreps
Secretary

National Bureau of Standards
Ernest Ambler, Director

National Bureau of Standards

Certificate of Analysis

Standard Reference Material 2657

Oxygen in Nitrogen

(Gas Standard)

This Standard Reference Material is intended for use in the calibration of instruments used for combustion control and respiratory gas analysis. It is not intended as a daily working standard, but rather as a primary standard to which the concentration of the daily working standards may be related.

Oxygen concentration: ± mole percent

Cylinder Number: Sample Number:

The concentration of oxygen is relative to all other constituents of the gas.

Each cylinder is individually analyzed and the concentration that appears on this certificate applies to the cylinder identified by cylinder and sample number.

The original development and evaluation of the oxygen in nitrogen series of Standard Reference Materials were performed at the National Bureau of Standards by W. D. Dorko and W. P. Schmidt.

The overall direction and coordination of technical measurements leading to certification were performed under the chairmanship of E. E. Hughes and H. L. Rook.

The technical and support aspects involved in the preparation, certification, and issuance of this Standard Reference Material were coordinated through the Office of Standard Reference Materials by R. Alvarez.

Washington, D.C. 20234
December 31, 1979

George A. Uriano, Chief
Office of Standard Reference Materials

(over)

Analysis:

The concentration of oxygen in this Standard Reference Material was determined by comparison with a set of gravimetric primary standards. The intercomparisons were performed using both a gas chromatograph equipped with a thermal conductivity detector and an analyzer sensitive to the paramagnetic properties of oxygen. The uncertainty shown is based on an estimate of the upper limit of the total uncertainty including the inaccuracy of the gravimetric primary standards and the imprecision of intercomparison of the Standard Reference Material with the gravimetric standards. This uncertainty at the 95% confidence level does not exceed 1.0% relative.

This sample is certified only for the concentration of oxygen.

A representative number of samples were examined to determine the argon concentration and it is estimated to be _____ mole percent.

Stability:

This SRM is contained in an aluminum cylinder. The stability is considered good and no change in concentration is anticipated. However, the value appearing on this certificate is considered valid for only 2 years from date of purchase. Periodic reanalyses of representative samples from this lot will be performed at NBS, and if significant changes are observed within the 2 year period, purchasers of the SRM will be notified.

Cylinder:

This SRM is supplied in cylinders at 12.4 MPa (1800 psi) pressure with a delivered volume of 0.88 m^3 (31 cubic feet) at STP. The cylinders conform to DOT specifications and are equipped with CGA-580 valves.

The cylinders become the property of the purchaser. However, they may be returned, prepaid, to the National Bureau of Standards for disposal.

SRM
2657

U.S. Department of Commerce
Juanita M. Kreps
Secretary

National Bureau of Standards
Ernest Ambler, Director

National Bureau of Standards

Certificate of Analysis

Standard Reference Material 2658

Oxygen in Nitrogen

(Gas Standard)

This Standard Reference Material is intended for use in the calibration of instruments used for combustion control and respiratory gas analysis. It is not intended as a daily working standard, but rather as a primary standard to which the concentration of the daily working standards may be related.

Oxygen concentration: ± mole percent

Cylinder Number: Sample Number:

The concentration of oxygen is relative to all other constituents of the gas.

Each cylinder is individually analyzed and the concentration that appears on this certificate applies to the cylinder identified by cylinder and sample number.

The original development and evaluation of the oxygen in nitrogen series of Standard Reference Materials were performed at the National Bureau of Standards by W. D. Dorko and W. P. Schmidt.

The overall direction and coordination of technical measurements leading to certification were performed under the chairmanship of E. E. Hughes and H. L. Rook.

The technical and support aspects involved in the preparation, certification, and issuance of this Standard Reference Material were coordinated through the Office of Standard Reference Materials by R. Alvarez.

Washington, D.C. 20234
December 31, 1979

George A. Uriano, Chief
Office of Standard Reference Materials

(over)

Analysis:

The concentration of oxygen in this Standard Reference Material was determined by comparison with a set of gravimetric primary standards. The intercomparisons were performed using both a gas chromatograph equipped with a thermal conductivity detector and an analyzer sensitive to the paramagnetic properties of oxygen. The uncertainty shown is based on an estimate of the upper limit of the total uncertainty including the inaccuracy of the gravimetric primary standards and the imprecision of intercomparison of the Standard Reference Material with the gravimetric standards. This uncertainty at the 95% confidence level does not exceed 1.0% relative.

This sample is certified only for the concentration of oxygen.

A representative number of samples were examined to determine the argon concentration and it is estimated to be _____ mole percent.

Stability:

This SRM is contained in an aluminum cylinder. The stability is considered good and no change in concentration is anticipated. However, the value appearing on this certificate is considered valid for only 2 years from date of purchase. Periodic reanalyses of representative samples from this lot will be performed at NBS, and if significant changes are observed within the 2 year period, purchasers of the SRM will be notified.

Cylinder:

This SRM is supplied in cylinders at 12.4 MPa (1800 psi) pressure with a delivered volume of 0.88 m^3 (31 cubic feet) at STP. The cylinders conform to DOT specifications and are equipped with CGA-580 valves.

The cylinders become the property of the purchaser. However, they may be returned, prepaid, to the National Bureau of Standards for disposal.

SRM
2658